

**Chain-transfer kinetics for free-radical homo-
and copolymerizations of styrene and
methyl methacrylate in supercritical carbon dioxide**

Dissertation

zur Erlangung des Doktorgrades

der Mathematisch-Naturwissenschaftlichen Fakultäten

der Georg-August-Universität zu Göttingen

vorgelegt von

Véronique El Rezzi

aus Beirut, Libanon

Göttingen 2001

D 7

Referent: Prof. Dr. M. Buback

Korreferent: Prof. Dr. K. Hoyer mann

Tag der mündlichen Prüfung: 27.06.2001

Table of contents

1.	Abstract	1
2.	Introduction	3
3.	Experimental	7
3.1	Apparatus	7
3.1.1	Optical high-pressure cell	7
3.1.2	Optical internal cell	9
3.1.3	Pressure generation and control	9
3.1.4	Heating and temperature control	10
3.1.5	Experimental set-up for polymerizations in scCO ₂	10
3.1.6	FT-IR/NIR spectrometer	12
3.1.7	Excimer laser	12
3.1.8	Size-Exclusion Chromatography (SEC)	12
3.1.9	Preparation of the mixtures containing the cobalt-complex	13
3.2	PLP-SEC technique	13
3.3	Determination of C _T and CO ₂ -content	14
3.4	Substances used	14
3.4.1	Monomers	14
3.4.2	Carbon dioxide	15
3.4.3	Initiators and inhibitor	15
3.4.4	Chain-transfer agents	16
3.5	FT-IR/NIR spectroscopy	18
3.6	Consideration of errors	19
3.7	References	20

4.	Experimental considerations and choice of reaction conditions	23
4.1	Selection of temperature and pressure	23
4.2	SEC calibration	23
4.3	Determination of C_T	25
4.3.1	Background	25
4.3.1.1	Mayo method	28
4.3.1.2	Chain-Length Distribution method	29
4.3.2	Comparison of both procedures	31
4.3.2.1	Theoretical comparison	31
4.3.2.2	Experimental comparison	32
4.3.3	CLD method	33
4.4	Conditions for the determination of C_T by PLP	34
4.5	Consideration of errors	39
4.6	References	40
5.	Results and discussions	43
5.1	DDM as chain-transfer agent	43
5.1.1	Homopolymerization of styrene	44
5.1.1.1	Mayo method	44
5.1.1.2	CLD method	46
5.1.1.3	Results	46
5.1.2	Homopolymerization of MMA	50
5.1.3	Copolymerization of styrene and MMA	53
5.1.4	Summary	57
5.2	COPhBF as catalytic chain-transfer agent	59
5.2.1	Preliminary investigations	60
5.2.2	Homopolymerization of MMA	62
5.2.3	Homopolymerization of styrene	66
5.2.4	Copolymerization of styrene and MMA	70
5.2.5	Closing remarks	77
5.3	MMA trimer as chain-transfer agent	79
5.3.1	Homopolymerization of styrene	81

5.3.2	Homopolymerization of MMA	85
5.3.3	Summary	89
5.4	Discussions	91
5.4.1	Mechanism of the chain-transfer reaction	91
5.4.1.1	DDM	92
5.4.1.2	MMA trimer	93
5.4.1.3	COPhBF	95
5.4.2	Activation volume ΔV^\ddagger and scCO ₂ influence on k_{tr}	98
5.4.2.1	DDM	98
5.4.2.2	MMA trimer	100
5.4.2.3	COPhBF	101
5.5	References	104
6.	Kinetic modeling	109
6.1	Theoretical background	109
6.1.1	Simulations of k_{tr} applying terminal and PUE models	109
6.1.2	Endgroups estimate	115
6.1.3	Simulation tool PREDICI [®]	116
6.2	Simulation of k_{tr} applying terminal and PUE models	116
6.2.1	Free-radical copolymerization	117
6.2.2	Copolymerizations in the presence of DDM	119
6.2.3	Copolymerizations in the presence of COPhBF	120
6.3	Modeling of full molecular weight distributions of styrene-MMA copolymers via PREDICI [®]	122
6.3.1	Experimental considerations	122
6.3.2	DDM as chain-transfer agent	126
6.3.3	COPhBF as catalytic chain-transfer agent	130
6.3.4	Closing remarks	131
6.4	Endgroups estimate	132
6.5	References	133

7.	Closing remarks	137
	7.1 References	138
8.	Abbreviations	139
9.	Appendix	143

1. Abstract

Chain-transfer kinetics have been studied for styrene and MMA homo- and copolymerizations in bulk and in solution of supercritical CO₂ (40 wt % scCO₂). Three chain-transfer agents (CTAs) were used in this work: *n*-dodecyl mercaptan (DDM), the bis(methanol) complex of bis(difluoroboryl) diphenylglyoximate cobalt (II) (COPhBF), and the methyl methacrylate trimer (MMA_t). Chain-transfer constants, C_T , which are defined as k_{tr}/k_p , the ratio of the transfer and propagation rate coefficients have been measured by the pulsed-laser polymerization (PLP)-size exclusion chromatography (SEC) technique. C_T values are derived by the chain-length distribution (CLD) procedure. k_{tr} is calculated from C_T by way of the known propagation rate coefficient, k_p . The pressure dependence of k_{tr} has been investigated between 300 and 1500 bar in both media, bulk and scCO₂, at 80°C.

k_{tr} obtained for the CTAs differ by orders of magnitude: In MMA homopolymerization k_{tr} is close to 10², 10³ and 10⁷ L·mol⁻¹·s⁻¹ for the MMA trimer, for DDM and for COPhBF, respectively. In styrene homopolymerization k_{tr} is close to 10², 10⁴ and 10⁵ L·mol⁻¹·s⁻¹ for the MMA trimer, for DDM and for COPhBF, respectively. The difference in k_{tr} for these CTAs is due to different transfer mechanisms.

The presence of scCO₂ has no influence on k_{tr} with the exception of MMA homopolymerizations with COPhBF being the catalytic CTA. In this case, k_{tr} is significantly higher in the presence of 40 wt % scCO₂. Even for the transfer reaction of MMA with COPhBF, the activation volume in bulk and in scCO₂ is the same.

The high k_{tr} value, the scCO₂ influence on k_{tr} , and the significant pressure dependence associated with an activation volume around + 35 cm³·mol⁻¹ observed in MMA homopolymerization with COPhBF are consistent with a diffusion-controlled transfer reaction.

The transfer reaction with DDM and MMA trimer as CTAs are chemically controlled. The activation volumes are around ± 3 cm³·mol⁻¹.

Kinetic modeling of k_{tr} indicates that the terminal model does not allow for an accurate description of the experimental results in the transfer process in styrene-MMA copolymerizations in the presence of DDM as CTA. Models, which consider penultimate units, describe the copolymerization k_{tr} behavior as a function of the monomer feed well. Estimates of the type of polymer endgroups for polymerizations with DDM as CTA clearly

indicate that even at very low f_S , styrene is the dominant endgroup. In case of CPhBF as CTA, kinetic modeling has shown that the simple terminal model is sufficient to describe the copolymerization k_{tr} observed.

MWDs obtained by simulations via PREDICI[®] considering a PUE model for the transfer process in styrene-MMA copolymerization with DDM as CTA are in excellent agreement with the experimental MWDs.

C_T values, thus k_{tr} values, obtained with DDM may be used for simulations of homo-, copolymerizations of styrene and methacrylates since it is known that C_T of DDM for methacrylates is independent of the ester size. In addition, knowing the activation energy of k_{tr} , simulations at different temperatures may be investigated.

2. Introduction

Environmental concern over the emission of volatile organic solvents used in polymer synthesis has prompted researchers to look for less harmful alternatives. A very promising technology area should be the polymerization in supercritical fluids¹. These fluids show gaslike diffusivities while having liquidlike densities that allow for solvation of many compounds. They exhibit a change in solvent density upon small variations in temperature or pressure without altering solvent composition². In addition, the low viscosity of supercritical fluids and their ability to plasticize glassy polymers have implications on polymer processing and kinetics. When carbon dioxide is used as a supercritical solvent, additional advantages can be realized. CO₂ is naturally occurring and abundant, it exists in natural reservoirs of high purity located throughout the world. CO₂ has a critical temperature of 31°C, a modest critical pressure of 74 bar and a critical density of 0.468 g·cm⁻³. These characteristics³ allow for liquidlike densities at temperatures slightly above room temperature and by implication, liquidlike solvent characteristics. DeSimone and co-workers have shown that scCO₂ is an ideal medium for both homogeneous and heterogeneous radical polymerizations⁴. Most of the investigations into polymerizations in scCO₂ focused on reaction in heterogeneous phase as polymer solubility in scCO₂ is generally rather low. Recently, several studies showed a significant influence of scCO₂ on homogeneous phase polymerizations. For example, in butyl acrylate homopolymerization scCO₂ was shown to have a significant influence on the propagation and termination rate coefficients^{5,6,7}.

The controlled synthesis of low molecular weight (MW) polymers is gaining greater importance as applications in coatings, detergents and water treatment industries continue to develop. The interest in the free-radical polymerization with respect to the preparation of these materials is originating from the fact that in contrast to ionic polymerization a greater number of monomers may be utilized. Although most common styrenic and meth(acrylic) polymers show only limited solubility, the synthesis of low molecular weight material in the presence of scCO₂ is a promising alternative process. Due to the significantly increased polymer solubility at low MW, high degrees of monomer conversion are accessible in homogeneous phase of scCO₂. For example styrene-methacrylate terpolymers which are used in coatings may be synthesized at complete monomer conversion ($M_n \approx 3000 \text{ g}\cdot\text{mol}^{-1}$) in scCO₂⁸. Because polymer properties are strongly dependent on MW, it is of great interest to effectively control

MW. One approach to molecular weight reduction involves the use of chain-transfer agents (CTAs). The knowledge of the transfer activity of a CTA, which is measured via the chain-transfer rate coefficient, k_{tr} , is necessary to predict the molecular weight of the polymer obtained. Thus, the aim of this work is to investigate the influence of $scCO_2$ as a solvent on the transfer process in free-radical polymerization. Three types of CTAs in styrene and MMA homo- and copolymerizations are studied: A mercaptan (*n*-dodecyl mercaptan, DDM), a cobalt-complex (bis(difluoroboryl)diphenylglyoximato cobalt (II), CPhBF), and a methyl methacrylate macromonomer (MMA_t). The use of these CTAs has two major advantages. Firstly, by using these CTAs it is possible to obtain polymers in very different MW ranges. Secondly, the polymer endgroups obtained are dissimilar: A saturated carbon bond is produced with DDM, whereas an unsaturated carbon bond is produced with CPhBF. In case of the MMA trimer, the polymer chain length is increased by three monomer units due to the incorporation of the MMA trimer into the polymer backbone and an unsaturated endgroup is obtained. This aspect is interesting as the type of terminal group in the polymer determines potential subsequent reactions and the properties of the polymer generated.

A great advantage of using mercaptans as CTA is that they have a good transfer activity towards usual vinyl monomers. However, mercaptans are incorporated into the propagating chains which may affect the polymer properties. A new technology has emerged in recent years^{9,10}: The use of catalytic chain transfer (CCT) agents, which is well known as a highly efficient method for producing oligomers. CCT has many favorable characteristics: The catalysts, which are generally cobalt complexes, are used in low concentration (ppm range), are generally non toxic and are regenerated during the polymerization. The mechanism is such that each polymer molecule has a terminal vinyl group, which can be used subsequently for copolymerization with other monomers, usually macromonomers such as MMA trimer, resulting in graft, comb, and star architectures^{11,12,13}. The mode of reaction is an addition-fragmentation reaction¹⁴. The type structure of the CCT substituents determines the functionality introduced at the polymer chain ends.

Literature shows only few reports on the chain-transfer activity, thus on the chain-transfer constant ($C_T = k_{tr}/k_p$) of cobalt complexes^{10,15,16} and macromonomers¹⁷. Even for the frequently used mercaptans only few informations on k_{tr} are available¹⁸.

Investigations into C_T in styrene and methacrylates homopolymerizations at ambient pressure have shown that the transfer activity of DDM is more effective with styrene than with methyl

methacrylate (MMA)¹⁸. C_T of 15.6 and 0.706 were reported for 60°C and 1 bar in styrene and MMA homopolymerization, respectively.

The chain-transfer activity of CPhBF has been tested in styrene and MMA polymerizations at ambient pressure and different temperatures¹⁵. The reported C_T values indicate that CCT is by one order of magnitude more effective in MMA homopolymerization than in styrene. However, even in case of styrene, C_T values are high, which implies a strong transfer activity of CPhBF compared to common CTAs¹⁹. C_T values reported at 60°C and 1 bar are in the range of 10^4 and 10^2 in MMA and in styrene homopolymerization, respectively.

Investigations into C_T for MMA homopolymerizations in the presence of MMA trimer¹⁷ result in C_T of 0.188 at 80°C and 1 bar. No literature data have been reported on C_T in styrene homopolymerization with MMA trimer as CTA so far.

In order to effectively control MW in polymerizations in scCO₂, knowledge of k_{tr} in the presence of CO₂ is required. However, so far only for MMA homopolymerization with CPhBF at 150 bar and 50°C the influence of CO₂ on the transfer process was studied¹⁶. Due to the lack of k_{tr} data in the presence of CO₂, this work is focused on the influence of scCO₂ as a solvent on k_{tr} of DDM, CPhBF, and MMA trimer in MMA and styrene homopolymerizations. The variation of k_{tr} with pressure has been studied between 300 and 1500 bar since the physical properties of the system, such as viscosity, are altered. In addition, investigations into the pressure dependence of k_{tr} are useful for the understanding of the mechanism of the transfer process. k_{tr} data are derived from the pulsed-laser polymerization (PLP) technique combined with the molecular weight distribution analysis of the resulting polymer by size exclusion chromatography (SEC).

The studies of the chain-transfer activity of CTAs are extended to styrene-MMA copolymerizations in case of DDM and CPhBF. These copolymers have many important applications in the polymer industry, e.g. are used in adhesive and coatings compositions, as dispersants and in the biomedical industry. In order to model and optimize the copolymerizations, the knowledge of copolymerization k_{tr} is required. In addition, copolymerization k_{tr} should improve the understanding of the transfer mechanisms.

In order to understand the results obtained for styrene-MMA copolymerizations in the presence of DDM and CPhBF, kinetic modeling is carried out. Chain-transfer rate coefficients are determined via different kinetic models, applying a penultimate unit effect model and a terminal unit model in the transfer reaction. With the knowledge of k_{tr} values

determined experimentally, simulations of molecular weight distribution are performed via the program PREDICI[®].²⁰

2.1 References

1. Jessop, P. G.; Leitner, W. *Chemical Synthesis using Supercritical Fluids*, Wiley-VCH, Weinheim **1999**.
2. McHugh, M. A.; Krukonis, V. J. J. *Supercritical Fluid Extraction: Principles and Practice*, 2nd Ed. Butterworth-Heinemann: Stoneham, **1993**.
3. Baser, S. J.; Stern, K. M.; *In Catalytic Activation of Carbon Dioxide*: Ayers, W. M.; Ed. American Chemical Society: Washington, DC, **1998**.
4. DeSimone, J. M.; Guan, Z.; Elsbernd, C. S. *Science* **1992**, 257, 945.
5. Beuermann, S.; Buback, M.; Schmaltz, C.; Kuchta, F.-D. *Macromol. Chem. Phys.* **1998**, 199, 1209.
6. Beuermann, S.; Buback, M.; Schmaltz, C. *Macromolecules* **1998**, 31, 8069.
7. Beuermann, S.; Buback, M.; Schmaltz, C. *Ind. Eng. Chem. Res.* **1999**, 38, 3338.
8. Jürgens, M. *Ph.-D* **2001**, Göttingen.
9. Gridnev, A.; *J. Polym. Sci., Polym. Chem. Ed.* **2000**, 38, 1753.
10. Heuts, J. P. A.; Kukulj, D.; Foster, D. J.; Davis, T. P. *Macromolecules* **1998**, 31, 2894.
11. Antonelli, J. A.; Scopazzi, C.; Doherty, M. M.; E. I. *Dupont de Nemours and Company*, invs.: US **1991**, 5 010 140.
12. Antonelli, J. A.; Scopazzi, C. E. I. *Dupont de Nemours and Company*, invs.: US **1994**, 5 362 813.
13. Chu, I. C.; Fryd, M.; Lynch, L. E. E. I. *Dupont de Nemours and Company*, invs.: US **1993**, 5 231 131.
14. Berge, C. T.; Darmon, M. J.; Antonelli, J. A. *US Patent US 5*, **1994**, 362, 826.
15. Heuts, J. P. A.; Foster, D. J.; Davis, T. P.; Yamada, B.; Yamazoe, H.; Azukizawa, M. *Macromolecules* **1999**, 32, 2511.
16. Foster, D. J.; Heuts, P. A.; Lucien, F. P.; Davis, T. P. *Macromolecules* **1999**, 32, 5514.
17. Moad, L. C.; Moad, G.; Rizzardo, E.; Thang, S. H. *Macromolecules* **1996**, 29, 7717.
18. Hutchinson, R. A.; Paquet, D. A.; Mc Minn, J. H. *Macromolecules* **1995**, 28, 5655.
19. Odian, G. *Principles of Polymerization*, 2nd Ed., Wiley: New York, **1981**.
20. Wulkow, M. *Macromol. Theory Simul.* **1996**, 5, 393.

3. Experimental

3.1 Apparatus

3.1.1 Optical high-pressure cell

The optical high-pressure cell used for spectroscopic investigations of pulsed laser induced homo- and copolymerizations under high pressure is illustrated in Fig. 3.1. The cell is designed for pressures up to 3500 bar and temperatures up to 350 °C. The cylindrical cell body and sealing flanges are made of a nickel-based alloy of high ultimate tensile strength (RGT 601, Material No. 2.4668, Arbed Saarstahl). The body length is 100 mm, and the outer and inner diameters are 80 and 22 mm, respectively. Four holes bored perpendicular to the cylindrical axis allow for fitting of high-pressure capillaries and insertion of a sheathed thermocouple (6) directly into the sample volume. Unused borings are sealed with plugs.

The cell is sealed at each end by a conical ram (5) (Material No. 2.4668, Arbed Saarstahl) which sits into the cell cone. The ram is pressed against the cell cone by the flange (2) (Material No. 2.4668, Saarstahl) which is secured by six high-pressure bolts (1) (Material No. 2.4969).

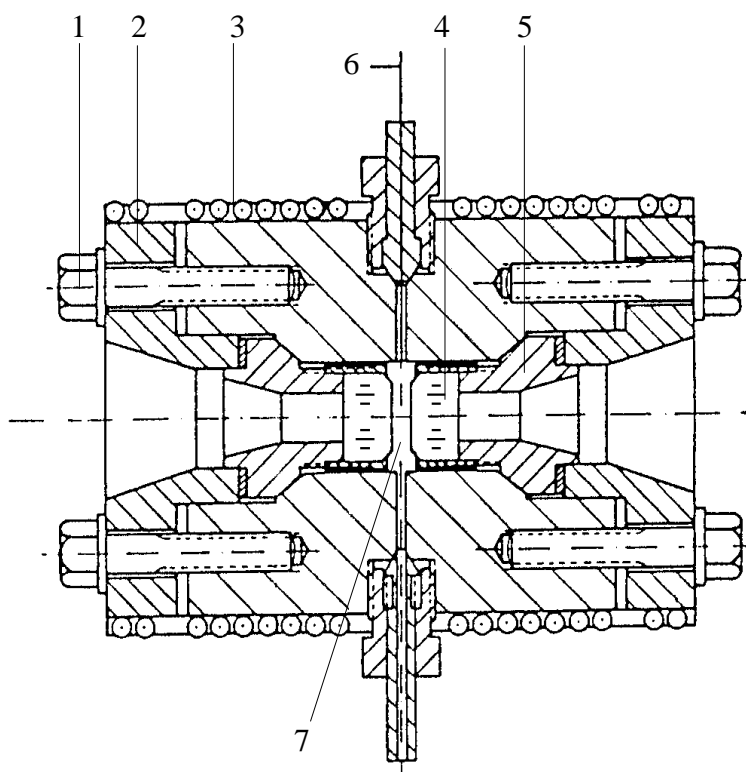


Figure 3.1: Optical high-pressure cell.

- (1) bolt, (2) flange, (3) heating jacket, (4) high-pressure window,
(5) ram, (6) sheathed thermocouple, (7) adjustable optical path length

Each high-pressure window (4) is fitted against the polished surface of the ram and held in place by a stainless steel ceiling cap. To compensate for surface area irregularities, a $\sim 12 \mu\text{m}$ thick teflon foil is placed between the polished surfaces of the window. This set-up is self-sealing under pressure in accordance with the Poulter principle¹. The high-pressure optical windows used in this work were synthetic sapphire crystals (diameter 18 mm, height 10 mm, UV grade, Roditi, Union Carbide) made by the Czochralski procedure. This material is transparent in the wavenumber range from 2000 to 50000 cm^{-1} . The optical transparency at the pulsed laser wavelength is not affected by laser irradiation or by changing the temperature.

The optical high-pressure cell is mounted on a metal holder with wooden grip for easy handling and fitting into the sample chamber of the FT-IR spectrometer.

3.1.2 Optical internal cell

The optical internal cell used for the kinetic investigations in bulk polymerizations is depicted in Fig. 3.2. The cell consists of a teflon tube (1) (outer diameter 10 mm, inner diameter 9 mm, length ~ 11 mm) which is closed at each end by a calcium fluoride window (2) (diameter 10 mm, thickness ~ 5 mm, Korth). To facilitate optimal sealing of the cylindrical cell, the sides of the CaF₂ windows are polished using a diamond micrometer suspension (4-8 micron, Mikrodiamant GmbH). CaF₂ was chosen as the window material as it is transparent in the wavenumber range above 1100 cm⁻¹, thus allowing detection in the desired IR region. The sample volume (3) is contained between the two windows. The distance between the CaF₂ windows determines the sample volume and optical path length, which was about 1.2 mm. The internal cell is fitted between the high-pressure windows of the high-pressure cell ((7) in Fig. 3.1) and held in place by a solid teflon spacer.

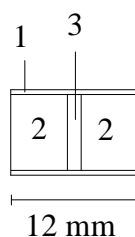


Figure 3.2: *Optical internal cell used for bulk investigations.*

(1) teflon tube, (2) CaF₂ window, (3) sample volume

An excellent survey on the high-pressure techniques described within this section can be found in ref. 2.

3.1.3 Pressure generation and control

For the kinetic investigations in bulk polymerizations, *n*-heptane served as the pressure transmitting medium. The system is pressurized using a manually driven ("syringe" type) pressure generator (volume 12 cm³). The pressure is measured using a high-pressure precision manometer (Class 0.1, 0 - 4 kbar, Wiegand). The pressure generating system is depicted in Fig. 3.3.

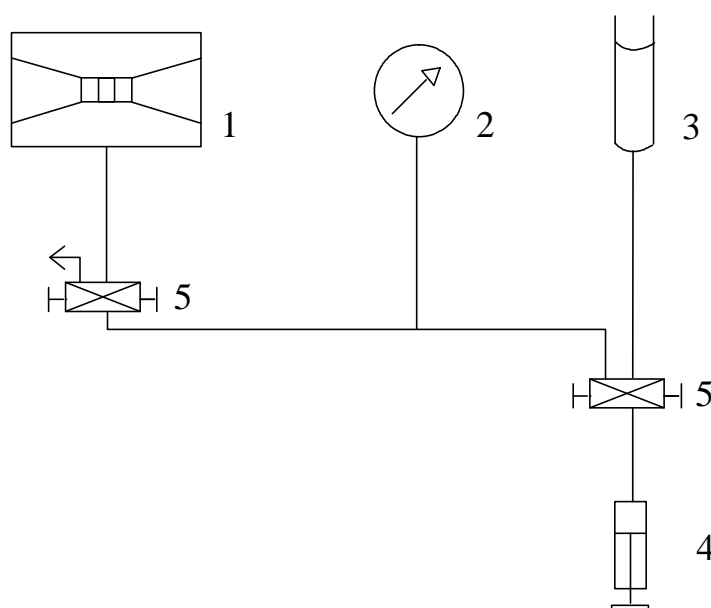


Figure 3.3: Pressure generating system for bulk polymerizations.

- (1) optical high-pressure cell, (2) manometer, (3) pressure medium *n*-heptane, (4) "syringe" type pressure generator, (5) valve

3.1.4 Heating and temperature control

The optical high-pressure cell is heated by two heating jackets. They consist of a brass matrix, into which is embedded a sheathed resistance heating wire (CGE-Asthom). The closely fitting jackets slide over each end of the cell body (see Fig. 3.1 (3)). The temperature is measured via a sheathed thermocouple (Nickel-chromium against nickel, CIA S250, CGE-Alsthom) and regulated by a PID-controller (Eurotherm 815).

3.1.5 Experimental set-up for polymerizations in scCO_2

The experimental set-up used for polymerization in supercritical CO_2 (scCO_2) is described in Fig. 3.4. The major components are a high-pressure liquid chromatography pump (HPLC), a pressure intensifier, an optical high-pressure cell and a mixing autoclave. The autoclave is equipped with a magnetic stir bar and a cooling device that keeps the mixture at 0°C to prevent polymerization. The pressure intensifier is used to compress CO_2 up to a supercritical pressure. The HPLC pump generates a pressure of 200 bar inside the mixing autoclave and keeps the pressure at a constant level of 250 bar while filling the optical high-pressure cell.

The reaction mixture consisting of monomer, photoinitiator and chain-transfer agent is filled into the autoclave and CO₂ is added by means of a syringe pump. The pressure intensifier is used to provide CO₂ at a pressure up to 400 bar. To achieve a homogeneous reaction system in the autoclave, the mixture is vigorously stirred for one hour at 0°C. Before filling, the optical high-pressure cell is purged with CO₂ to remove O₂.

While part of the reaction mixture is transferred from the autoclave into the optical high-pressure cell via the HPLC pump, the pressure is kept at a sufficiently high level to ensure homogeneity of the monomer/photoinitiator/chain-transfer agent/CO₂ mixture. Further compression of the system is achieved by means of the syringe pump. Once the reaction pressure and temperature are reached, the high-pressure cell is disconnected from the pressure branch, inserted into the sample compartment of a Fourier-Transform infrared spectrometer, and subsequently into the laser irradiation assembly.

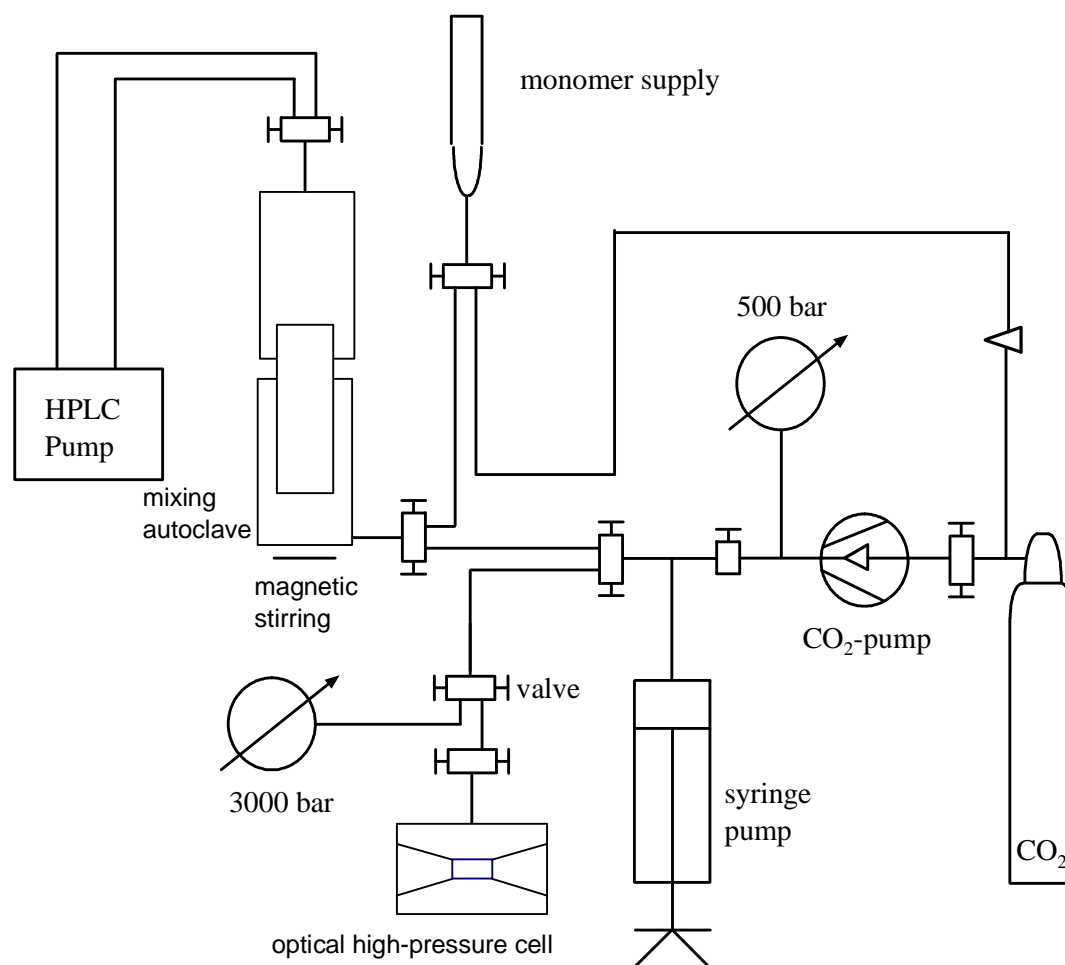


Figure 3.4: Set-up for the preparation of the polymerization mixtures containing scCO₂

3.1.6 FT-IR/NIR spectrometer

Infrared and near infrared spectra were recorded on a Bruker IFS-88 Fourier-Transform spectrometer. To accommodate the heated optical high-pressure cell, the sample chamber of the spectrometer is enlarged (heightened) and fitted with a water-cooled cell holder (to prevent heat transfer). The chamber is purged with compressed air that has been freed from water and carbon dioxide.

The optical configuration of the present work consisted of a halogen source, a silicon-coated calcium fluoride beam splitter, and an InSb detector. This configuration allows for optimal recording in the spectral range of 4000 to 10000 cm^{-1} .

Data acquisition and data processing were performed using the Opus software.

3.1.7 Excimer laser

The polymerizations were carried out with the pulsed-laser polymerization (PLP) technique. The XeF line (351 nm) of an LPX 200 excimer laser (Lambda Physik, EMG 103 MSC) was used to induce initiator decomposition and thus polymerization. The laser repetition rate is of 1 Hz, see section 4.4. The incident laser energy was chosen to be close to 4 mJ per single pulse.

3.1.8 Size-Exclusion Chromatography (SEC)

The molecular weight distributions (MWDs) were determined by size-exclusion chromatography (SEC)³ using a Waters 515 pump, Waters 410 refractive index detector, PSS–SDV–columns with nominal pore sizes of 10^5 , 10^3 and 10^2 Å with tetrahydrofuran (THF) at 30°C as the eluent and toluene as the internal standard. The calibration of the SEC was carried out with PS standards (M_w between 410 and $2 \cdot 10^6$ $\text{g} \cdot \text{mol}^{-1}$) and PMMA standards (M_w between 670 and $2.4 \cdot 10^6$ $\text{g} \cdot \text{mol}^{-1}$) supplied from PSS, Mainz.

A part of the molecular weight distributions analysis was determined at the Polymer Institute in Bratislava, Slovakia by Dr. I. Lacík.

3.1.9 Preparation of the mixtures containing the cobalt-complex

The Co-complex was kept in a glove box because of its air sensitivity. Very careful precautions were taken to prevent any air contact of the complex. All mixtures were prepared in a glove box and deoxygenated by four freeze-pump-thaw cycles. It should also be mentioned that the cobalt-complex was dissolved in the monomer mixture using an ultra-son bad. In case of the bulk polymerizations, the solution was filled into an internal cell (described in section 3.1.2) under argon atmosphere. For the CO₂ polymerizations, the solution was filled in the glove box into a Schlenk flask which was closed with a valve. The CO₂ set-up described in section 3.1.5 was evacuated with a vacuum pump and purged several times with CO₂. A bulb was connected between the CO₂ set-up and the Schlenk flask containing the solution. The equipment was evacuated for ten minutes. Then, the solution contained in the Schlenk flask was filled into the bulb by opening the valve and transferred into the autoclave.

3.2 PLP-SEC Technique

The pulsed laser polymerizations were performed using an optical high-pressure cell as described in section 3.1.1.

In this work, the homo- and copolymerizations of styrene and methyl methacrylate (MMA) were performed in bulk and in supercritical CO₂ (~ 40 wt % scCO₂) at 80°C under pressure with *n*-dodecyl mercaptan, methyl methacrylate trimer, and a cobalt complex as chain-transfer agents. The influence of scCO₂ acting as solvent and the pressure dependence of k_{tr} were studied for these three chain-transfer agents.

For the bulk experiments, monomer, photoinitiator, and chain-transfer agent were mixed and the solution was filled into an internal cell. The internal cell, consisting of a teflon tube and two CaF₂ windows is then inserted into the optical high-pressure cell and the assembly is brought to reaction conditions. The polymerization in scCO₂ is described in the section 3.1.5.

The excimer laser was used to induce initiator decomposition and thus polymerization, as described in section 3.1.7. Samples were initiated by successive laser pulses with a repetition rate of 1 Hz, an incident single pulse energy of about 4 mJ and a photoinitiator concentration of about 0.2 mmol·L⁻¹. After irradiation of the sample, near infrared (NIR) spectra were recorded in order to determine monomer conversion, which is typically below 4 %. The

resulting polymer was then precipitated with an excess of a mixture of methanol with hydroquinone and isolated.

Molecular weight distributions were determined by means of size-exclusion chromatography.

3.3 Determination of C_T and CO_2 -content

As explained in section 4.3, the chain-length distribution method is used to determine the chain-transfer constant, C_T . Eq. 4.17 indicates that C_T is derived from $[\text{CTA}]/[\text{M}]$, thus the monomer concentration under conditions is not required for data evaluation. The ratio $[\text{CTA}]/[\text{M}]$ was calculated from the weighted masses of monomer and chain-transfer agent, and their respective molecular weights:

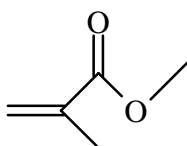
$$\frac{[\text{CTA}]}{[\text{M}]} = \frac{m_{\text{CTA}} / M_{\text{CTA}}}{m_{\text{M}} / M_{\text{M}}}$$

The CO_2 content was calculated from the weighted masses of styrene and MMA and the known amount of CO_2 used for the preparation of the reaction mixture^{4,5}.

3.4 Substances used

3.4.1 Monomers

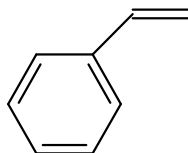
Methyl methacrylate (MMA)



Methyl methacrylate (MMA, 99.5 %, stabilized by 0.02 wt % hydroquinone, Fluka Chemie AG, Buchs, Switzerland) was distilled (using a Vigreux column) under reduced pressure ($\approx 47^\circ\text{C}$, 240 Torr) in the presence of K_2CO_3 to remove the stabilizer. Great care has to be

taken to avoid contamination of the monomer by vacuum grease. Therefore the distillation apparatus is kept sealed by teflon washers.

Styrene



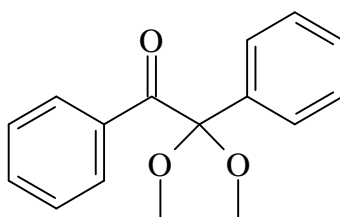
Styrene (99.5%, stabilized with 0.005 % 4-tert-butylbrenzkatechlin, Fluka Chemie AG, Buchs, Switzerland) was washed several times with aqueous NaOH and water to remove the inhibitor, then dried with Na₂SO₄ and distilled under reduced pressure (≈ 45 °C, 20 Torr).

3.4.2 Carbon dioxide

CO₂ (grade 4.5, Messer Griesheim, Krefeld, F.R.G) was used without further purification.

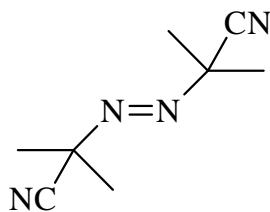
3.4.3 Initiators and inhibitor

2,2-Dimethoxy-2-phenylacetophenone (DMPA)



The photoinitiator DMPA (Aldrich, 99 %) was used as received.

Azo-bis-isobutyronitril (AIBN)



AIBN (Aldrich, 99.5 %) was recrystallized twice from diisopropylether prior to use.

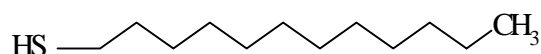
AIBN was used for the polymerization in section 5.2.1.

Hydroquinone

Hydroquinone (Aldrich, >99%) was used as received.

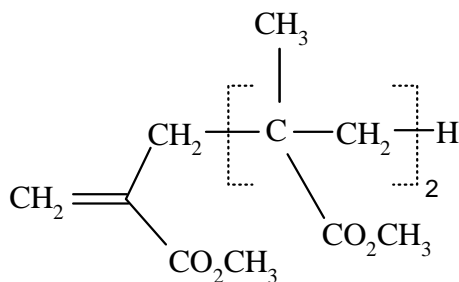
3.4.4 Chain-transfer agents

n-dodecyl mercaptan (DDM)



DDM (97%, Fluka chemie, AG, Buchs, Switzerland) was used as received.

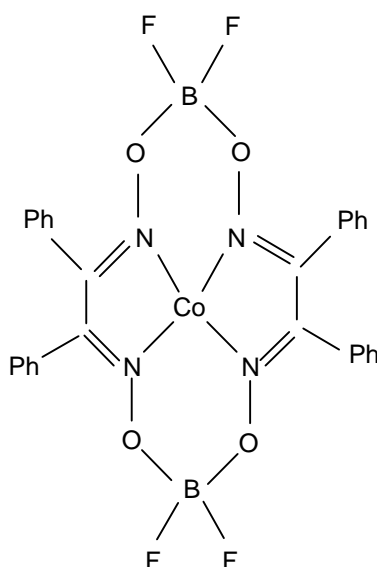
Methyl methacrylate trimer (MMA_t)



A mixture of low molecular weight MMA oligomers was provided by DuPont Performance Coatings. The fraction of MMA trimer was isolated by fractional distillation under reduced

pressure (90°C, 0 Torr). The separation was confirmed by size-exclusion chromatography analysis. The SEC analysis of MMA trimer fractions showed the presence of a small amount of MMA dimer.

bis(methanol) complex of bis(difluoroboryl)diphenylglyoximato cobalt (II) (COPhBF)



The bis(methanol) complex of COPhBF was prepared according to the method described by Bakac et al.⁶, replacing the dimethylglyoxime in the given procedure by diphenylglyoxime:

A suspension of 2 g of cobalt (II) acetate tetrahydrate ($\text{Co}(\text{OAc})_2 \cdot 4\text{H}_2\text{O}$, 99%, Lancaster) and 1.9 g of diphenylglyoxime (dpgH_2 , 99%, Lancaster) in 150 ml of oxygen free diethyl ether was treated with an excess (100 ml) of freshly distilled boron trifluoride diethyl ether complex ($\text{BF}_3 \cdot \text{Et}_2\text{O}$, 99%, Lancaster). The mixture was stirred at room temperature for 6 hours, while the desired product precipitated. The brown solid obtained by filtration was washed several times with ice-cold water and air-dried. The powder obtained was recrystallized from methanol and isolated as the bismethanol adduct.

X-ray Structure of the complex was carried out but was not a success. The crystals obtained were not enough structured for this analysis. Therefore, the purity of the complex was checked by elemental analysis. The composition of the complex ($(\text{CH}_3\text{OH})_2$, COPhBF) was calculated from the relative carbon (C), hydrogen (H) and nitrogen (N) masses. The values found are in a good agreement with the calculated values:

	C %	H %	N %
experimental	51.59	4.12	7.92
calculated	51.64	4.01	8

3.5 FT- IR/NIR spectroscopy

The monomer conversion was controlled by FT-NIR spectroscopy. It has become standard practice^{5,7,8} to use the first overtone of the CH-vibration where the hydrogen atom is linked to a C=C double bond for quantitative analysis of olefinic monomers. This absorbance is located at around 6140 cm⁻¹ for styrene and at 6170 cm⁻¹ for methyl methacrylate. The peak is integrated over the high wavenumber half-band from the band maximum toward higher wavenumbers against a horizontal baseline determined by the absorbance at 6300 cm⁻¹. The monomer conversion X is obtained from the ratio of peak integrals after pulsing Int_p and the integral prior irradiation by the UV laser Int_o : $X = [1 - (Int_p/Int_o)] \cdot 100$.

For a reaction mixture with CO₂ a shift of the peak maximum to higher wavenumbers is observed. For example, a styrene homopolymerization at 800 bar and 80°C with 40 wt % CO₂ shows an absorbance peak at 6144 cm⁻¹, whereas the peak for the homopolymerization in bulk is located at 6137 cm⁻¹. Schmaltz⁵ showed the same trend for the homopolymerization of butyl acrylate (a shift by 11 cm⁻¹ to higher wavenumbers for a polymerization in 40 wt % CO₂ at 11°C and 200 bar).

Fig. 3.5 shows typical NIR spectra of styrene (solid line) and of CO₂ (dotted line) at 80°C and 300 bar. The insert shows the absorbance spectra between 6000 cm⁻¹ and 6500 cm⁻¹. The spectrum of CO₂ exhibits two weak absorptions at around 6325 cm⁻¹ and 6200 cm⁻¹.

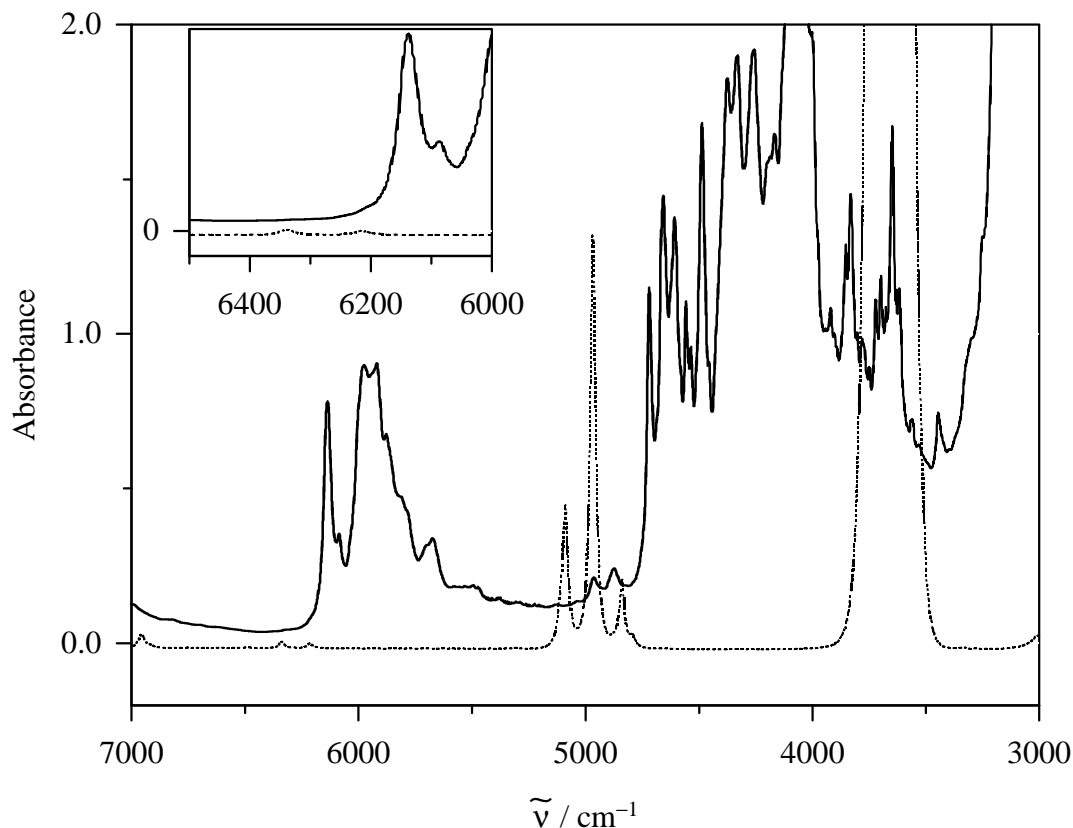


Figure 3.5: NIR spectra of styrene (solid line) and CO₂ (dotted line) at 80°C and 300 bar (optical path length of 0.25 cm).

3.6 Consideration of errors

Measurement of the reaction temperature in the direct vicinity of the optical path of the high-pressure cell is achieved with the sheathed thermocouple to better than ± 0.3 K. The PID controller regulates the temperature within an error of ± 0.2 K. Temperature is assumed to be accurate within ± 0.5 K.

The high-pressure precision manometer of class 0.1 offers an accuracy of ± 0.1 % of the scale limit, resulting in an error of ± 6 bar. Due to the volume contraction associated with the polymerization activity, the pressure in the reacting system is reduced. For example, the pressure decreases at 1000 bar by approximately 50 bar between zero and 100 % of monomer conversion. Therefore, the pressure variation during the experiments can be neglected in this

work, because monomer conversions are around 3 %. The precise description of the technique used to determine this uncertainty can be found in ref. 5.

For the preparation of the solutions, an analysis balance (Sartorius) was used which allows measurement up to 4 decimal places. The absolute error should therefore be ± 0.5 mg. However, the actual error in concentration measurement is greater than this, as the balance is very sensitive to small disturbances. It is estimated that the actual error in the concentration of the comonomer solutions does not exceed 2 % for CTA masses of 50 mg or higher. The polymerizations with the cobalt-complex as catalytic chain-transfer agent require a very small amount of the complex (few mg). To reduce the error several dilutions were carried. The error in the Co-complex concentration is assumed to be less than 5 % for CTA masses of 10 mg or higher.

The error in the CO₂ content is composed of the uncertainties in monomer and CO₂ densities. The error in the styrene⁹ and MMA¹⁰ density at 20°C and 1 bar is about 4 %. The CO₂ content was calculated using the density¹¹ of CO₂ at 10°C and 1 bar considering an error of 3 %.

The error induced by the SEC calibration procedure is given by the uncertainties of the Mark-Houwink coefficients of the copolymers under investigation and by SEC broadening.

3.7 References

1. Poulter, T. C. *Phys. Rev.* **1932**, 40, 860.
2. Buback, M., Hinton, C. in *High-pressure Techniques in Chemistry and Physics - A practical approach*, Holzappel, B. W and Isaacs, N.S, eds., Oxford University Press: Oxford, **1997**.
3. Olaj, O. F.; Bitai, I.; Hinkelmann, F. *Makromol. Chem.* **1987**, 188, 1689.
4. Beuermann, S.; Buback, M.; Schmaltz, C.; Kuchta, F.-D.; *Macromol. Chem. Phys.* **1998**, 199, 1209.
5. C. Schmaltz, *Ph.-D. Thesis* **1997**, Göttingen.
6. Bakac, A.; Brynildson, M. E.; Espenson, J. H. *Inorg. Chem.* **1986**, 25, 4108.
7. Buback, M.; Kuchta, F.-D. *Macromol. Chem. Phys.* **1995**, 198, 1455.
8. Wahl, A.; *Ph.-D. Thesis* **2000**, Göttingen.
9. Kuchta, F.-D. *Ph.-D. Thesis* **1996**, Göttingen.

10. Beuermann, S. *Ph.-D. Thesis* **1993**, Göttingen.
11. Angus, S.; Armstrong, B.; de Renck, K. M. "*International Thermodynamic Tables of the Fluid State Carbon Dioxide*", Pergamon Press, Oxford **1976**.

4. Experimental considerations and choice of reaction conditions

4.1 Selection of temperature and pressure

Polymerizations were performed at 80°C and at pressures between 300 and 1500 bar. The temperature of 80°C was chosen because it is a good compromise of achieving reasonable polymerization rate and avoiding significant contributions of thermally induced decomposition of the initiator. The temperature dependence was not studied, because literature already reported the influence of temperature on C_T . E.g. Hutchinson and co-workers¹ studied the temperature dependence of C_T in homopolymerizations of methacrylates with DDM as chain-transfer agent. Measurement of C_T at ambient pressure and temperature between 20 and 80°C did not show a variation of C_T with temperature. In case of the cobalt-complex as chain-transfer agent, the temperature dependence of styrene and MMA homopolymerization was investigated². The temperature does not significantly influence the chain-transfer constant for MMA, whereas a decrease of C_T was observed for higher temperatures for styrene. A study of C_T in MMA homopolymerization with MMA trimer as CTA has shown only a slight temperature dependence³.

Informations on the pressure dependence of C_T , thus of k_{tr} , are not yet available. Therefore, pressures ranging from 300 to 1500 bar were applied.

4.2 SEC calibration

The molecular weight distributions, which are required for the derivation of C_T , were determined by means of size-exclusion chromatography⁴ (SEC). Thus, the accuracy of C_T is largely governed by the calibration of the SEC system. This is especially important for copolymer analysis. In this section, the methods used for the calibration of the SEC for the homo- and copolymers are presented.

The polystyrene (PS) and poly(methyl methacrylate) (PMMA) samples were directly calibrated against PS standards and PMMA standards, respectively.

For the copolymer samples, two methods may be used to determine the molecular weight by SEC. The first method is based on the knowledge of the Mark-Houwink (MH) constants, a and K , for the copolymers, applying the principle of universal calibration⁵. To apply this technique, the SEC is calibrated against polystyrene. The Mark-Houwink (MH) constants for the copolymers are obtained from a linear interpolation between the MH constants of PMMA and PS considering the fraction of styrene in the copolymer (F_S), as suggested by Coote et al⁶. The MH constants for the different copolymers are listed in Table 4.1.

In this case, the absolute weight average molecular weight, M_w , of the copolymer is directly determined from a single molecular weight distribution analysis.

F_S	a_{copo}	$K_{\text{copo}} 10^5 / \text{dL} \cdot \text{g}^{-1}$
0	0.7190	9.44 ref. 7
0.30	0.7181	10.04
0.55	0.7173	10.52
0.78	0.7166	10.97
1	0.7160	11.40 ref. 8

Table 4.1: Mark-Houwink parameters a and K for copolymers of styrene and MMA.

The second method used to obtain the molecular weight distribution of the copolymer is based on the knowledge of the MH constants of styrene and MMA homopolymers. Since the solution behavior of styrene and MMA homopolymers in tetrahydrofuran is very similar (as evidenced by their MH constants), the following approximations for their copolymers can be made⁹:

$$M_{n,\text{copo}} \approx F_S M_{n,S} + (1-F_S) M_{n,\text{MMA}} \quad (4.1)$$

where $M_{n,\text{copo}}$ is the number average molecular weight of the copolymer, $M_{n,S}$ and $M_{n,\text{MMA}}$ are the number average molecular weights considering the polymer to be PS and PMMA, respectively.

For the determination of the chain-transfer constant via the chain-length distribution method (see section 4.3), the following expression is used:

$$\Lambda_{\text{copo}}^{-1} \approx F_S \cdot \Lambda_S^{-1} + (1-F_S) \cdot \Lambda_{\text{MMA}}^{-1} \quad (4.2)$$

Λ_{copo} is the slope of the $\ln f(M)$ vs M plot for the copolymer, and Λ_S and Λ_{MMA} are the slopes considering the polymer to be PS and PMMA, respectively.

In order to check the validity of the C_T values obtained by using these two methods, some investigations on styrene-MMA copolymerizations were carried out with DDM as chain-transfer agent in bulk at 80°C and 300 bar. Table 4.2 lists the chain-transfer constants obtained with both procedures. Close agreement of the results was obtained, indicating that both methods are equivalent.

F_S	a and K copolymers	a and K homopolymers
0.55	$C_T = 3.34$	$C_T = 3.38$
0.78	$C_T = 8.14$	$C_T = 8.68$

Table 4.2: Chain-transfer constants obtained with both methods of calibration of the SEC.

Both procedures are actually based on the knowledge of homopolymer MH constants and require the same amount of experimental work, the difference lies in the analysis of the size-exclusion chromatograms. A single analysis of the molecular weight distribution is required for the first method, whereas the second method affords two molecular weight analyses. Therefore, in this work the chain-transfer constants for the copolymerization were determined by applying the first method.

4.3 Determination of C_T

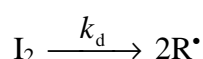
4.3.1 Background

According to the classical mechanism for free-radical polymerization, as shown in the following reaction scheme, a propagating radical R^* , once generated, has three options to

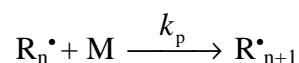
react. It may propagate, terminate in a radical-radical reaction, or undergo a chain-transfer reaction.

Chain transfer involves the reaction of a propagating chain R_n^\bullet with a transfer agent to terminate one polymer chain and produce a new radical X^\bullet , which initiates another chain XR_1^\bullet . The substrate for the chain transfer may be a chain-transfer agent (X), or the initiator (I_2), the monomer (M), or some other component of the polymerization medium.

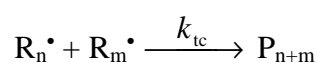
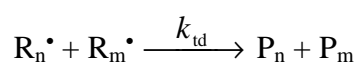
Initiation



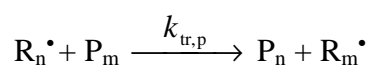
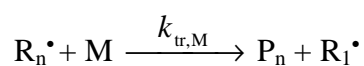
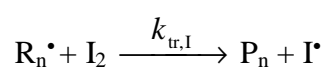
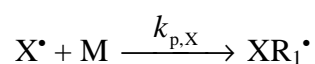
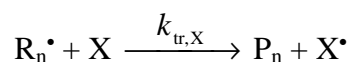
Propagation



Termination



Transfer



k_d and k_p are the decomposition and propagation rate coefficients, respectively. k_{td} and k_{tc} are the termination rate coefficients for termination by disproportionation and by combination, respectively. $k_{tr,X}$, $k_{tr,M}$, $k_{tr,I}$ and $k_{tr,p}$ are the transfer rate coefficients to CTA, initiator, monomer and polymer, respectively.

At any given instant of the polymerization process, the probability of propagation S , is simply the rate of propagation divided by the sum of reaction rates of the entire set of potential reactions of the propagating radical, as follow:

$$S = R_p / (R_p + R_{tr} + R_t) \quad (4.3)$$

where,

$$R_p = k_p[M][R_n\cdot] \quad (4.4)$$

$$R_{tr} = k_{tr,X}[CTA][R_n\cdot] + k_{tr,I}[I][R_n\cdot] + k_{tr,M}[M][R_n\cdot] + k_{tr,P}[P_m][R_n\cdot] \quad (4.5)$$

$$R_t = 2 \cdot k_t[R_n\cdot]^2 \quad (4.6)$$

Replacing the rate expressions into Eq 4.3 yields:

$$S = \frac{k_p[M][R_n\cdot]}{k_p[M][R_n\cdot] + k_{tr,X}[CTA][R_n\cdot] + k_{tr,I}[I][R_n\cdot] + k_{tr,M}[M][R_n\cdot] + k_{tr,P}[P_m][R_n\cdot] + 2 \cdot k_t[R_n\cdot]^2} \quad (4.7)$$

which may be written as:

$$S = \frac{1}{1 + C_T \frac{[CTA]}{[M]} + C_I \frac{[I]}{[M]} + C_M + C_P \frac{[P_m]}{[M]} + \frac{2 \cdot k_t[R_n\cdot]}{k_p[M]}} \quad (4.8)$$

where C_T , C_M , C_I , C_P are the transfer constants for transfer to the chain-transfer agent, to monomer, to initiator, and to polymer, respectively.

$$\frac{1}{S} = 1 + C_T \frac{[CTA]}{[M]} + C_I \frac{[I]}{[M]} + C_M + C_P \frac{[P_m]}{[M]} + \frac{2 \cdot k_t[R_n\cdot]}{k_p[M]} \quad (4.9)$$

The probability that a chain will propagate and terminate to yield a polymer molecule of length i is given by the product of the probability of individual propagation steps and the probability of termination of the chain of length i . If termination is independent of chain length, this can be expressed as the probability of propagation raised to a power of $(i-1)$ multiplied by the probability of termination $(1-S)$. Thus, the chain-length distribution is:

$$P_i = (1-S) S^{i-1} \quad (4.10)$$

This is the well known Schulz-Flory¹⁰ most probable distribution, for which the following equations hold:

$$DP_n = \frac{S}{1-S} \quad (4.11)$$

$$S = \frac{DP_n}{1+DP_n} \quad (4.12)$$

Substitution of S in Eq. 4.9 gives the Mayo equation¹¹ (Eq. 4.13):

$$\frac{1}{DP_n} = C_T \frac{[\text{CTA}]}{[\text{M}]} + C_I \frac{[\text{I}]}{[\text{M}]} + C_M + C_P \frac{[\text{P}_m]}{[\text{M}]} + \frac{2 \cdot k_t [\text{R}_n \cdot]}{k_p [\text{M}]} \quad (4.13)$$

In the absence of an added chain-transfer agent the number average degree of polymerization is given by Eq. 4.14.

$$\frac{1}{DP_{n_0}} = C_I \frac{[\text{I}]}{[\text{M}]} + C_M + C_P \frac{[\text{P}_m]}{[\text{M}]} + \frac{2 \cdot k_t [\text{R}_n \cdot]}{k_p [\text{M}]} \quad (4.14)$$

Comparison of Eqs 4.13 and 4.14 shows that:

$$\frac{1}{DP_n} = \frac{1}{DP_{n_0}} + C_T \frac{[\text{CTA}]}{[\text{M}]} \quad (4.15)$$

The chain-transfer constant, C_T , is defined as the ratio of $k_{tr,X}$ and k_p .

The higher C_T is, the lower is the concentration of chain-transfer agent that is required for a particular molecular weight reduction¹². This effect on polymer molecular weight is quantitatively given by the Mayo-equation¹¹ which expresses the reciprocal of the number average degree of polymerization, DP_n , as a function of the rates of chain growth and chain stopping^{11,12} (Eq. 4.13).

There are two possible procedures for determining C_T data, the Mayo method and the chain-length distribution (CLD) method.

4.3.1.1 Mayo method

The usually applied procedure for measuring chain-transfer constants proceeds via the determination of the average degree of polymerization for a range of $[\text{CTA}]/[\text{M}]$ values and plotting the data as DP_n^{-1} vs $[\text{CTA}]/[\text{M}]$, i.e., the so called Mayo plot. The value of C_T is then determined as the slope of the straight line in the results. This procedure assumes that the product $k_t[\text{R}_n \cdot]$ is independent of the variation of $[\text{CTA}]/[\text{M}]$. However, if termination is chain

length dependent, then $k_t[\text{R}_n^\bullet]$ will vary with $[\text{CTA}]/[\text{M}]$ as the average degree of polymerization varies and hence the frequency of termination varies, even if the initiator concentration remains constant. This implies that the last term on the right hand side of Eq. 4.13 is generally not a constant and so the Mayo plot needs not to be linear. In principle, this is a weakness of the Mayo method for determining C_T . However, in practice, this effect does not seem to be significant, which suggests that, in system with added chain-transfer agent, the last term of the right hand side of Eq 4.13 generally makes a negligible contribution to DP_n^{-1} .

There is two ways to use the Mayo equation for determining C_T . The number average degree of polymerization can be obtained directly from the number average molecular weight, M_n , by dividing M_n by monomer molecular weight, M_0 . Although, this procedure is in principle the only correct way to determine DP_n from a molecular weight distribution, in practice this procedure has an important shortcoming. The number average molecular weight is very sensitive to errors in the analysis of the size-exclusion chromatogram (e.g., peak and baseline selection), and it often leads to scattered results¹³. This is especially true for low molecular weight polymers. An alternative procedure for obtaining DP_n from the molecular weight distribution is from the weight average molecular weight¹⁴, M_w . In a chain transfer dominated system, M_w is equal to $2M_n$ (except for very low molecular weights), and hence $DP_n = M_w/(2M_0)$ for such system. The use of M_w is often more reliable because M_w is much less sensitive to errors in the analysis of the size-exclusion chromatogram.

4.3.1.2 Chain-Length Distribution method

A more recent procedure for determining C_T has been developed by Gilbert and co-workers^{15,16,17}. It is called the **Chain Length Distribution (CLD)** method. This procedure is based upon taking the high molecular weight slope of the number molecular weight distribution, $f(M)$, plotted as $\ln f(M)$ vs. M . The high molecular weight slope of a line on this plot, denoted as Λ , is related to the kinetic parameters as follows:

$$\Lambda = \lim_{M \rightarrow \infty} \frac{d \ln f(M)}{d M} = - \left(\frac{2 \cdot k_t [\text{R}_n^\bullet]}{k_p [\text{M}]} + C_M + C_I + C_P + C_T \frac{[\text{CTA}]}{[\text{M}]} \right) \frac{1}{M_0} \quad (4.16)$$

and,

$$\Lambda M_0 = \frac{d \ln f(n)}{d n} = a - C_T \frac{[\text{CTA}]}{[\text{M}]} \quad (4.17)$$

where, a includes the contributions of all other chain stopping events.

According to Eq. 4.17, $-C_T$ is equal to the slope of a straight line of the CLD plot, which refers to the plot of $\Lambda \cdot M_0$ vs $[CTA] / [M]$.

Recently, a discussion has started about the adequate molecular weight region from which Λ should be determined¹³, i.e., whether the slope should be determined in the high molecular weight region (Λ_{high} : between A and B), which is the correct theoretical limit¹⁵, or in the region of the peak molecular weight (Λ_{peak} : starting near M_w and ending at around M_z), which suffers less from experimental uncertainties¹³. These molecular weight regions are illustrated in Fig. 4.1. In a previous study Davis and co-workers⁹ found that Λ_{peak} results compare most favorably with the $M_w/2$ results of the Mayo method, and therefore concluded that this should be the preferred option, which has been also confirmed by several other authors^{21,2}. The choice of the peak molecular weight region is also justified by results obtained by Moad and Moad¹³, who argue that this high molecular weight region may be less affected by deviations in the baseline. In principle, C_T can be evaluated from any part of the \ln CLD plot.

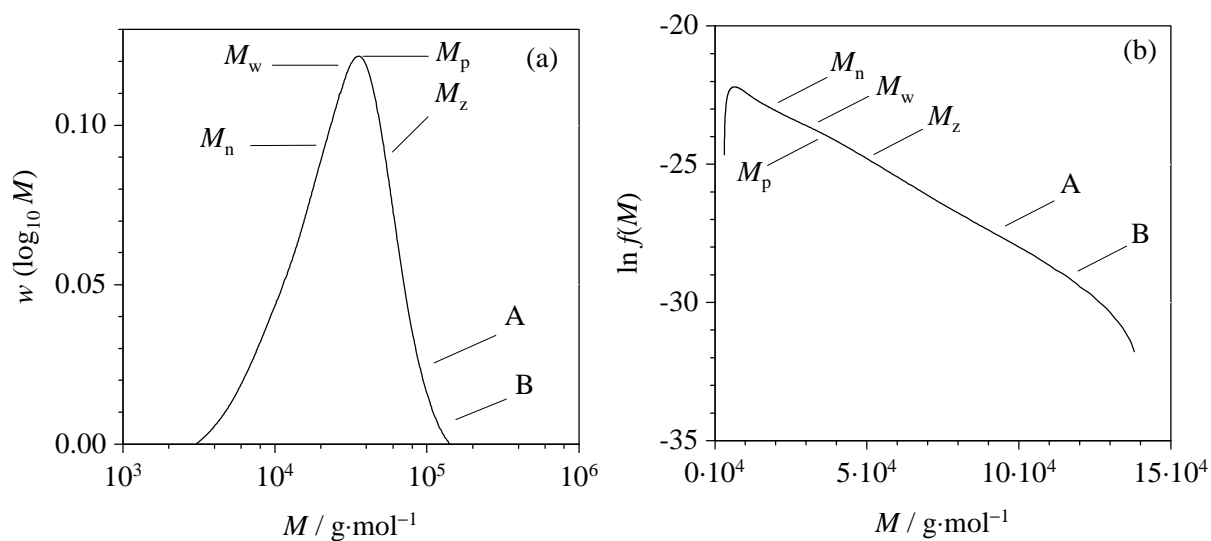


Figure 4.1: Typical molecular weight distribution plotted as (a) $w(\log M)$ vs M and (b) $\ln f(M)$ vs M . The positions of the most important molecular weight averages used for the determination of C_T are indicated.

4.3.2 Comparison of both procedures

4.3.2.1 Theoretical comparison

The formats of Eqs 4.15 and 4.17 for determination of C_T according to the Mayo method and to the CLD method, respectively, are very similar. However, calculation of C_T via the slope of the MWD (CLD method) provides a more robust estimate, since it is less dependent on the tails of the distribution. Since in each type of plot the ordinates are different, DP_n^{-1} for the Mayo plot and ΛM_0 for the CLD plot, one might get the impression that the two procedures for determining C_T are different. With respect to the required experimental material, both procedures are identical, only the analysis of the size-exclusion chromatograms is different.

It is now generally accepted that the rate coefficient of termination in radical polymerization is chain-length dependent. Bamford¹⁸ and Olaj et al.¹⁹ have considered the effect of a chain-length dependence of the termination rate coefficient on the applicability of the Mayo method. They concluded that transfer constants should be slightly overestimated by the Mayo method. Gilbert and co-workers^{15,16} have indicated that by examining the high molecular weight tail of the distribution, the effects of some termination by combination and the chain-length dependence of propagation and termination rate constants on the slope of a CLD plot should be negligible.

As explained before, both the Mayo and the CLD methods can be used in two different ways to determine the chain-transfer constant: Using M_n or M_w for the Mayo method and Λ_{peak} or Λ_{high} for the CLD. In general, M_w and Λ_{peak} are used^{17,9}. Indeed, it has been previously shown^{9,20} that in cases in which significant curvature occurs, the results based upon the Mayo procedure using M_w agree very well with the results obtained from the CLD procedure using Λ_{peak} . As already mentioned, the CLD method is less sensitive to the presence of artefacts in the GPC traces caused by experimental noise or poor baseline selection. One major benefit of the CLD method is that the requisite information can be obtained by analyzing a small segment of the chain-length distribution. Thus problems, that may arise from an incomplete separation of low molecular weight material, e.g. residual monomer, which affects M_n and M_w are excluded or are minimized. In addition, problems resulting from difficulties in the accurate analysis of the high molecular weight side of the MWD, or due to spontaneous polymerization, or due to a lack of reliable calibration standards, or due to branching of polymer as a result of transfer to polymer reactions, may be reduced or even eliminated. In these cases, the Mayo method may not be applicable since M_n and M_w values are affected:

This was the case in this work for styrene homopolymerizations with DDM as CTA (for comparison see section 5.1). Moreover, the C_T values determined with the CLD method, via Λ_{peak} and Λ_{high} , are seen to be very close to each other in most experiments performed in this work (more details in section 4.3.3).

4.3.2.2 Experimental comparison

As explained in section 4.3.2.1, theoretically both methods may be used, however it seems that the CLD method is more robust. In the following section, both procedures are compared via the calculated C_T values. The weight average molecular weight, M_w , was used for the Mayo method and the peak region, Λ_{peak} , for the CLD method for the reasons already explained.

The chain-transfer constants determined are listed in Table 4.3, as example for the copolymerizations of styrene and MMA ($f_S = 0.2$ and 0.8) with DDM and CPhBF at 300 bar and 80°C .

		C_T CLD (Λ_{peak})		C_T Mayo (M_w)	
CTA		bulk	scCO ₂	bulk	scCO ₂
$f_S = 0.2$	DDM	2.03	2.10	2.10	1.90
	CPhBF	$42.2 \cdot 10^2$	$125 \cdot 10^2$	$39.4 \cdot 10^2$	$111 \cdot 10^2$
$f_S = 0.8$	DDM	8.14	8.98	7.82	7.75
	CPhBF	$9.34 \cdot 10^2$	$10.1 \cdot 10^2$	$9.73 \cdot 10^2$	$9.85 \cdot 10^2$

Table 4.3: Chain-transfer constants, C_T , determined via the Mayo and the CLD methods for the copolymerization of styrene and MMA at 80°C and 300 bar with DDM and CPhBF as chain-transfer agents.

The C_T values obtained via the CLD method are mostly slightly higher than the C_T values obtained using the Mayo method. The difference is not significant, less than 15 %, and close to uncertainties observed in the literature^{9,21,22}. Madruga et al.²¹ determined C_T values for the homopolymerization of styrene at 50°C in bulk using the Mayo and CLD methods. The reported values are 12.6 and 15.1, respectively. This difference is larger than the one reported

here. Some literature data show a larger difference of the C_T values ($C_{T, \text{Mayo}} = 550$ and $C_{T, \text{CLD}} = 1.5 \cdot 10^3$ for the same system²³). The C_T values which are listed in Appendices 2, 3, and 4 show also a good agreement between both methods.

This section has shown that both procedures are almost equivalent. In this thesis, the analysis technique suggested by Gilbert and co-workers, the so-called CLD method, was preferentially used for the determination of C_T in section 5.

4.3.3 CLD method

For all experiments performed in this work, the CLD procedure was used to determine C_T via Λ_{peak} and via Λ_{high} . The results obtained for styrene and MMA homopolymerizations at 300 bar and 80°C with DDM as CTA are shown in Fig. 4.2.

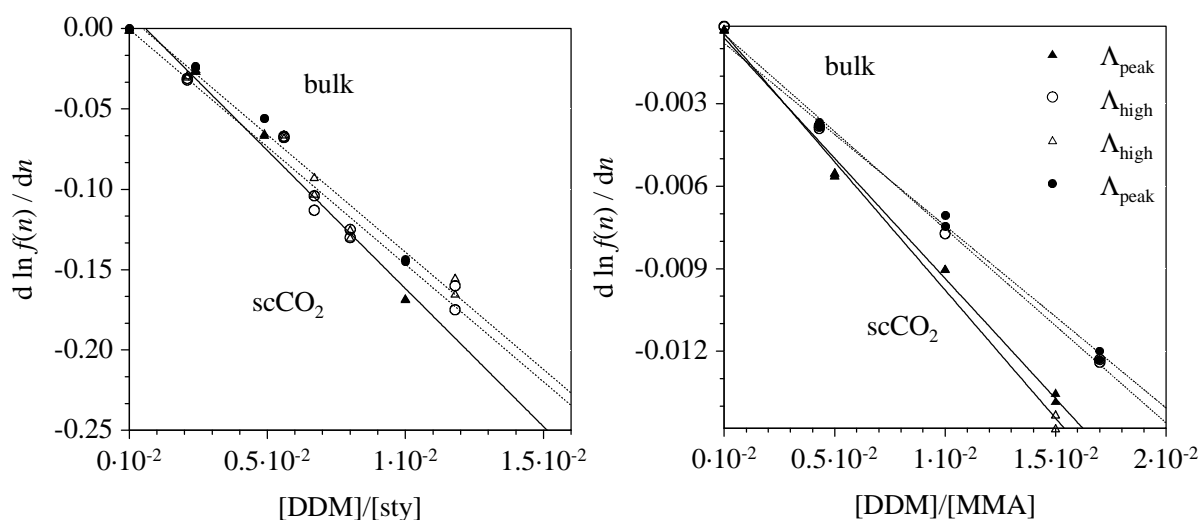


Figure 4.2: CLD plots for DDM as CTA. The left hand side pictures the CLD plots of styrene homopolymerizations, on the right hand side are shown the CLD plots of MMA homopolymerizations.

It is clearly seen that the slopes, corresponding to $-C_T$, are the same in both cases, using the peak and the high molecular weight regions for analysis. The values of C_T , which are summarized in Table 4.4 are independent of the considered region. Since there seems to be no convincing argument for an a priori choice of a particular region, the peak region was used to determine C_T in section 5. However, for all systems it was verified that both C_T (Λ_{high} and Λ_{peak}) are in good agreement.

C _T from CLD				
	Λ _{high}		Λ _{peak}	
	bulk	scCO ₂	bulk	scCO ₂
MMA	0.681	0.801	0.702	0.811
styrene	14.9	15.8	14.6	16.3

Table 4.4: C_T values obtained in styrene and MMA homopolymerizations at 300 bar and 80°C using the CLD method.

The good agreement of C_T obtained by the two approaches is not surprising. Upon examination of Fig. 4.1b it can be seen that there is no curvature over the complete range of molecular weights. The same observation is made for most of the samples investigated in this thesis.

4.4 Conditions for the determination of C_T by PLP

Initiation by PLP has been shown to be a reliable technique for the determination of k_p if certain criteria are met. The advantages of PLP, e.g, the easy variability of the radical concentration in the polymerizing system and short reaction time, should also apply to the measurement of k_{tr}^{24,25,26,27}.

The limitations for the estimation of C_T are examined and criteria are defined for the use of PLP in chain-transfer studies.

As explained in the preceding section, the method used for the determination of chain-transfer constants in this work is the CLD¹⁵ method. It is based on the following equation:

$$\frac{d \ln f(n)}{dn} = a - \left(\frac{k_{tr,X}}{k_p} \right) \frac{[CTA]}{[M]} \quad (4.18)$$

The best estimate for k_{tr,X} / k_p (C_T) is obtained when the contributions from other chain-stopping mechanisms are small compared to that from the chain-transfer mechanism under consideration. In other words, the intercept value *a* should be close to zero. In this work,

experimental conditions are chosen such that chain transfer to chain-transfer agent dominates the MWD.

It is necessary to determine under which conditions it is feasible to combine PLP, inherently a non-steady-state process, with a procedure developed assuming steady state conditions.

The PLP technique involves the exposure of a monomer/photoinitiator system to laser flashes, which generate a burst of initiator radicals in a controlled and periodic fashion. Between two flashes, which occur every t_0 seconds, the radical concentration in the system decreases due to radical-radical termination:

$$d[\mathbf{R}\cdot] / dt = - 2 \cdot k_t [\mathbf{R}\cdot]^2 \quad x \cdot t_0 < t < (x + 1) \cdot t_0 \quad (4.19)$$

where x is the number of pulses.

Integration of this equation leads to an explicit expression for the variation of the total radical concentration with time:

$$[\mathbf{R}\cdot](t) = \frac{[\mathbf{R}\cdot]^{\max}}{1 + k_t [\mathbf{R}\cdot]^{\max} (t - x \cdot t_0)} \quad (4.20)$$

where, $[\mathbf{R}\cdot]^{\max}$ is the radical concentration immediately following the x th laser pulse.

In PLP, a fraction of the growing polymer radicals survives without undergoing a termination or transfer event until the next pulse of radicals is generated t_0 seconds later. A typical radical concentration-time profile is shown in Fig. 4.3.

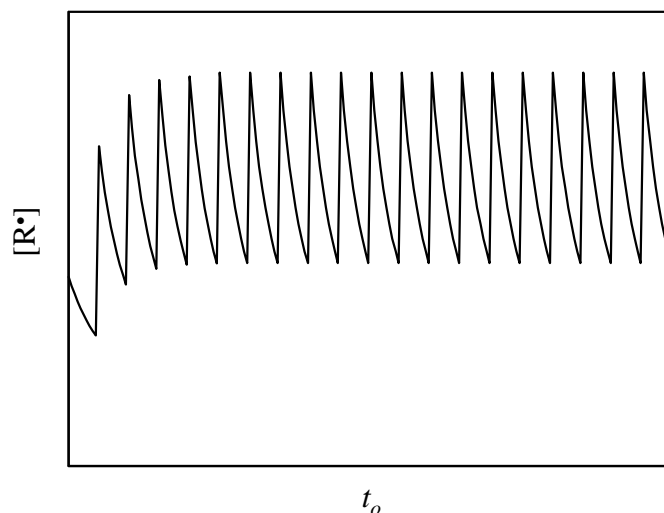


Figure 4.3: Typical radical concentration-time profile for the determination of k_p .

The conditions required for the study of chain transfer are very different. It is necessary to design the experiments such that the majority of radicals undergoes a chain-transfer event before the next pulse arrives. Moreover, the calculation of k_{tr} / k_p from pulsed laser generated polymer is valid only as long as chain transfer is the molecular weight controlling mechanism. Fig. 4.4 shows a typical radical concentration time profile for the case of a transfer dominated system:

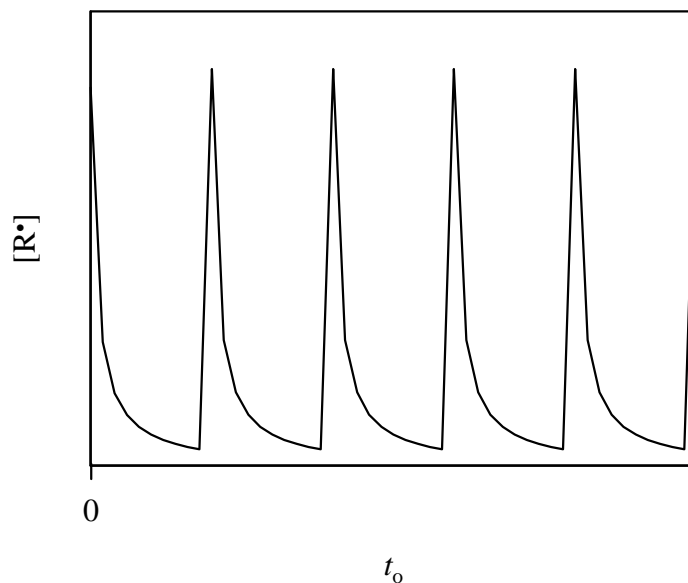


Figure 4.4: Typical radical concentration-time profile for transfer dominated system.

Two conditions must be met in order to get a transfer dominated MWD and to measure transfer rates by PLP.

1) Chain-transfer events must dominate termination events:

$$2 \cdot k_t [R^\bullet] \ll k_{tr,X} [CTA] \quad (4.21)$$

where $[R^\bullet]$ varies with time according to Eq. 4.20.

Transfer is favored if:

- (a) the time between pulses is increased, allowing the radical concentration to decline to lower values,
- (b) the radical concentration generated per pulse is lowered,
- (c) the rate of chain-transfer events is increased.

2) Transfer should have taken place before the arrival of the next pulse:

After each pulse, the total radical concentration in the system increases up to a value of $[R\cdot]^{\max}$. At that time most radicals from the previous pulse will have undergone at least one chain-transfer event in t_0 seconds. Mathematically, this second condition is expressed by:

$$1 / t_0 \ll k_{tr,X} \cdot [CTA] \quad (4.22)$$

Again this condition is favored by increasing $k_{tr,X} \cdot [CTA]$ or increasing t_0 .

Eq. 4.22 provides a more easily observable criterion than Eq. 4.21; The above given condition is met if the MWD for the monomer/chain-transfer agent system is shifted to lower molecular weights compared to a MWD from a termination dominated system without chain-transfer agent. Note that establishing Eq. 4.22 as a criterion for analyzing PLP results for chain transfer implies that k_p and k_{tr} cannot be estimated¹ from a single experiment*. To ensure that the criterion of Eq. 4.21 is satisfied, it is necessary to perform experiments to ensure that the results are not affected by the level of termination in the system.

This highlights the limitations of PLP as a tool for measuring k_{tr} . PLP offers advantages for studying chain transfer in systems for which the transfer can easily made to be the dominant event.

Hutchinson and co-workers¹ proved experimentally that reproducible results are obtained without excessive monomer purification. Although, the radical concentration is high immediately after a pulse, it is lower toward the end of the interval between pulses. Thus the effect of termination reactions between radicals and impurities (e.g. O_2) on the chain transfer dominated part of the MWD is minimized by the CLD technique. It is of importance to verify that experimental conditions are chosen to create transfer dominated system.

In this work the conditions required were as follow:

- (a) a very low repetition rate of laser pulses, 1 Hz
- (b) low initiator concentration for controlling the level of termination
- (c) variation of CTA concentration should be reflected in a systematic change in MW

* Although, by a special choice of the laser pulse pattern, k_p and k_{tr} may be determined from a single experiment²⁸.

Different means of controlling the level of termination in PLP experiments were tested. The condition (c) for each polymerization was checked and described in section 5. The condition (b) is developed for a styrene homopolymerization system below.

The MWDs, obtained for styrene homopolymerization in bulk at 80°C and 300 bar, for three different concentrations of the photoinitiator ($[DMPA] = 0.2, 1$ and $2 \text{ mmol}\cdot\text{L}^{-1}$) and with *n*-dodecyl mercaptan as chain-transfer agent, are plotted in Fig. 4.5.

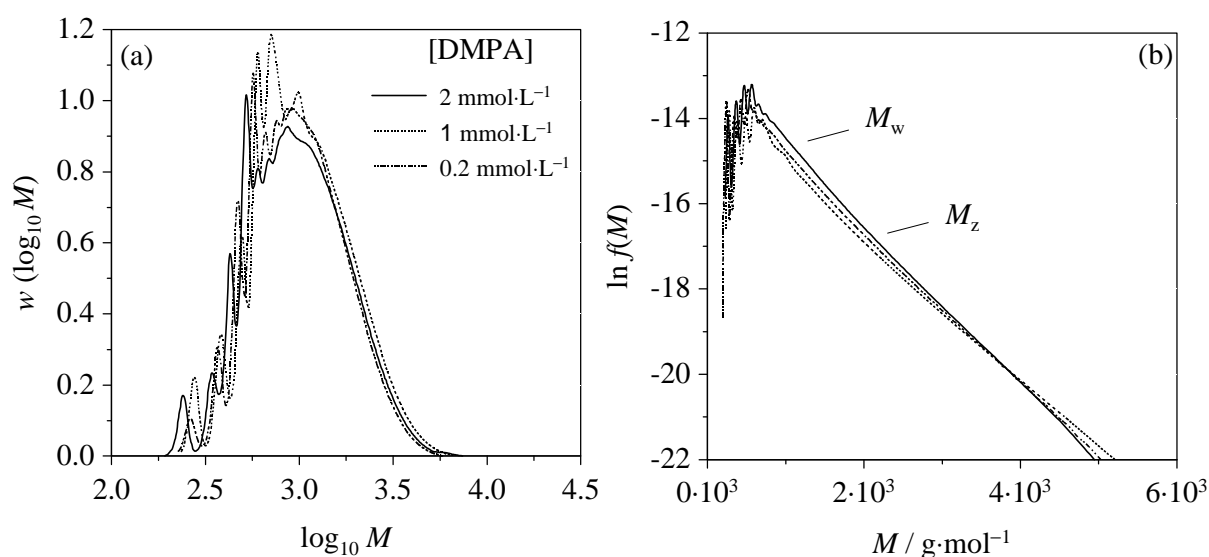


Figure 4.5: Polystyrene produced at 80°C and 300 bar, with 3 vol % of DDM and varying amount of the photoinitiator DMPA: (a) molecular weight distributions obtained from SEC; (b) number MWD on a semilog scale.

It can be immediately seen from the GPC traces (Fig. 4.5a) that the concentration of DMPA has the most significant effect on the styrene samples on the low molecular weight side. On the high MW side, the distributions are more similar. This can be understood by considering the periodic radical concentration generated per pulse. Immediately following a laser pulse, radical-radical termination of the very short chains makes a large contribution to the total number of polymer chains being formed. Thus, the low molecular weight side of the distribution is the most affected by the concentration of DMPA. As the remaining living chains grow, the radical concentration in the system is much reduced. These chains have a high probability of being terminated through transfer with DDM; The high MWD side of the

distribution is less affected by [DMPA]. This fact is very important since it is from the slope of this high MWD side that k_{tr}/k_p is estimated.

Fig. 4.5b shows a plot of the distribution transformed to a semilog number scale. A slight initiator effect can be seen from the slopes but the high molecular weight side and particularly the slope between M_w and M_z used for the determination of C_T (see section 4.3) are not really affected. Indeed, the slopes obtained for the concentration of DMPA of 0.2, 1, and 2 mmol·L⁻¹ are $1.7 \cdot 10^{-2}$, $1.8 \cdot 10^{-2}$, $1.75 \cdot 10^{-2}$, respectively. It is obvious from theory¹ that better estimates for C_T will be obtained if radical concentration (and thus concentration of DMPA) is kept low. Therefore, all the experiments in this work were carried out at a photoinitiator concentration of 0.2 mmol·L⁻¹.

4.5 Consideration of errors

The errors in the chain-transfer rate coefficient, k_{tr} , and in the chain-transfer constant, C_T , which are determined by the PLP-SEC technique described within this section, are difficult to estimate and depend on the chain-transfer agent used. The error in C_T was estimated using the chain-length distribution (CLD) technique, as described in section 4.3. In order to determine the uncertainty of the slope of the number of distribution plot, $\ln f(M)$ vs M , the slope was determined from several molecular weight ranges, with M_w always being the lower limit. The error in C_T is estimated to be about 10, 20 and 10 % with *n*-dodecyl mercaptan, the cobalt-complex and MMA trimer as chain-transfer agents, respectively.

In summary, the error of the k_{tr}/k_p data is composed of several contributions: The error in the masses of the monomer mixture and chain-transfer agent, the error resulting from the ambiguity in selection of the molecular weight region for the semilog $\ln f(M)$ vs M plot and the error of the SEC calibration procedure. These errors sum up to a total of ± 30 % for the chain-transfer rate constant of this work. For the homopolymerization systems, the error is reduced to ± 25 %, as direct calibration using PMMA or PS standards may be carried out.

4.6 References

1. Hutchinson, R. A.; Paquet, D. A.; Mc Minn, J. H. *Macromolecules* **1995**, 28, 5655.
2. Kukulj, D.; Davis, T. P. *Macromol. Chem. Phys.* **1998**, 199, 1697.
3. Moad, C. L.; Moad, G.; Rizzardo, E.; Thang, S. H. *Macromolecules* **1996**, 29, 7717.
4. Olaj, O. F.; Bitai, I.; Hinkelmann, F. *Makromol. Chem.* **1987**, 188, 1689.
5. Grubisic, Z.; Rempp, P.; Benoit, H. A. *J. Polym. Sci., Polym. Lett.* **1967**, 5, 753.
6. Coote, J. M.; Zammit, M. D.; Willett, G. D.; Davis, T. P. *Macromolecules* **1997**, 30, 8182.
7. Beuermann, S.; Paquet, D. A.; McMinn, Jr. J. H.; Hutchinson, R. A. *Macromolecules* **1996**, 29, 4206.
8. Beuermann, S.; Paquet, D. A.; McMinn, Jr. J. H.; Hutchinson, R. A.; Jackson, C. *Ind. Eng. Chem. Res.* **1997**, 36, 1103.
9. Heuts, J. p. A.; Kukulj, D.; Foster, D. J.; Davis, T. P. *Macromolecules* **1998**, 31, 2894.
10. Flory, P. J. *Principles of Polymer Chemistry*, Cornell University Press, Ithaca, NY, **1953**, p 317.
11. Mayo, F. R. *J. Am. Chem. Soc* **1943**, 65, 2324.
12. Moad, G.; Solomon, D. H. *The chemistry of Free Radical Polymerization*; Pergamon: Oxford, **1995**.
13. Moad, G.; Moad, C. *Macromolecules* **1996**, 29, 7727.
14. Sticker, M.; Meyerhoff, G. *Makromol. Chem.* **1978**, 179, 2729.
15. Clay, P. A.; Gilbert, R. G. *Macromolecules* **1995**, 28, 552.
16. Whang, B. C. Y.; Ballard, M. J.; Napper, D. H.; Gilbert, R. G. *Aust. J. Chem.* **1991**, 44, 1133.
17. Heuts, J. P. A.; Clay, P. A.; Christie, D. I.; Piton, M., C.; Hutovic, J., Kable, S. H.; Gilbert, R. G. *Prog. Pac. Polym. Sci. Proc.* **1994**, 3, 203.
18. Bamford, C. H. *Eur. Polym. J.* **1990**, 26, 1245.
19. Olaj, O. F.; Zifferer, G.; Gleixner, G. *Macromolecules* **1987**, 20, 839.
20. Heuts, J. P. A.; Foster, D. J.; Davis, T. P.; Yamada, B.; Yamazoe, H.; Azukizawa, M. *Macromolecules* **1999**, 32, 2511.
21. de la Fuente, J. L.; Madruga, E. L. *J. Polym. Sci., Polym. Chem.* **1998**, 36, 2913.
22. de la Fuente, J. L.; Madruga, E. L. *J. Polym. Sci., Polym. Chem.* **2000**, 38, 170.
23. Mang, A. S.; Dokolas, P.; Holmes, A. B. *Am. Chem. Soc. Org. Lett.* **1999**, 1, 125.

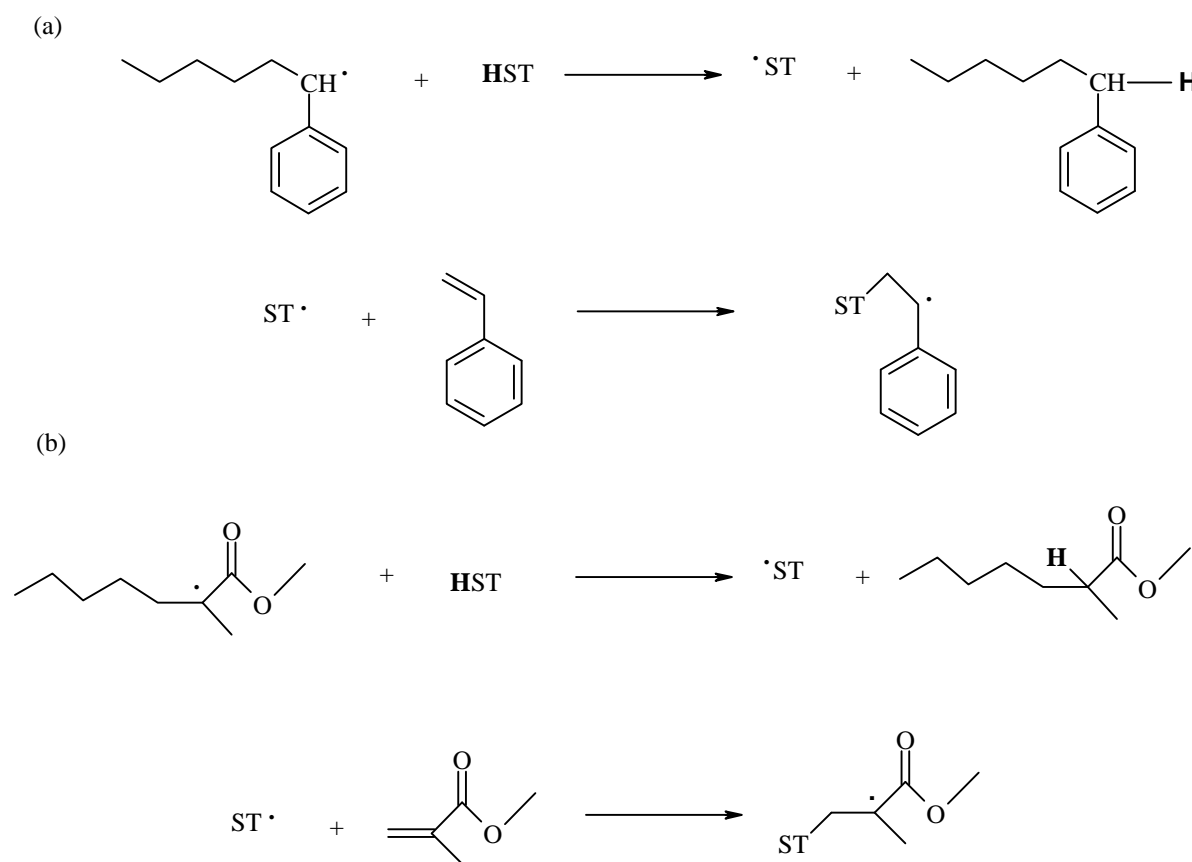
24. Olaj, O. F.; Bitai, I. *Angew. Makromol. Chem.* **1987**, 155, 177.
25. Buback, M.; Gilbert, R. G.; Russell, G. T.; Hill, D. J. T.; Moad, G.; O'Driscoll, K. F.; Shen, J.; Winnik, M. A. *J. Polym. Sci., Polym. Chem. Edn.* **1992**, 30, 851.
26. Beuermann, S.; Buback, M.; Schmaltz, C.; Kuchta, F.-D. *Macromol. Chem. Phys.* **1998**, 199, 1209.
27. Buback, M.; Hippler, H.; Schweer, J.; Vögele, H.-P. *Makromol. Chem. Rapid. Commun.* **1986**, 7, 261.
28. Buback, M.; Laemmel, R. A. *Macromol. Theory Simul.* **1997**, 6, 145.

5. Results and discussions

5.1 DDM as chain-transfer agent

The use of mercaptans as chain-transfer agents has proven to be an effective method to reduce the molecular weight. In this section, the interest was focused on the *n*-dodecyl mercaptan (DDM). The mechanism of the chain-transfer reaction is illustrated in scheme 5.1 for styrene (a) and MMA (b) homopolymerizations. The mercaptan HST acts through a hydrogen transfer reaction with the radical chain, creating a dead polymer chain and a thiyl radical ST^\bullet which initiates a new chain.

The terminal group of the polymer obtained consists of a saturated carbon-carbon bond, as described by scheme 5.1. The thiyl group is the initiator and hence a possible functionality to be introduced as an endgroup needs to be present in the chain-transfer agent.



Scheme 5.1: Reaction scheme for the chain-transfer of DDM in homopolymerization of styrene (a) and MMA (b). HST represents DDM.

In the literature, only few reports^{1,2,3} deal with DDM as chain-transfer agent for the polymerization of styrene and MMA. The pressure dependence of C_T and k_{tr} as well as the influence of scCO₂ as a solvent on the chain-transfer reaction of DDM have not been studied so far. Previously, Hutchinson et al.¹ investigated the temperature dependence of C_T for DDM in methacrylate homopolymerizations at ambient pressure. The values reported showed that C_T is temperature independent.

In this work, the pressure dependence of the chain-transfer rate coefficient of DDM as CTA in the homo- and copolymerization of styrene and MMA is determined in bulk and in scCO₂. The PLP technique is applied using a laser pulse repetition rate of 1 Hz and a photoinitiator concentration, [DMPA], of 0.2 mmol·L⁻¹, as explained in section 4. The same amounts of DDM are used for the different systems.

The detailed discussion about DDM as CTA in homo- and copolymerizations of styrene and MMA is given in section 5.4.

5.1.1 Homopolymerization of styrene

5.1.1.1 Mayo method

The molecular weight distributions of polymer obtained in the presence of DDM as CTA contain oligomer peaks in the low molecular weight region. As explained in section 4, the presence of oligomers in the MWD may influence the values of the number and weight average molecular weights, M_n and M_w , respectively. The program PREDICI[®] (for comparison see section 6) was used to estimate M_n and M_w for the corresponding MWDs in the absence of oligomer peaks. Fig. 5.1 shows as example the MWD obtained without (dotted line) and after applying simulation via PREDICI[®] (full line) for homopolymerization in scCO₂ with [DDM]/[sty] = 0.01.

M_n and M_w values obtained for both MWDs, without and after simulation, are listed in Table 5.1 for styrene homopolymerizations in 40 wt % scCO₂. As expected, M_n and M_w are very different when the peaks are eliminated to the molecular weight distribution. As explained in section 4, M_n and M_w are the parameters used in the Mayo method. Thus, it is obvious that the C_T values determined using the Mayo method depend on the presence or not of these peaks. In other words, the Mayo method is not adequate for this system.

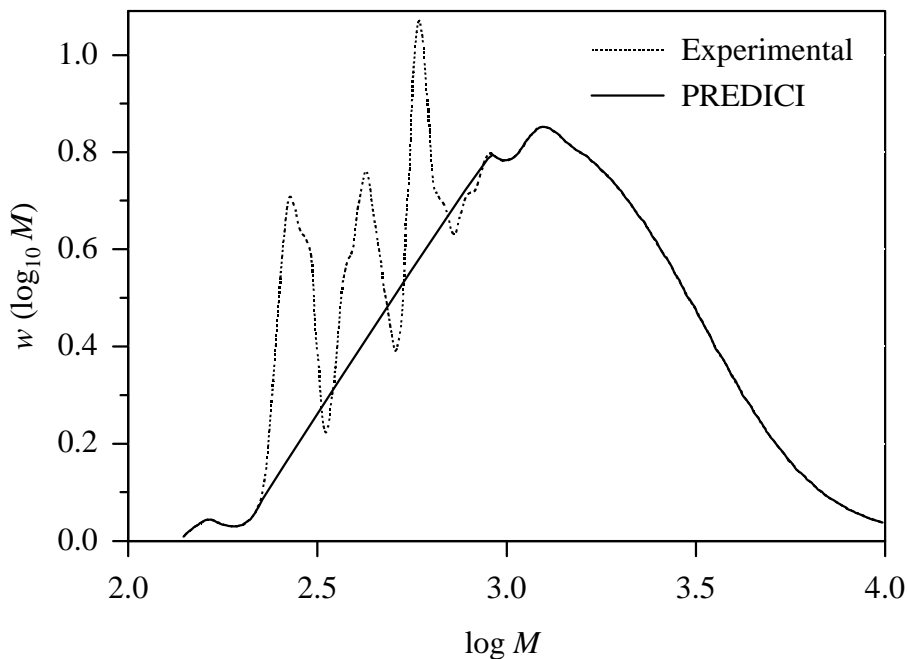


Figure 5.1: Molecular weight distribution obtained without (dotted line) and after applying the program PREDICI[®] (full line) for polystyrene from homopolymerization with DDM as CTA in $scCO_2$ at 80°C, 300 bar and $[DDM]/[sty] = 0.01$.

[DDM]/[sty]	Experimental MWD		Simulated MWD	
	M_n	M_w	M_n	M_w
0.0025	$1.51 \cdot 10^3$	$5.88 \cdot 10^3$	$1.62 \cdot 10^3$	$6.1 \cdot 10^3$
0.005	$8.95 \cdot 10^2$	$2.67 \cdot 10^3$	$1.40 \cdot 10^3$	$3.37 \cdot 10^3$
0.01	$6.92 \cdot 10^2$	$1.33 \cdot 10^3$	$9.17 \cdot 10^2$	$1.57 \cdot 10^3$
0.015	$6.53 \cdot 10^2$	$9.51 \cdot 10^2$	$6.88 \cdot 10^2$	$1.01 \cdot 10^3$

Table 5.1: Summary of the average numbers M_n and M_w determined experimentally and simulated with the program PREDICI[®] for styrene homopolymerizations with DDM as CTA at 80°C and 300 bar in $scCO_2$.

5.1.1.2 CLD method

As shown in Fig. 5.1, the oligomer peaks are only present in the low molecular weight region at $M < 10^3 \text{ g}\cdot\text{mol}^{-1}$. This was also observed in the MWD of polystyrene obtained with tetrabromo methane (CBr_4) as CTA in the same conditions of temperature and pressure⁴. In both cases, here and ref. 4, the MWDs of oligomer differ by one monomer unit. However, the presence of oligomers in the low molecular weight region should not affect the high molecular weight region that is used for the CLD method. As explained in section 4, MWD is shifted to lower values when the concentration of CTA is increased. Thus, the influence of oligomers on the high molecular weight region will be enhanced when [DDM] increases. Therefore small amounts of DDM were used in order to prevent the obtention of too low molecular weight. In summary, the CLD method is adequate for determining C_T in this condition when using restricted amounts of CTA in styrene homopolymerization.

5.1.1.3 Results

Homopolymerizations of styrene were carried out with DDM as chain-transfer agent in 40 wt % scCO_2 and in bulk at 80°C varying the pressure between 300 and 1500 bar.

The MWDs of PS obtained for polymerizations in scCO_2 at 80°C , 300 bar, and various amounts of DDM are shown in Fig. 5.2.

The MWDs are strongly shifted to lower molecular weights when the concentration of DDM increases. In the absence of DDM, the reaction yields polymer with a weight average molecular weight of $3.77\cdot 10^5 \text{ g}\cdot\text{mol}^{-1}$, and upon the addition of DDM (0.5 wt %, $[\text{DDM}]/[\text{sty}] = 0.0025$) M_w decreases to $5.91\cdot 10^3 \text{ g}\cdot\text{mol}^{-1}$. Therefore, the addition of only a small amount of CTA leads to a strong shift of the MWD to lower values.

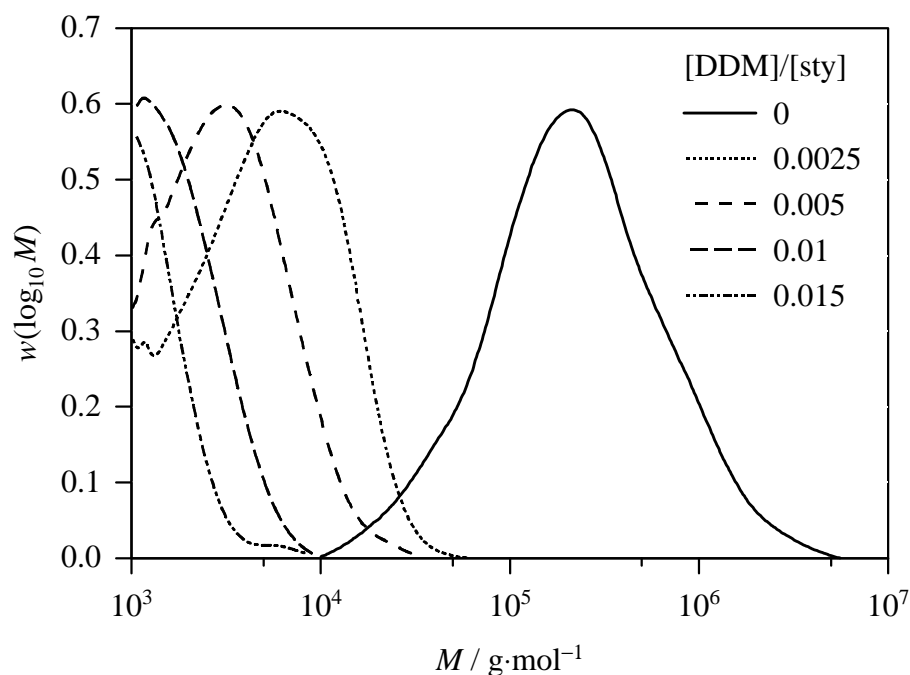


Figure 5.2: Molecular weight distributions of polystyrene from polymerizations in 40 wt % $scCO_2$ at 80°C, 300 bar, and DDM concentration as indicated.

The corresponding $\ln f(M)$ plots shown in Fig. 5.3 exhibit a linear part in the high molecular weight region between M_w and M_z (as indicated for the lowest value of $[DDM]/[sty]$), which slope is used to determine C_T , as explained in section 4.

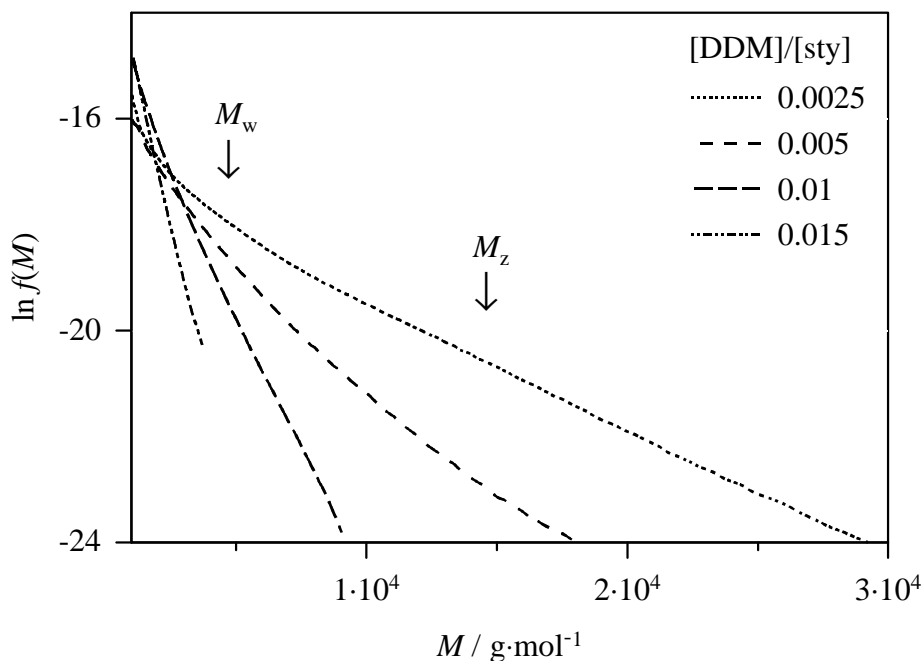


Figure 5.3: $\ln f(M)$ distributions for polystyrene from polymerizations in 40 wt % $scCO_2$ at 80°C, 300 bar, and DDM concentration as indicated.

The slope of the linear part increases with DDM concentration, which indicates a change in the chain-transfer activity. Fig. 5.4 exhibits the so called CLD plots for the styrene homopolymerizations at 80°C and 300 bar in scCO₂ and in bulk. The magnitude of the slopes is not significantly different in bulk and in scCO₂, which traducts very close C_T values. The values of C_T determined are 14.6 ± 1.8 and 16.3 ± 1.5 in bulk and in 40 wt % scCO₂, respectively. Thus, scCO₂ has no significant influence on C_T .

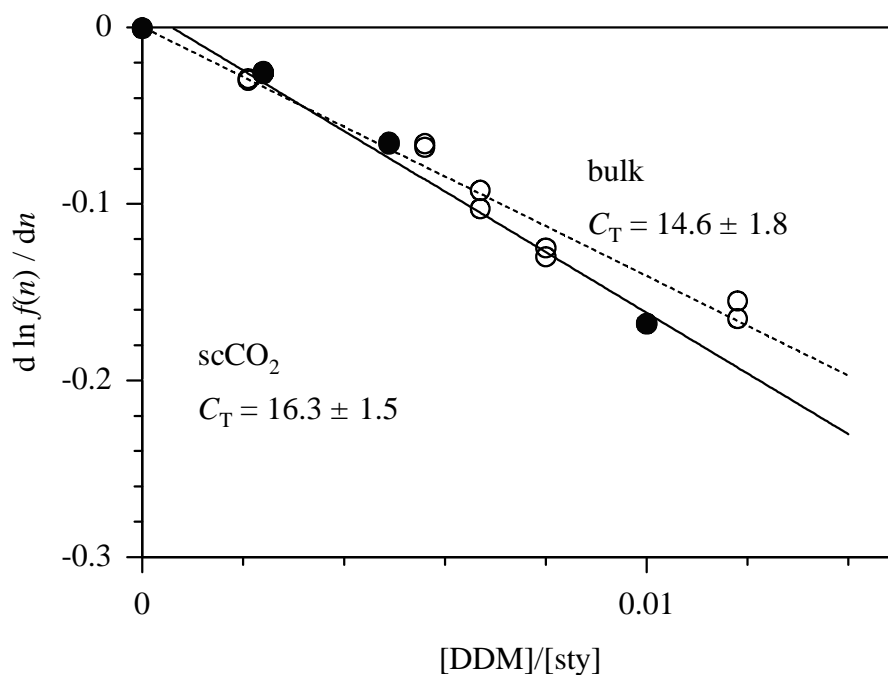


Figure 5.4: Determination of the chain-transfer constant, C_T , from a plot of $d \ln f(n)/dn$ vs. $[DDM]/[sty]$ for styrene homopolymerizations at 80°C, 300 bar in 40 wt % scCO₂ (solid line) and in bulk (dotted line).

Pressure dependence of C_T and k_{tr}

The pressure dependence of C_T and k_{tr} for the homopolymerization of styrene was studied at 80°C and at pressures between 300 and 1500 bar.

The corresponding chain-transfer rate coefficients, k_{tr} , were determined using the C_T values calculated in this study and the propagation rate coefficients, k_p , reported in the literature^{5,6} under the same conditions of pressure and temperature. The k_p values used are listed in Appendix 1 and those are nearly equivalent in bulk and in scCO₂.

Fig. 5.5 shows the pressure dependence of C_T (a) and k_{tr} (b) for polymerizations in scCO₂ and in bulk at 80°C. In addition, the literature value¹ obtained by PLP at 60°C and ambient

pressure is compared to the data of this work. C_T of 15.5 determined in bulk polymerization at 80°C and ambient pressure is in very good agreement with the literature data¹ of 15.6. This finding indicates that C_T may be temperature independent in styrene homopolymerization.

C_T measured in both media decreases significantly with the pressure: For example, C_T values at 300 and 1500 bar in scCO₂ are 16.3 and 11, respectively. The values determined in scCO₂ are very close to the bulk values in the entire pressure range. In contrast to C_T , k_{tr} for polymerizations in bulk and in scCO₂ slightly increases with pressure. In addition, the difference on k_{tr} in both media is not significant.

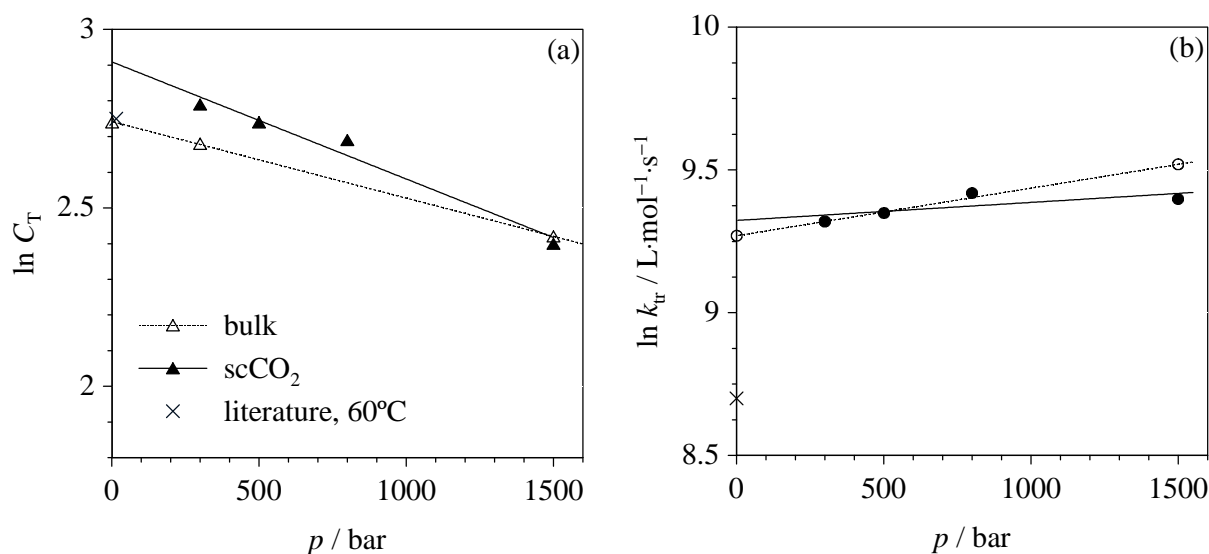


Figure 5.5: Pressure dependence of the chain-transfer constant, C_T , (a) and of the chain-transfer rate coefficient, k_{tr} , (b) for styrene homopolymerizations at 80°C in 40 wt % scCO₂ and in bulk. Experimental data are reported in Appendix 2. The literature data is taken from ref. 1.

Eqs. 5.1 to 5.4 correspond to the linear fits of the experimental data for C_T and k_{tr} given in Fig. 5.5.

$$\ln C_T = (2.74 \pm 0.01) - (2.16 \pm 0.31) \cdot 10^{-4} (p / \text{bar}) \quad (5.1)$$

$$\ln [k_{tr} / (\text{L} \cdot \text{mol}^{-1} \cdot \text{s}^{-1})] = (9.26 \pm 0.02) + (1.54 \pm 0.34) \cdot 10^{-4} (p / \text{bar}) \quad (5.2)$$

(bulk, 80°C, 300 ≤ p ≤ 1500 bar)

$$\ln C_T = (2.91 \pm 0.11) - (3.31 \pm 1.29) \cdot 10^{-4} (p / \text{bar}) \quad (5.3)$$

$$\ln [k_{tr} / (\text{L} \cdot \text{mol}^{-1} \cdot \text{s}^{-1})] = (9.33 \pm 0.1) + (0.62 \pm 1.18) \cdot 10^{-4} (p / \text{bar}) \quad (5.4)$$

(40 wt % scCO₂, 80°C, 300 ≤ p ≤ 1500 bar)

According to $\delta (\ln k_{tr}) / \delta p = -\Delta V^\ddagger / (R \cdot T)$ and $\delta (\ln C_T) / \delta p = -\Delta V^\ddagger / (R \cdot T)$, the activation volumes for C_T and k_{tr} are determined as:

$$\text{bulk: } \Delta V^\ddagger(C_T) = + (6.3 \pm 0.7) \text{ cm}^3 \cdot \text{mol}^{-1} \qquad \Delta V^\ddagger(k_{tr}) = - (4.5 \pm 1.0) \text{ cm}^3 \cdot \text{mol}^{-1}$$

$$\text{scCO}_2: \Delta V^\ddagger(C_T) = + (9.7 \pm 3.8) \text{ cm}^3 \cdot \text{mol}^{-1} \qquad \Delta V^\ddagger(k_{tr}) = - (1.8 \pm 3.5) \text{ cm}^3 \cdot \text{mol}^{-1}$$

Within experimental uncertainty, the activation volumes for C_T , which are close in both media, indicate that C_T is pressure dependent. In contrast, the low values of $\Delta V^\ddagger(k_{tr})$ suggest that the transfer reaction is not pressure dependent in both media. This finding will be discussed in section 5.4.

5.1.2 Homopolymerization of MMA

MMA homopolymerizations were carried out in 40 wt % scCO₂ and in bulk at 80°C and at pressures between 300 and 1000 bar.

Figs. 5.6a and 5.6b show typical molecular weight distributions and their corresponding $\ln f(M)$ plots obtained for MMA homopolymerizations in scCO₂ at 80°C and 300 bar with the indicated amount of DDM.

The MWDs are shifted to lower molecular weights with increasing CTA concentration, as seen in Fig. 5.6a. In the absence of DDM, the reaction yields polymer with a weight average molecular weight of $5 \cdot 10^5 \text{ g} \cdot \text{mol}^{-1}$, and upon addition of 1 wt % DDM ($[\text{DDM}]/[\text{MMA}] = 0.005$) M_w decreases to $3.3 \cdot 10^4 \text{ g} \cdot \text{mol}^{-1}$. In Fig. 5.6b the part of the distribution used to calculate C_T is indicated by the bold line. The slope of this MW region is enhanced with increasing the concentration of DDM.

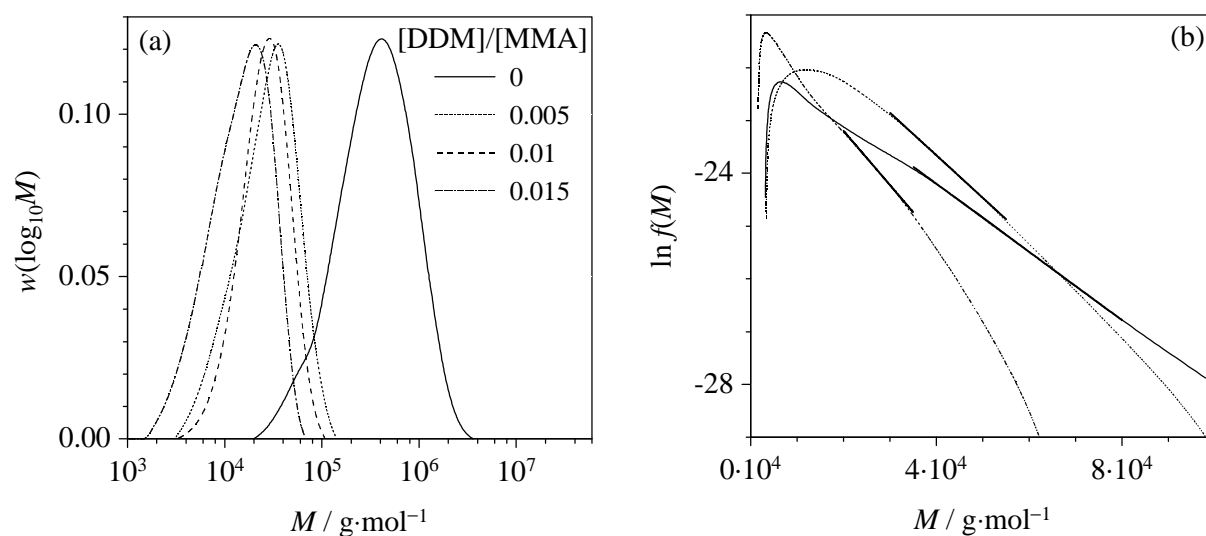


Figure 5.6: Molecular weight distributions (a) and corresponding $\ln f(M)$ distributions (b) for MMA homopolymerizations in 40 wt % scCO_2 at 80°C , 300 bar, and DDM concentration as indicated. The bold line indicates the region where the slope is measured.

Fig. 5.7 exhibits the CLD plots of MMA homopolymerizations at 300 bar and 80°C in bulk and in scCO_2 .

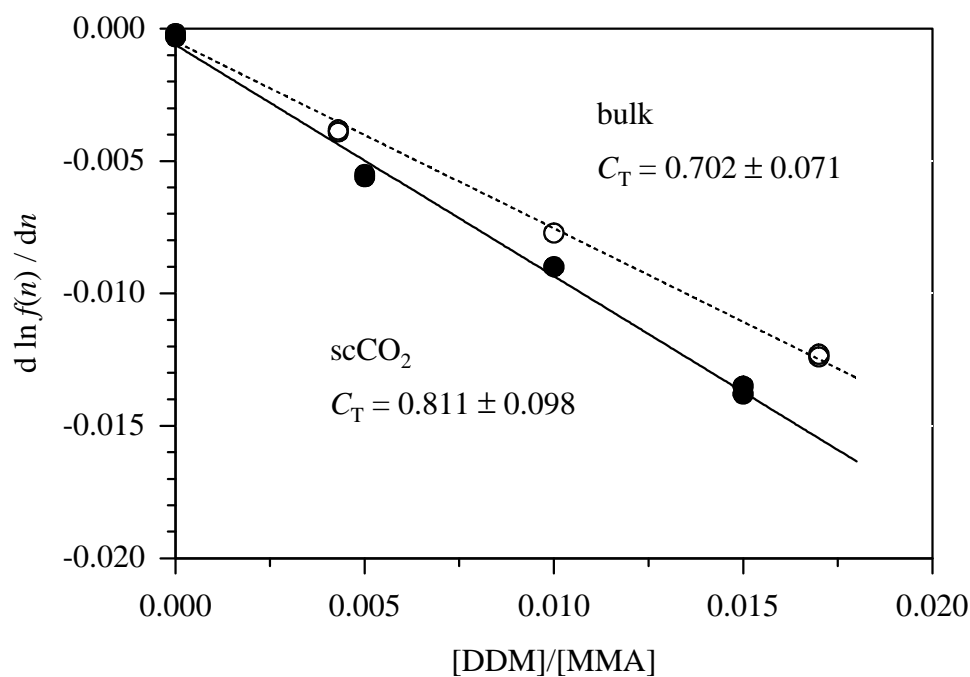


Figure 5.7: Determination of the chain-transfer constant from a plot of $d \ln f(n)/dn$ vs. $[\text{DDM}]/[\text{MMA}]$ for MMA homopolymerizations at 80°C , 300 bar in 40 wt % scCO_2 (solid line) and in bulk (dotted line).

The C_T values obtained in $scCO_2$ and in bulk are 0.811 ± 0.098 and 0.702 ± 0.071 , respectively. Within experimental uncertainty, the chain-transfer constants obtained for MMA are close in both media. Thus, $scCO_2$ as a solvent has no significant effect on the chain-transfer activity.

Pressure dependence of C_T and k_{tr}

The pressure dependence of C_T and k_{tr} for MMA homopolymerization was studied in a pressure range from 300 to 1000 bar. The values of k_{tr} were calculated from the C_T values and k_p data. For bulk polymerization the propagation rate coefficient is determined using the equation given by Beuermann et al.⁷. k_p values in $scCO_2$ were determined in this work using the PLP-SEC method, as described in the literature⁶. k_p at 1000 bar in $scCO_2$ was estimated using a ratio of $k_{p,bulk} / k_{p,scCO_2}$ of 0.9, which is calculated for the different pressures measured. The k_p values used in bulk and in $scCO_2$ are listed in Appendix 1.

Fig. 5.8 shows the pressure dependence of k_{tr} and C_T for polymerizations in $scCO_2$ and in bulk at 80°C.

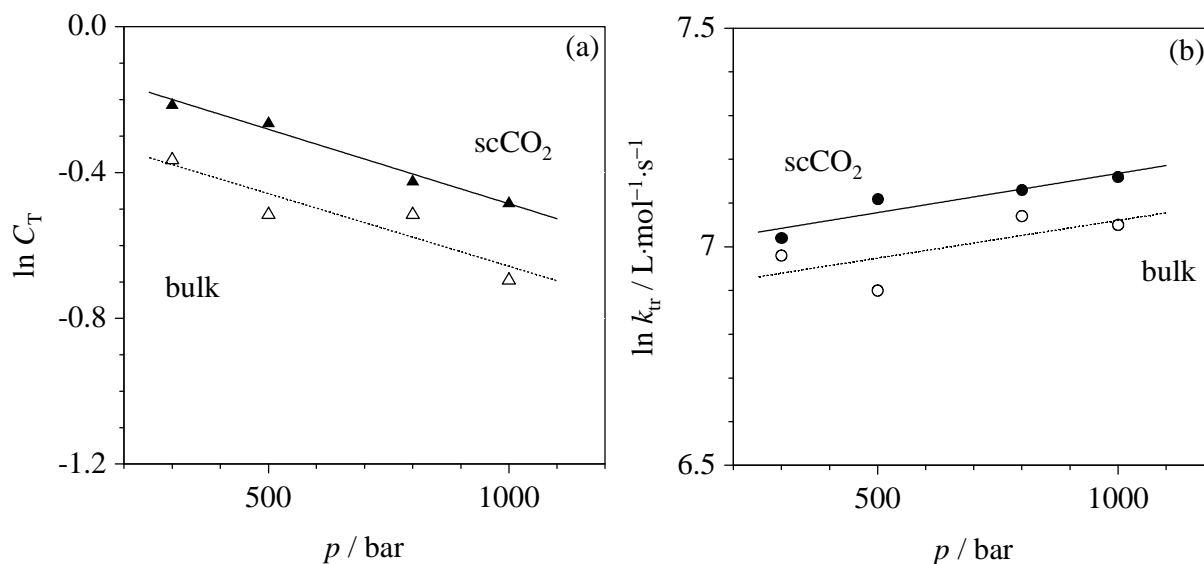


Figure 5.8: Pressure dependence of the chain-transfer constant (a) and of the chain-transfer rate coefficient (b) for MMA homopolymerizations in 40 wt % $scCO_2$ and in bulk at 80°C. Experimental data are reported in Appendix 2.

C_T decreases with increasing pressure in bulk and in $scCO_2$. The lines fitted to the experimental C_T data in both reaction media are parallel. Moreover, C_T values determined in

scCO₂ are very close to the bulk values in the entire pressure range. In contrast to C_T , k_{tr} is enhanced in both media, as seen in Fig. 5.8b. However, the pressure dependence of k_{tr} is low: For example, in scCO₂ the k_{tr} values are $1.14 \cdot 10^3$ and $1.28 \cdot 10^3$ L·mol⁻¹·s⁻¹ at 300 and 1000 bar, respectively. In addition, $k_{tr,bulk} / k_{tr,scCO_2}$ are 0.95 and 0.9 at 300 and 1000 bar, respectively, which shows a minor difference in the pressure dependence of k_{tr} in both media.

The pressure dependence of k_{tr} and C_T for polymerizations in bulk and in scCO₂ may be expressed by Eqs. 5.5-5.8:

$$\ln C_T = - (0.267 \pm 0.086) - (3.72 \pm 2) \cdot 10^{-4} (p / \text{bar}) \quad (5.5)$$

$$\ln [k_{tr} / (\text{L} \cdot \text{mol}^{-1} \cdot \text{s}^{-1})] = (6.88 \pm 0.27) + (1.79 \pm 1.27) \cdot 10^{-4} (p / \text{bar}) \quad (5.6)$$

(bulk, 80°C, $300 \leq p \leq 1000$ bar)

$$\ln C_T = - (0.095 \pm 0.024) - (3.61 \pm 1.02) \cdot 10^{-4} (p / \text{bar}) \quad (5.7)$$

$$\ln [k_{tr} / (\text{L} \cdot \text{mol}^{-1} \cdot \text{s}^{-1})] = (7.02 \pm 0.11) + (1.44 \pm 1.01) \cdot 10^{-4} (p / \text{bar}) \quad (5.8)$$

(40 wt % scCO₂, 80°C, $300 \leq p \leq 1000$ bar).

The respective activation volumes are as follows:

$$\text{bulk: } \Delta V^\ddagger(C_T) = + (10.9 \pm 10.6) \text{ cm}^3 \cdot \text{mol}^{-1} \quad \Delta V^\ddagger(k_{tr}) = - (5.3 \pm 3.7) \text{ cm}^3 \cdot \text{mol}^{-1}$$

$$\text{scCO}_2: \Delta V^\ddagger(C_T) = + (10.6 \pm 3.0) \text{ cm}^3 \cdot \text{mol}^{-1} \quad \Delta V^\ddagger(k_{tr}) = - (4.4 \pm 2.9) \text{ cm}^3 \cdot \text{mol}^{-1}$$

The activation volume of C_T is around $-11 \text{ cm}^3 \cdot \text{mol}^{-1}$ in both media, which confirms the significant pressure dependence of C_T . Within experimental uncertainty, $\Delta V^\ddagger(k_{tr})$ in bulk and in scCO₂ are slightly pressure dependent. $\Delta V^\ddagger(k_{tr})$ values are equivalent in both media. The extrapolation of C_T in bulk to 1 bar via Eq. 5.5 gives a value of 0.765, which is in very good agreement with the value of 0.711 determined by Hutchinson et al.¹.

5.1.3 Copolymerization of styrene and MMA

The chain-transfer reaction of DDM in copolymerizations of styrene and MMA was studied at 80°C and four different pressures. The chain-transfer rate coefficients were obtained using the C_T values measured and k_p data for copolymerizations listed in Appendix 1, which were

obtained as explained in section 6.1 applying the IPUE model. Fig. 5.9 shows the C_T values obtained at 80°C and 300 bar for different mole fractions of styrene in the monomer feed, f_S .

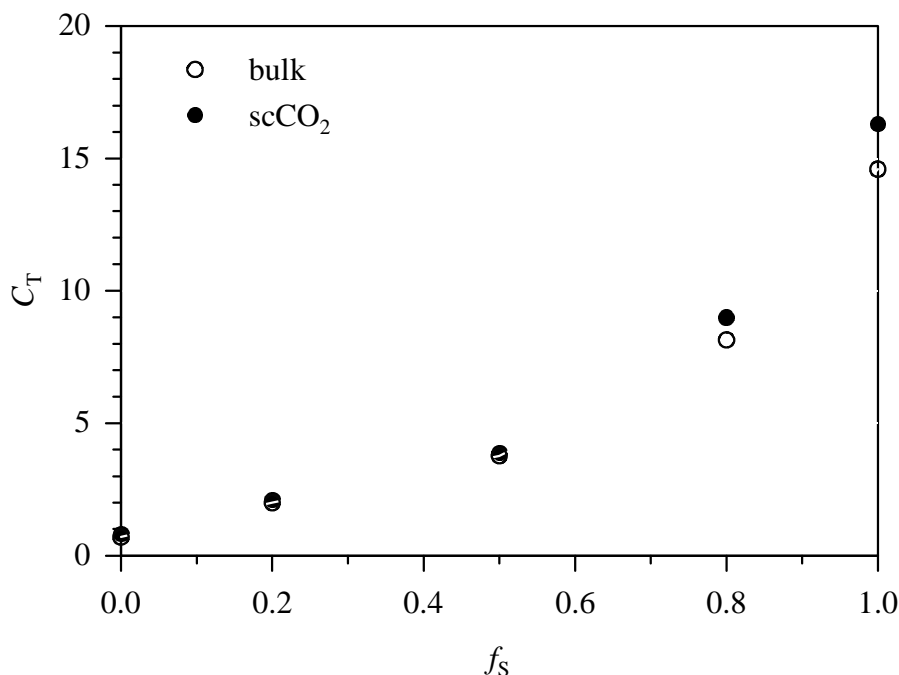


Figure 5.9: Variation of C_T with the mole fraction of styrene in the monomer feed for copolymerizations of styrene and MMA in 40 wt % scCO₂ (full circles) and in bulk (open circles) at 80°C and 300 bar. Experimental data are reported in Appendix 2.

The variation of C_T with f_S is not linear for reactions in bulk and in scCO₂. C_T increases with f_S , which means that C_T of styrene is higher than C_T of MMA. It is also seen that the difference in bulk and scCO₂ measurements is not significant in the entire range of f_S .

Fig. 5.9 shows that the increase of C_T with f_S is slow at low f_S values. This aspect will be discussed in section 6.

The variation of the corresponding k_{tr} values with f_S is shown in Fig. 5.10.

Fig. 5.10 exhibits a linear increase of $\ln k_{tr}$ with f_S for copolymerizations in scCO₂ and in bulk. It is clear that the presence of scCO₂ has no influence on k_{tr} at 80°C. The literature data included in Fig. 5.10 are calculated from the C_T values reported in refs. 1 and 2 and from k_p given in ref. 2.

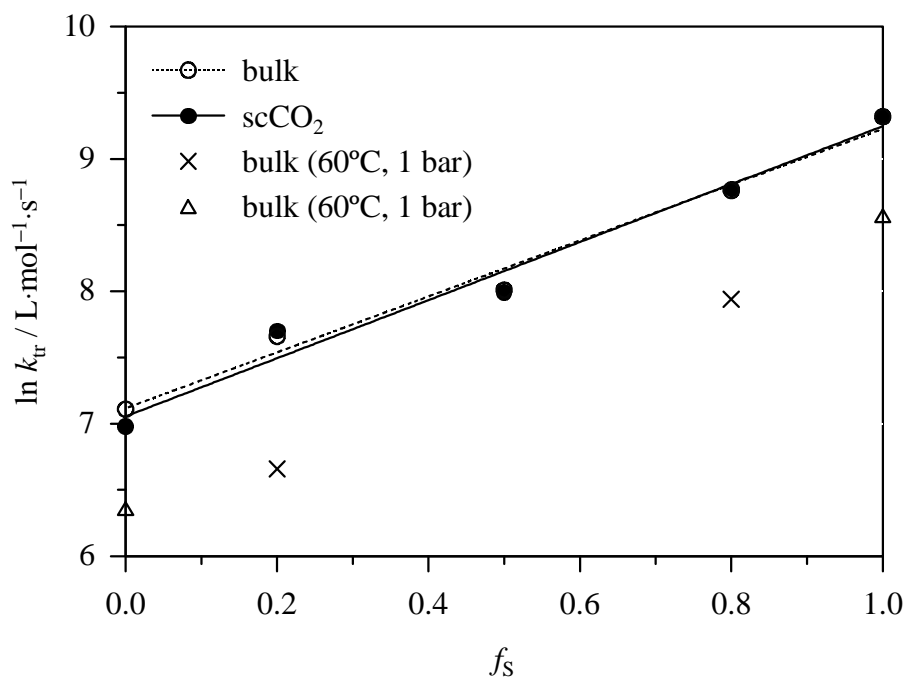


Figure 5.10: Variation of the chain-transfer rate coefficients with the mole fraction of styrene in the monomer feed for copolymerizations of styrene and MMA at 80°C and 300 bar. Literature data are taken from ref. 1 (Δ) and ref. 2 (\times). Experimental data are reported in Appendix 2.

The literature data show the same trend as k_{tr} from this work: $\ln k_{tr}$ increases linearly with f_s . Moreover, the plots of $\ln k_{tr}$ vs. f_s at 1 bar, 60°C and at 300 bar, 80°C are parallel, indicating that the variation of $\ln k_{tr}$ with f_s does not depend on the polymerization conditions (temperature, pressure, and reaction medium). In addition, comparison of k_{tr} determined at 60°C and 1 bar and at 80°C and 300 bar shows that k_{tr} may be temperature and pressure dependent.

Pressure dependence of C_T and k_{tr}

The pressure dependencies of C_T and k_{tr} for copolymerization with $f_s = 0.5$ at 80°C are plotted in Fig. 5.11. The C_T and k_{tr} values determined at each pressure are very close in bulk and in scCO₂: $C_{T,\text{bulk}}/C_{T,\text{scCO}_2}$ are in the range from 0.9 to 1. As seen for styrene and MMA homopolymerizations, C_T decreases, whereas k_{tr} slightly increases with pressure. Moreover, the effect of CO₂ as a solvent on C_T and k_{tr} is not significant in the entire pressure range.

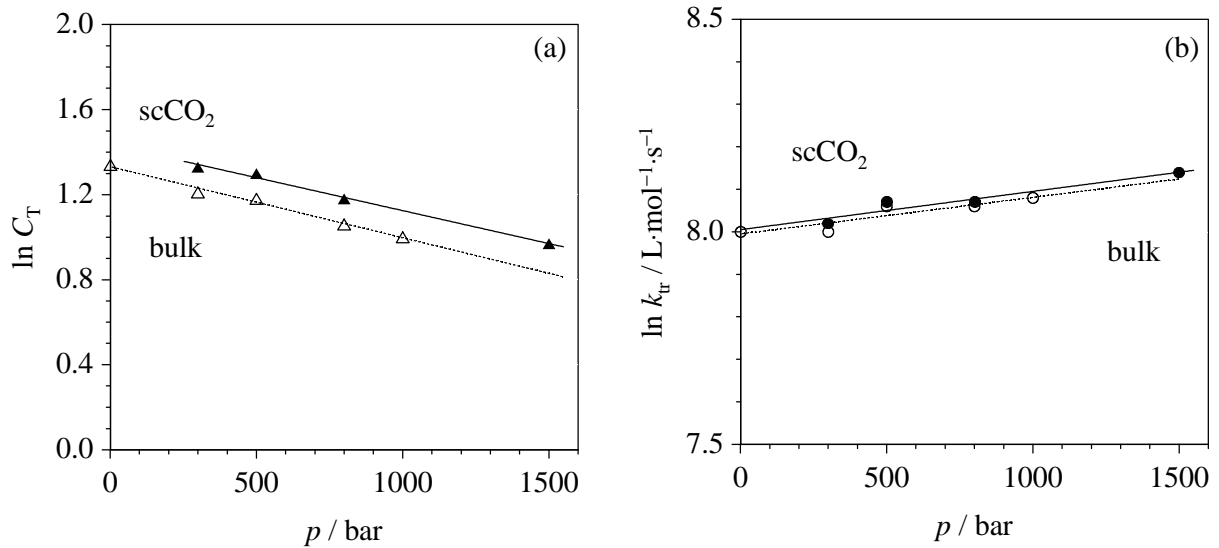


Figure 5.11: Pressure dependence of the chain-transfer constant (a) and of the chain-transfer rate coefficient (b) for copolymerizations of styrene and MMA ($f_S = 0.5$) in 40 wt % $scCO_2$ and in bulk at $80^\circ C$. Experimental data are given in Appendix 2.

The pressure dependence of k_{tr} and C_T for copolymerizations ($f_S = 0.5$) in bulk and in $scCO_2$ may be expressed by Eqs. 5.9-5.12:

$$\ln C_T = (1.33 \pm 0.05) - (3.33 \pm 0.71) \cdot 10^{-4} (p / \text{bar}) \quad (5.9)$$

$$\ln [k_{tr} / (\text{L} \cdot \text{mol}^{-1} \cdot \text{s}^{-1})] = (7.99 \pm 0.04) + (8.82 \pm 7.08) \cdot 10^{-5} (p / \text{bar}) \quad (5.10)$$

$$(\text{bulk}, f_S = 0.5, 80^\circ C, 300 \leq p \leq 1000 \text{ bar})$$

$$\ln C_T = (1.43 \pm 0.05) - (3.07 \pm 0.58) \cdot 10^{-4} (p / \text{bar}) \quad (5.11)$$

$$\ln [k_{tr} / (\text{L} \cdot \text{mol}^{-1} \cdot \text{s}^{-1})] = (8.00 \pm 0.05) + (9.46 \pm 6.43) \cdot 10^{-5} (p / \text{bar}) \quad (5.12)$$

$$(40 \text{ wt } \% \text{ } scCO_2, f_S = 0.5, 80^\circ C, 300 \leq p \leq 1000 \text{ bar})$$

The corresponding activation volumes are as follows:

$$\text{bulk: } \Delta V^\#(C_T) = + (9.8 \pm 2.1) \text{ cm}^3 \cdot \text{mol}^{-1}$$

$$\Delta V^\#(k_{tr}) = - (2.6 \pm 2.8) \text{ cm}^3 \cdot \text{mol}^{-1}$$

$$scCO_2: \Delta V^\#(C_T) = + (9.0 \pm 1.7) \text{ cm}^3 \cdot \text{mol}^{-1}$$

$$\Delta V^\#(k_{tr}) = - (2.8 \pm 1.9) \text{ cm}^3 \cdot \text{mol}^{-1}$$

The activation volume for C_T is approximately $+ 9.5 \text{ cm}^3 \cdot \text{mol}^{-1}$ in bulk and in scCO_2 . This value indicates a significant pressure dependence of C_T in both media. The variation of C_T with pressure is close to the one determined in homopolymerizations of styrene and MMA. In contrast, the activation volume for k_{tr} is approximately $- 2.7 \text{ cm}^3 \cdot \text{mol}^{-1}$ in bulk and in scCO_2 , thus k_{tr} shows a minor pressure dependence. Within experimental uncertainty, the values of $\Delta V^\ddagger (k_{tr})$ in copolymerizations are similar to the values for homopolymerizations. This finding indicates that $\Delta V^\ddagger (k_{tr})$ is not dependent on the monomer feed used, which will be discussed in section 5.4.

Since k_{tr} is not pressure dependent, the difference in k_{tr} between literature data and data from this work, shown in Fig. 5.10, is due to the different temperatures applied. Thus, k_{tr} is temperature dependent in styrene and MMA copolymerization.

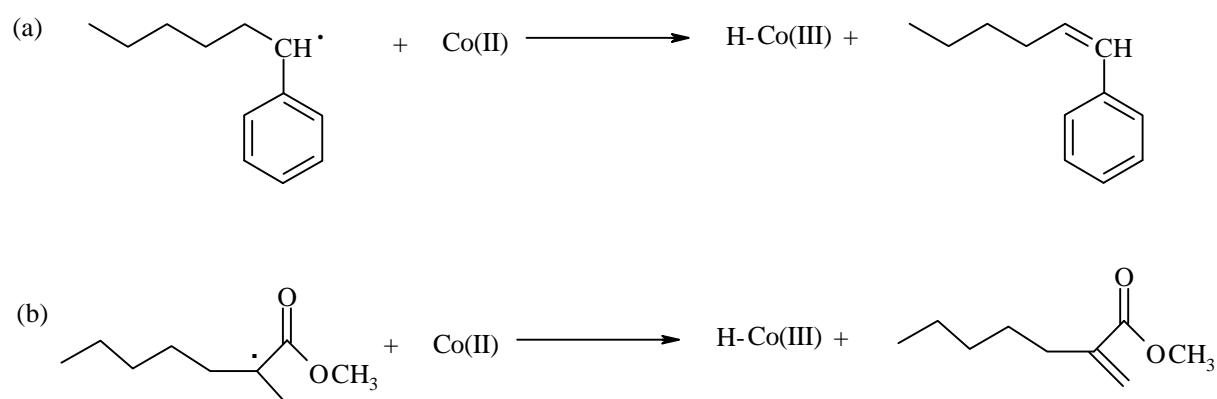
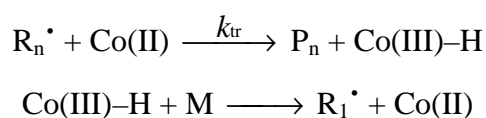
5.1.4 Summary

The table below summarizes the results obtained for homo- and copolymerizations of MMA and styrene in bulk and in scCO_2 at 80°C with DDM as chain-transfer agent. C_T and k_{tr} are given for polymerizations at 80°C and 300 bar.

MMA		
	C_T	k_{tr}
scCO₂	0.811 ± 0.098	(1.14 ± 0.25)·10 ³ L·mol ⁻¹ ·s ⁻¹
bulk	0.702 ± 0.071	(1.08 ± 0.21)·10 ³ L·mol ⁻¹ ·s ⁻¹
scCO₂ influence	no influence in the entire pressure range	no influence in the entire pressure range
DV[#] / cm³·mol⁻¹	<i>bulk</i> : + (10.9 ± 10.6)	<i>bulk</i> : – (5.3 ± 3.7)
	<i>scCO₂</i> : + (10.6 ± 3.0)	<i>scCO₂</i> : – (4.4 ± 2.9)
styrene		
	C_T	k_{tr}
scCO₂	16.3 ± 1.5	(11.2 ± 2.1)·10 ³ L·mol ⁻¹ ·s ⁻¹
bulk	14.6 ± 1.8	(11.2 ± 1.4)·10 ³ L·mol ⁻¹ ·s ⁻¹
scCO₂ influence	no influence in the entire pressure range	no influence in the entire pressure range
DV[#] / cm³·mol⁻¹	<i>bulk</i> : + (6.3 ± 0.7)	<i>bulk</i> : – (4.5 ± 1.0)
	<i>scCO₂</i> : + (9.7 ± 3.8)	<i>scCO₂</i> : – (1.8 ± 3.5)
styrene / MMA ($f_s = 0.5$)		
	C_T	k_{tr}
scCO₂	3.77 ± 0.35	(3.03 ± 0.62)·10 ³ L·mol ⁻¹ ·s ⁻¹
bulk	3.34 ± 0.25	(2.98 ± 0.55)·10 ³ L·mol ⁻¹ ·s ⁻¹
scCO₂ influence	no influence in the entire pressure range	no influence in the entire pressure range
DV[#] / cm³·mol⁻¹	<i>bulk</i> : + (9.8 ± 2.1)	<i>bulk</i> : – (2.6 ± 2.8)
	<i>scCO₂</i> : + (9.0 ± 1.7)	<i>scCO₂</i> : – (2.8 ± 1.9)

5.2 CPhBF as catalytic chain-transfer agent

Catalytic chain-transfer agents (CCTAs) have been developed during recent years^{8,9}. Frequently cobalt (II)-complexes are used, which are able to catalyze chain-transfer reaction. The mechanism of the catalytic chain-transfer reaction is illustrated in scheme 5.2. Cobalt (II)-complexes abstract a hydrogen atom from a β -carbon on the radical chain, creating a dead polymer with a vinyl end-group and a Co(III)-H species. This Co(III)-H species transfers the hydrogen atom to a monomer molecule, initiating a new chain. CCTAs are advantageous as compared to conventional CTAs, because the CCTA is regenerated during the polymerization and only a small amount (ppm range) of the complex is required.



Scheme 5.2: Typical reaction scheme for catalytic chain-transfer. Chain-transfer reaction for styrene (a) and for MMA (b) homopolymerizations.

The mechanism of scheme 5.2 is usually presented for the catalytic chain-transfer reaction with cobalt-complexes. Although, recently several authors^{10,11,12} suspected the formation of a cobalt-carbon bond in the Co(II)/styrene system, as discussed in section 5.4. In the following part C_T , thus k_{tr} values are based using scheme 5.2. C_T and k_{tr} observed are noted as C_T^{obs} and k_{tr}^{obs} since the reaction scheme is not clear.

Investigations reported in the literature focus on CCTAs in MMA and styrene polymerizations at ambient pressure. The only C_T^{obs} data reported¹³ so far in MMA

polymerization in solution of scCO₂ shows a significant influence of scCO₂ as a solvent. The pressure dependence of C_T for catalytic chain-transfer has not yet been studied. Thus, the pressure dependencies of C_T^{obs} and $k_{\text{tr}}^{\text{obs}}$ are investigated in scCO₂ and in bulk in this work.

The cobalt-complex used is the bis(methanol) complex of bis(difluoroboryl) diphenylglyoximato cobalt (II), the so-called CPhBF (description in section 3.4). This complex is known to be air sensitive, therefore few polymerizations with CPhBF are carried out in section 5.2.1 in order to evaluate its air sensitivity.

The polymerizations are carried out in bulk and in 40 wt % scCO₂ applying the PLP technique with a laser pulse repetition rate of 1 Hz and a photoinitiator concentration of 0.2 mmol·L⁻¹, as explained in section 4. The [CPhBF]/[M] range from 10⁻⁸ to 10⁻⁶ is used for the different systems: Homo- and copolymerizations. Low CPhBF concentrations are used in order to prevent the obtention of polymer with too low molecular weight. The homogeneity of the system is checked visually and by IR monitoring during the polymerization.

5.2.1 Preliminary investigations

Preliminary investigations are performed under the same experimental conditions as in the literature^{9,12} in order to compare the C_T^{obs} values obtained, thus to check the validity of the technique used to prepare the mixtures of monomer, initiator, and CTA. In the following part, MMA polymerizations are performed in bulk at 60°C and ambient pressure using CPhBF as CTA and AIBN as initiator. In this case, the PLP-technique is not applied and the polymerization is thermally initiated. The time required for a monomer conversion of approximately 2 % is about 10 minutes.

Fig. 5.12 shows the CLD plots obtained for MMA homopolymerizations performed in bulk at 60°C and ambient pressure. One set of experiments is performed without any precautions towards oxygen (insert of Fig. 5.12). The mixtures of CPhBF, monomer, and initiator are not degassed and prepared under normal atmosphere. The polymerization is carried out as described in section 3.1. Two others sets of experiments are performed under oxygen free conditions (circles in Fig. 5.12). In one set the reaction mixtures are prepared in a glove box (full circles) and in the other one, the stock solutions are degassed using a freeze-pump-thaw procedure prior to preparation of the reaction mixtures in the glove box (open circles).

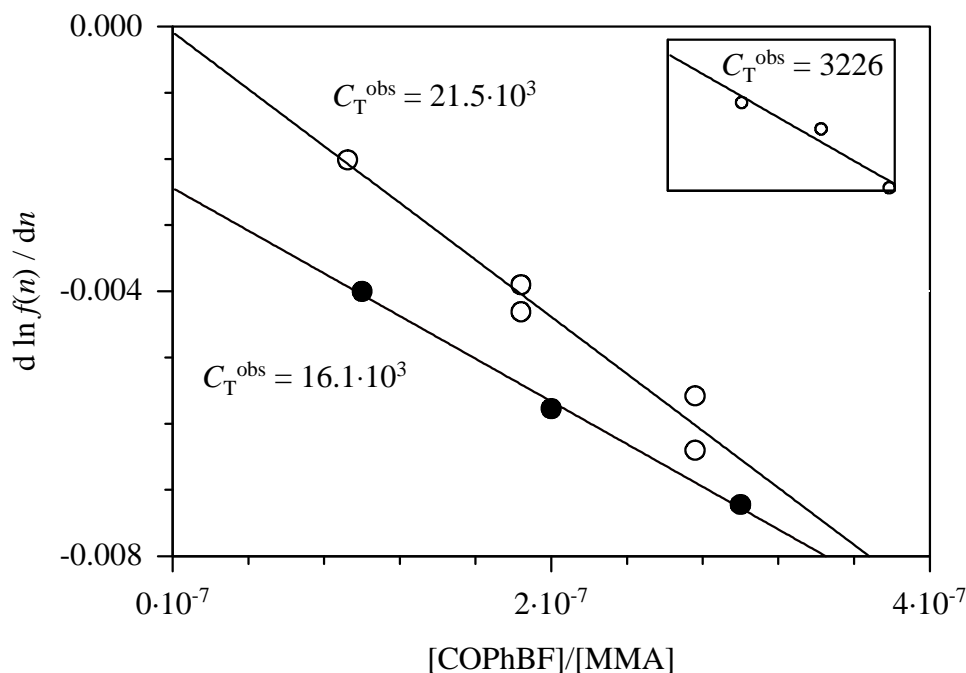


Figure 5.12: CLD plots for MMA polymerizations at 1 bar and 60°C using AIBN as initiator. The methods used to prepare the mixtures are given in the preceding text.

Fig. 5.12 clearly shows a difference in the slope, thus in C_T^{obs} , for the different methods used for the preparation of the reaction mixture. C_T^{obs} of $21.5 \cdot 10^3$, which corresponds to the reaction mixtures prepared in a glove box and degassed, is higher than the C_T^{obs} value of $16.1 \cdot 10^3$ obtained for polymerizations where the reaction mixtures are prepared in a glove box but are not degassed. The value of C_T^{obs} determined for experiments without any oxygen free precautions is 3226, which is about one order of magnitude lower than C_T^{obs} determined in oxygen free conditions. It is obvious that COPhBF in solution is less reactive in terms of the chain-transfer reaction when it is in contact with oxygen.

Davis et al.¹² performed MMA polymerizations at 60°C and ambient pressure considering the air sensitivity of the cobalt-complex. The solutions of MMA, initiator, and COPhBF were degassed by the freeze-pump-thaw procedure and the reactions performed using standard Schlenk apparatus and syringe techniques under oxygen free conditions. The values reported are in the range from $19.5 \cdot 10^3$ to $25.8 \cdot 10^3$, which is consistent with the C_T^{obs} value of $21.5 \cdot 10^3$ determined in this work.

In summary, precautions have to be taken to measure the kinetics of COPhBF as catalytic chain-transfer agent. Thus, all reaction mixtures are prepared under oxygen free conditions: The solutions of monomer, initiator, and CTA are prepared in a glove box and degassed using

the freeze-pump-thaw procedure. The method followed for preparation of the reactions mixtures in scCO₂ is described in section 3.1.9.

5.2.2 Homopolymerization of MMA

MMA is the most frequently studied monomer in polymerizations with CPhBF as CCTA. As already mentioned, the pressure dependence of C_T^{obs} and $k_{\text{tr}}^{\text{obs}}$ was not studied so far. Several reports with cobalt-complexes as CCTA for MMA polymerization^{14,15,16} suggest that C_T^{obs} is temperature independent. Therefore, MMA homopolymerizations were performed at 80°C in bulk and in 40 wt % scCO₂ at pressures between 300 and 1000 bar.

The molecular weight distributions obtained from MMA homopolymerizations in scCO₂ at 80°C, 300 bar and different CPhBF concentrations are shown in Fig. 5.13.

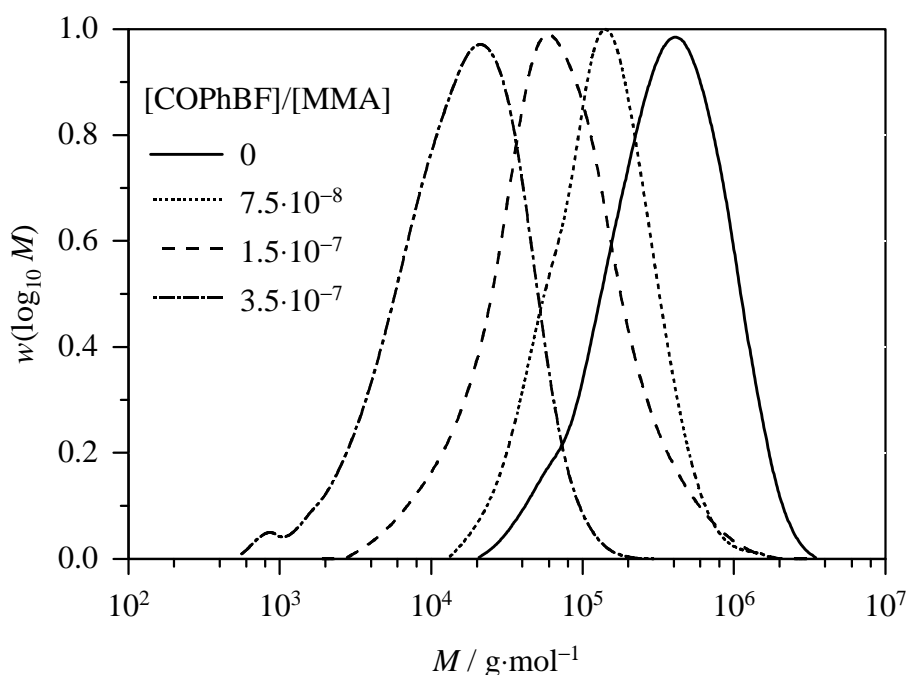


Figure 5.13: Molecular weight distributions of PMMA from polymerizations in 40 wt % scCO₂ at 80°C, 300 bar, and CPhBF concentration as indicated.

The addition of CPhBF shifts the resulting MWDs to lower molecular weights. PMMA obtained in the absence of CPhBF yields M_w of $5 \cdot 10^5$ g·mol⁻¹ and in the presence of only $5 \cdot 10^{-5}$ wt % of CPhBF ($[CPhBF]/[MMA] = 7.5 \cdot 10^{-8}$) M_w is shifted to a value of $2.1 \cdot 10^5$ g·mol⁻¹. For the highest amount of CPhBF, $2 \cdot 10^{-4}$ wt % ($[CPhBF]/[MMA] = 3.5 \cdot 10^{-7}$), a value of $2.6 \cdot 10^4$ g·mol⁻¹ is obtained for M_w . The addition of small amounts of CPhBF

strongly shifts M_w to lower values. The results demonstrate the exceptional transfer capacity of the cobalt-complex.

The corresponding $\ln f(M)$ vs. M plots of Fig. 5.13 are reported in Fig. 5.14. The bold lines indicate the region where the slope required for the determination of C_T^{obs} is measured, as explained in section 4.

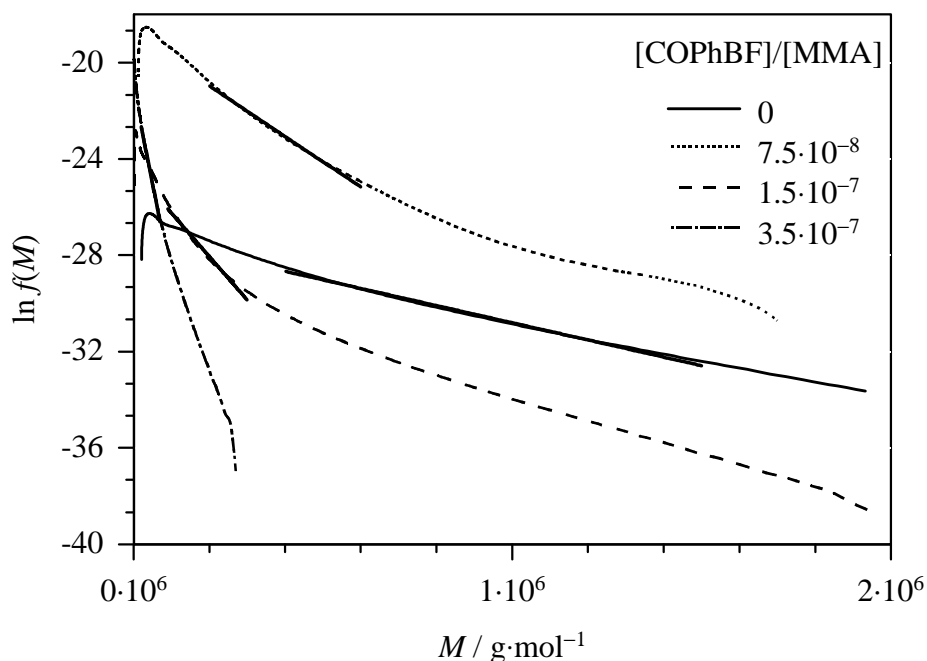


Figure 5.14: $\ln f(M)$ plots for PMMA from polymerizations in 40 wt % scCO_2 at 80°C , 300 bar, and CPhBF-concentration as indicated.

The slope is strongly enhanced with increasing CPhBF concentration. For example, the slopes corresponding to polymerizations without CTA and with $[\text{COPhBF}]/[\text{MMA}]$ of $1.5 \cdot 10^{-7}$ are $-3.56 \cdot 10^{-6}$ and $-1.80 \cdot 10^{-5}$, respectively. This indicates a change in the transfer activity when the concentration of CPhBF increases.

The CLD plots for MMA homopolymerizations in scCO_2 and in bulk at 80°C , 300 bar (a) and 1000 bar (b) are shown in Fig. 5.15, which slope gives $-C_T^{\text{obs}}$.

The values of C_T^{obs} determined at 300 bar are $(21.1 \pm 5.1) \cdot 10^3$ and $(14.1 \pm 2.2) \cdot 10^3$ in scCO_2 and bulk, respectively, which indicates a high chain-transfer activity of CPhBF. The difference in C_T^{obs} between bulk and in scCO_2 is clearly illustrated in Fig. 5.15b: C_T^{obs} in scCO_2 is 3 times higher than in bulk. In addition, C_T^{obs} determined at 300 bar is higher than C_T^{obs} at 1000 bar.

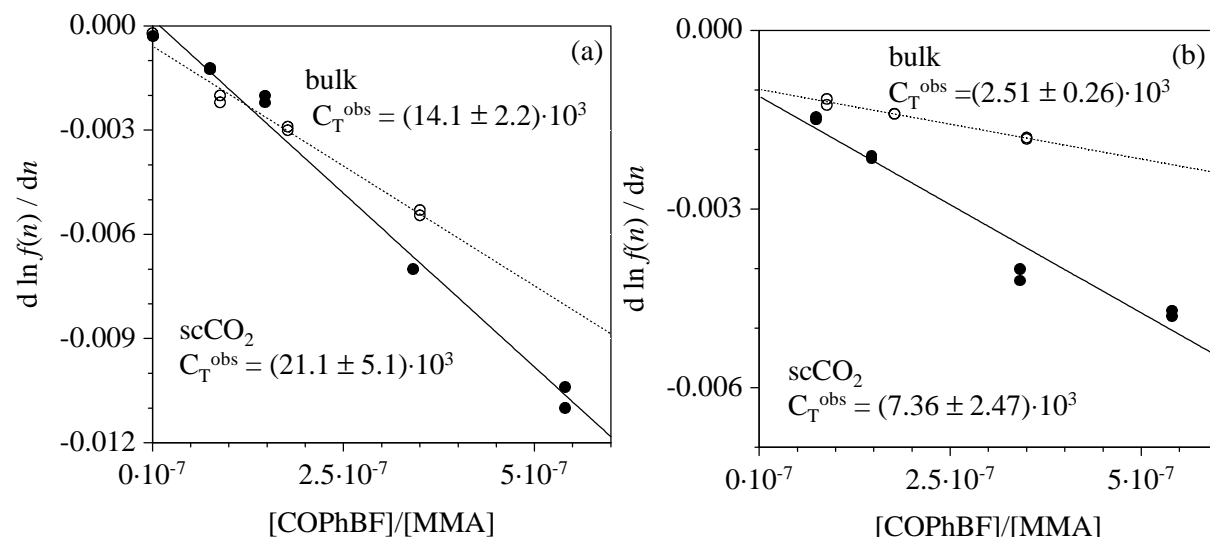


Figure 5.15: CLD plots for MMA homopolymerizations in 40 wt % $scCO_2$ (full circles) and in bulk (open circles) at 80°C, 300 bar (a) and 1000 bar (b) with COPhBF as catalytic chain-transfer agent.

Pressure dependence of k_{tr} and C_T

The pressure dependence of C_T^{obs} and k_{tr}^{obs} was studied for MMA homopolymerizations in bulk and in $scCO_2$ at 80°C and pressures varying between 300 and 1000 bar, as seen in Fig. 5.16. The values of k_{tr}^{obs} were calculated with C_T^{obs} values and k_p data given in Appendix 1 (for comparison see section 5.1.2).

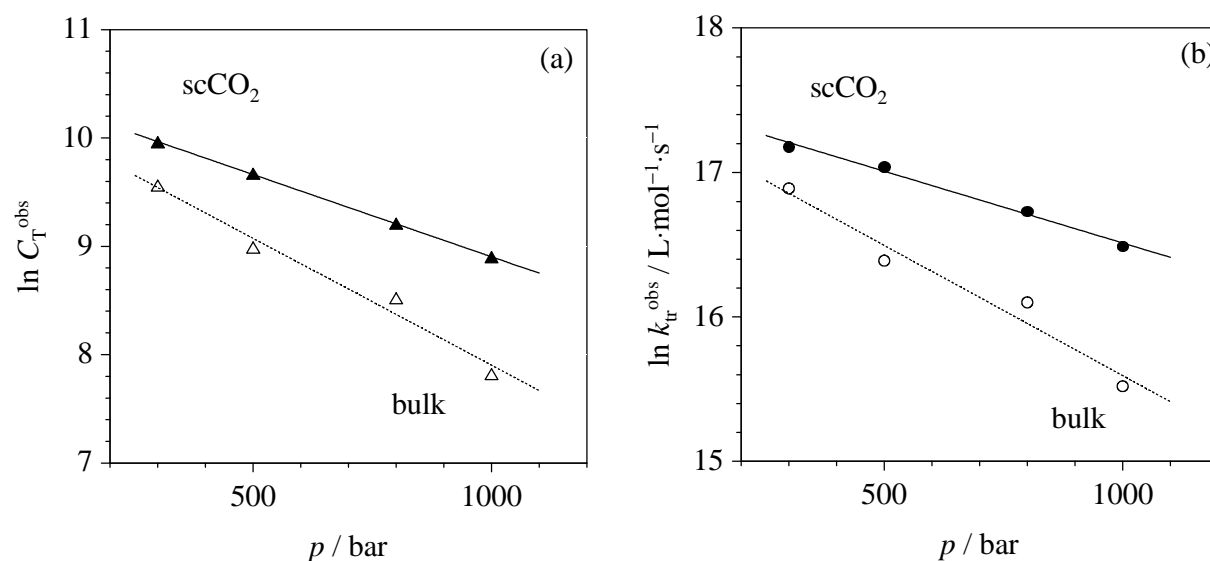


Figure 5.16: Pressure dependence of the chain-transfer constant (a) and of the chain-transfer rate coefficient (b) for MMA homopolymerizations in bulk and in 40 wt % CO_2 at 80°C. Experimental data are listed in Appendix 3.

As seen in Fig. 5.16, C_T^{obs} decreases with increasing pressure, which is slightly more pronounced in bulk than in scCO₂. In addition, $k_{\text{tr}}^{\text{obs}}$ determined in bulk and in scCO₂ polymerizations decreases with increasing pressure.

The values of $k_{\text{tr}}^{\text{obs}}$, reported in Appendix 3, are very high in the range of $10^7 \text{ L}\cdot\text{mol}^{-1}\cdot\text{s}^{-1}$ and are similar in size to the rate coefficients for bimolecular termination reactions in free-radical polymerizations, which are known to be diffusion controlled¹⁷. This finding will be discussed in section 5.4.

Eqs. 5.13 to 5.16 correspond to the linear fits of the experimental data for C_T^{obs} and $k_{\text{tr}}^{\text{obs}}$ given in Fig. 5.16.

$$\ln C_T^{\text{obs}} = (10.2 \pm 0.2) - (2.33 \pm 0.80) \cdot 10^{-3} (p / \text{bar}) \quad (5.13)$$

$$\ln [k_{\text{tr}}^{\text{obs}} / (\text{L}\cdot\text{mol}^{-1}\cdot\text{s}^{-1})] = (17.4 \pm 0.3) - (1.61 \pm 0.54) \cdot 10^{-3} (p / \text{bar}) \quad (5.14)$$

(bulk, 80°C, $300 \leq p \leq 1000 \text{ bar}$)

$$\ln C_T^{\text{obs}} = (10.4 \pm 0.2) - (1.51 \pm 0.41) \cdot 10^{-3} (p / \text{bar}) \quad (5.15)$$

$$\ln [k_{\text{tr}}^{\text{obs}} / (\text{L}\cdot\text{mol}^{-1}\cdot\text{s}^{-1})] = (17.5 \pm 0.16) - (1.07 \pm 0.25) \cdot 10^{-3} (p / \text{bar}) \quad (5.16)$$

(40 wt % scCO₂, 80°C, $300 \leq p \leq 1000 \text{ bar}$)

According to $\delta (\ln k_{\text{tr}}) / \delta p = -\Delta V^{\#} / (R \cdot T)$ and $\delta (\ln C_T) / \delta p = -\Delta V^{\#} / (R \cdot T)$, the activation volumes for C_T and k_{tr} are calculated as:

$$\text{bulk: } \Delta V^{\#}(C_T^{\text{obs}}) = + (68.7 \pm 23.5) \text{ cm}^3 \cdot \text{mol}^{-1} \quad \Delta V^{\#}(k_{\text{tr}}^{\text{obs}}) = + (47.5 \pm 15.8) \text{ cm}^3 \cdot \text{mol}^{-1}$$

$$\text{scCO}_2: \Delta V^{\#}(C_T^{\text{obs}}) = + (44.3 \pm 12.1) \text{ cm}^3 \cdot \text{mol}^{-1} \quad \Delta V^{\#}(k_{\text{tr}}^{\text{obs}}) = + (31.5 \pm 7.3) \text{ cm}^3 \cdot \text{mol}^{-1}$$

The above given activation volumes for C_T^{obs} and $k_{\text{tr}}^{\text{obs}}$ demonstrate the strong pressure dependence of the transfer reaction in bulk and in scCO₂ polymerizations. Within experimental uncertainty, $\Delta V^{\#}(k_{\text{tr}}^{\text{obs}})$ and $\Delta V^{\#}(C_T^{\text{obs}})$ are close in bulk and in scCO₂. The activation volumes of $\Delta V^{\#}(k_{\text{tr}}^{\text{obs}})$, in the range of $+35 \text{ cm}^3 \cdot \text{mol}^{-1}$, are surprisingly high. For comparison, $\Delta V^{\#}$ of the termination rate coefficient is typically in the order of $20 \text{ cm}^3 \cdot \text{mol}^{-1}$. These findings will be discussed in section 5.4.

The C_T^{obs} value of $2.68 \cdot 10^4$, which is extrapolated to ambient pressure via Eq. 5.13 in bulk, is in the same order of magnitude as C_T^{obs} of $21.5 \cdot 10^3$ determined at 60°C and 1 bar in section

5.2.1. Thus, this extrapolated value is in good agreement with the literature data¹² determined at 1 bar and 60°C in the range from $19.5 \cdot 10^3$ to $25.8 \cdot 10^3$. Davis et al¹³ performed polymerizations of MMA in 80 wt % scCO₂ at 50°C and 150 bar. The reported C_T^{obs} value was $1.13 \cdot 10^5$, which is approximately one order of magnitude higher than C_T^{obs} of $2.62 \cdot 10^4$ extrapolated to 150 bar, in 40 wt % scCO₂ via Eq. 5.15. The difference is certainly due to the fact that pressure, temperature, and CO₂ content are not the same. More details about this aspect are given in section 5.4.

5.2.3 Homopolymerization of styrene

The only study¹⁴ on the temperature dependence of catalytic chain-transfer polymerizations of styrene reported in the literature up to date indicates a different behavior as observed in MMA polymerizations: Although a large scatter in the data, C_T^{obs} appears to decrease with temperature at ambient pressure. This induces that k_{tr} is only slightly temperature dependent. Informations on the pressure dependence of C_T^{obs} and $k_{\text{tr}}^{\text{obs}}$ as well as the influence of scCO₂ on CCT in styrene polymerizations are not yet available.

In the following section, the pressure dependence of $k_{\text{tr}}^{\text{obs}}$ and C_T^{obs} and the influence of scCO₂ as a solvent in styrene polymerization are investigated.

Fig. 5.17a shows the molecular weight distributions for polystyrene obtained in 40 wt % scCO₂ at 80°C and 300 bar with different amounts of CPhBF. The MWDs are shifted to lower molecular weights when the concentration of the cobalt-complex increases. In the absence of CPhBF, the reaction yields polymer with a M_w of $3.77 \cdot 10^5 \text{ g} \cdot \text{mol}^{-1}$ and upon the addition of $7 \cdot 10^{-5}$ wt % of CPhBF ($[\text{CPhBF}]/[\text{sty}] = 10^{-7}$), the M_w decreases to $1.9 \cdot 10^5 \text{ g} \cdot \text{mol}^{-1}$.

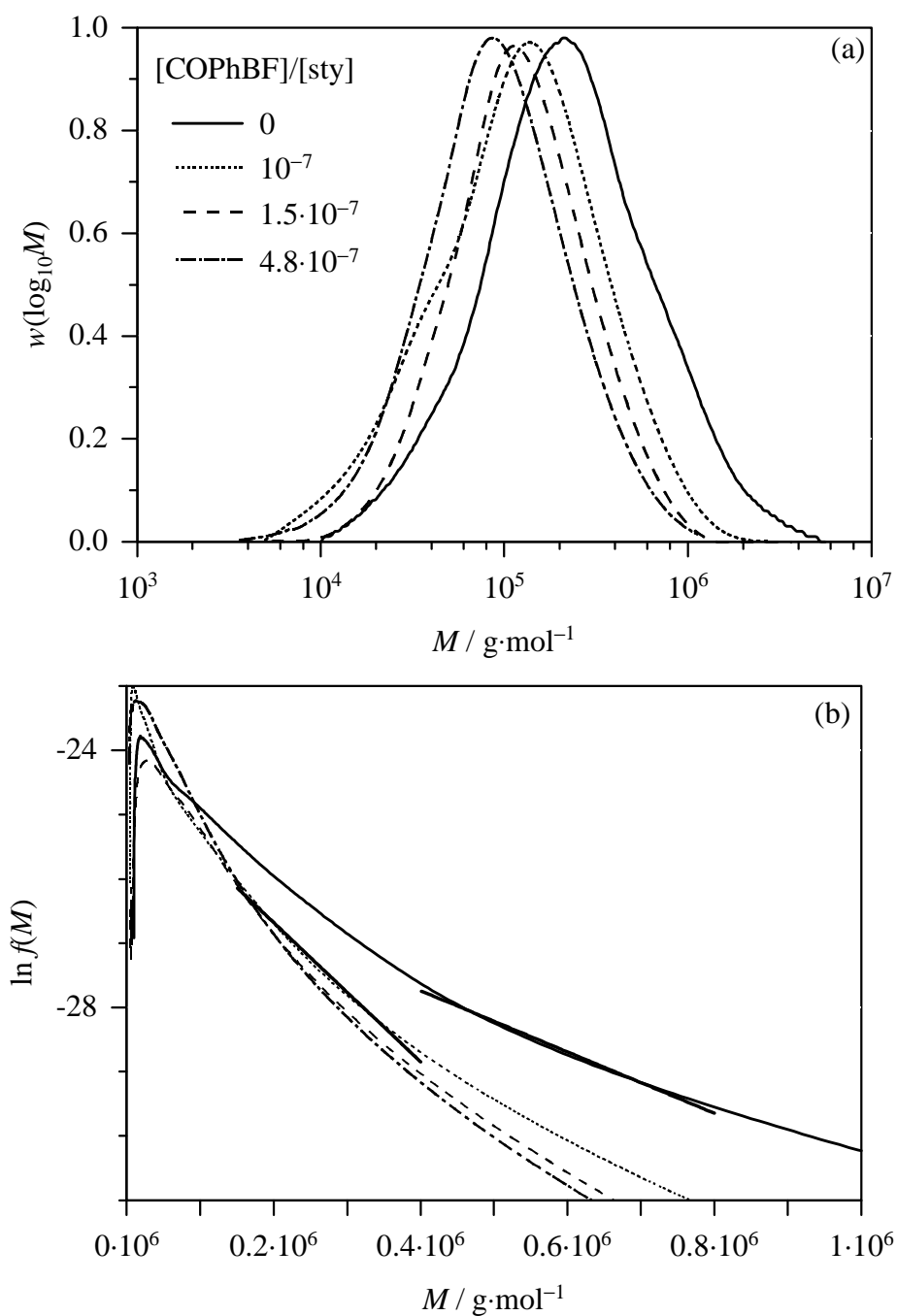


Figure 5.17: Molecular weight distributions (a) and corresponding $\ln f(M)$ vs. M plots (b) of polystyrene from polymerizations in 40 wt % scCO_2 at 80°C and 300 bar and COPhBF concentration as indicated. The bold lines indicate the region where the slope is measured for $[COPhBF]/[styrene] = 0$ and 10^{-7} .

As expected, the corresponding $\ln f(M)$ vs. M plots (Fig. 5.17b) show that the slope increases with increasing the amount of the complex. Although the slopes represented by the bold lines seem to be not linear, correlation coefficients of 0.998 are obtained. This indicates that the

slight curvature of the plot may not affect the determination of C_T (for comparison see section 4). The CLD plots for polymerizations in bulk and in 40 wt % scCO₂ at 80°C and 300 bar are pictured in Fig. 5.18.

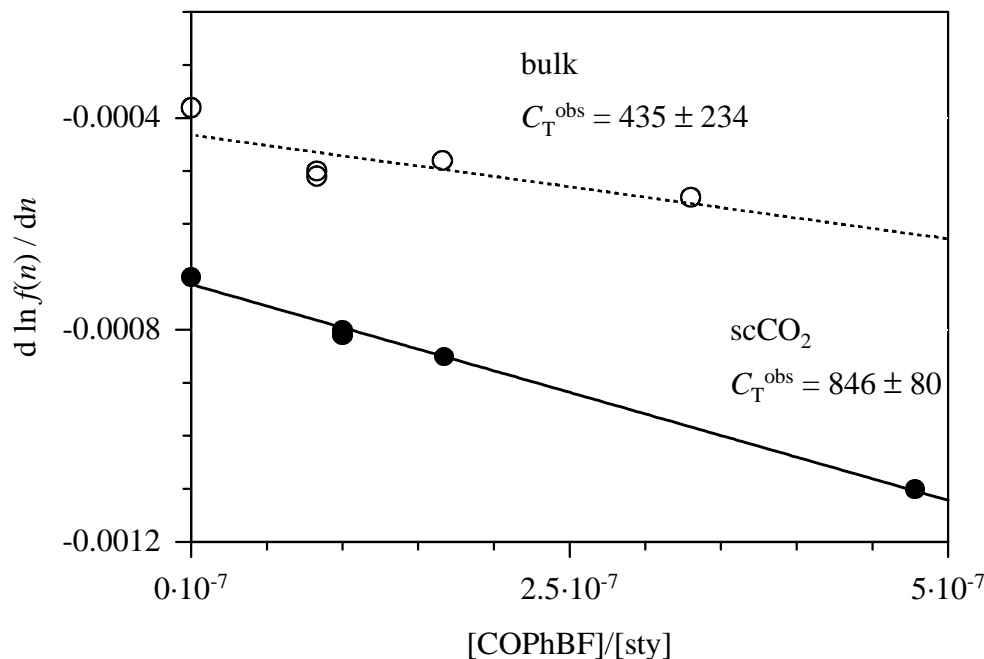


Figure 5.18: CLD plots for styrene homopolymerizations in 40 wt % scCO₂ (full circles) and in bulk (open circles) at 80°C and 300 bar.

The C_T^{obs} values determined are (846 ± 80) and (435 ± 234) in scCO₂ and in bulk, respectively. The influence of scCO₂ on the chain-transfer activity of COPhBF is not obvious: The significant error calculated in bulk polymerization shows that scCO₂ has probably a little influence in the C_T^{obs} value.

Pressure dependence of k_{tr} and C_T

The pressure dependence of C_T^{obs} and k_{tr}^{obs} was determined varying the pressure between 300 and 1000 bar. The k_{tr}^{obs} values were calculated from the experimental C_T^{obs} values and the k_p values reported in the literature^{5,6} under the same conditions of pressure and temperature, which are listed in Appendix 1. Fig. 5.19 shows the pressure dependence of C_T^{obs} and k_{tr}^{obs} in styrene homopolymerizations at 80°C.

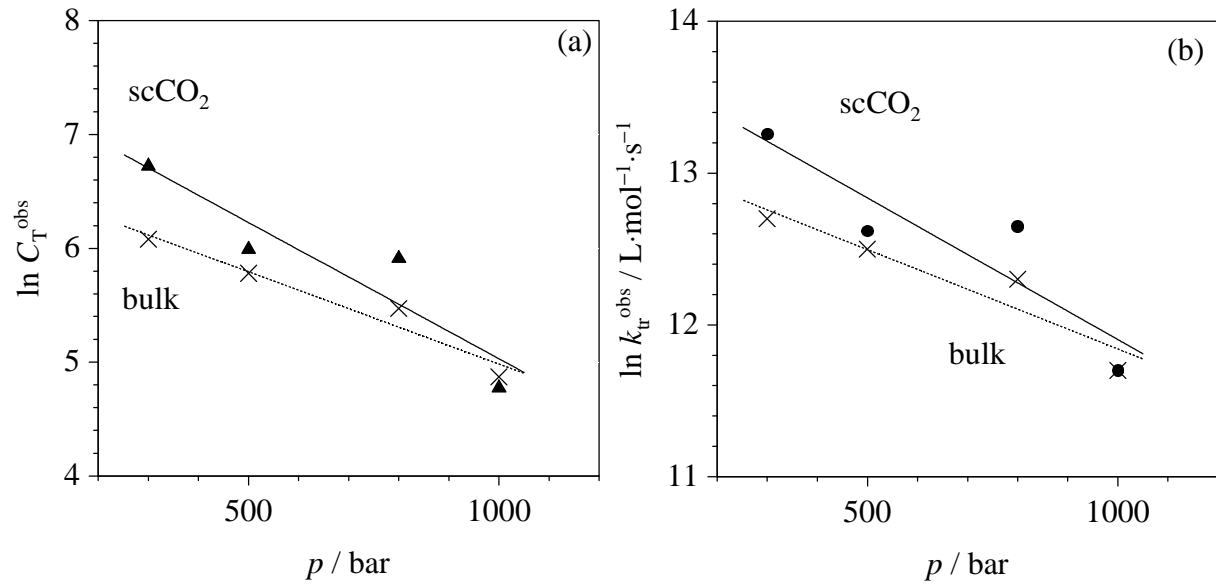


Figure 5.19: Pressure dependence of the chain-transfer constant (a) and the chain-transfer rate coefficient (b) for styrene homopolymerizations in bulk and in 40 wt % CO_2 at 80°C . Experimental data are listed in Appendix 3.

Fig. 5.19 shows a large scatter in the data, which is stronger in scCO_2 . C_T and k_{tr} decrease with increasing pressure in bulk and in scCO_2 . The values determined at 500 and 1000 bar are almost equivalent in bulk and in scCO_2 . In contrast, the values determined at 300 and 800 bar differ in both media. Nevertheless, considering the significant errors calculated in C_T^{obs} and k_{tr}^{obs} , the values are close in both media in the entire pressure range which indicates that C_T and k_{tr} in styrene polymerization at 300 bar are not influenced by scCO_2 .

The pressure dependence of C_T^{obs} and k_{tr}^{obs} may be expressed by Eqs. 5.17-5.20:

$$\ln C_T^{\text{obs}} = (6.60 \pm 0.18) - (1.62 \pm 0.52) \cdot 10^{-3} (p / \text{bar}) \quad (5.17)$$

$$\ln [k_{tr}^{\text{obs}} / (\text{L} \cdot \text{mol}^{-1} \cdot \text{s}^{-1})] = (13.2 \pm 0.2) - (1.31 \pm 0.33) \cdot 10^{-3} (p / \text{bar}) \quad (5.18)$$

(bulk, 80°C , $300 \leq p \leq 1000$ bar)

$$\ln C_T^{\text{obs}} = (7.42 \pm 0.49) - (2.39 \pm 0.69) \cdot 10^{-3} (p / \text{bar}) \quad (5.19)$$

$$\ln [k_{tr}^{\text{obs}} / (\text{L} \cdot \text{mol}^{-1} \cdot \text{s}^{-1})] = (13.8 \pm 0.4) - (1.86 \pm 0.63) \cdot 10^{-3} (p / \text{bar}) \quad (5.20)$$

(40 wt % scCO_2 , 80°C , $300 \leq p \leq 1000$ bar)

The corresponding activation volumes in bulk and in 40 wt % scCO₂ are as follows:

$$\text{bulk: } \Delta V^\#(C_T^{\text{obs}}) = + (45.6 \pm 15.3) \text{ cm}^3 \cdot \text{mol}^{-1} \quad \Delta V^\#(k_{\text{tr}}^{\text{obs}}) = + (38.5 \pm 9.6) \text{ cm}^3 \cdot \text{mol}^{-1}$$

$$\text{scCO}_2: \Delta V^\#(C_T^{\text{obs}}) = + (70.2 \pm 20.3) \text{ cm}^3 \cdot \text{mol}^{-1} \quad \Delta V^\#(k_{\text{tr}}^{\text{obs}}) = + (54.6 \pm 18.4) \text{ cm}^3 \cdot \text{mol}^{-1}$$

The above activation volumes for C_T^{obs} and $k_{\text{tr}}^{\text{obs}}$ indicate a strong pressure dependence of the transfer reaction in both media. The activation volumes in bulk and in scCO₂ are very close considering the uncertainty in $\Delta V^\#$. As seen in MMA polymerization, $\Delta V^\#$ for $k_{\text{tr}}^{\text{obs}}$ is exceptionally high, as compared to the activation volume of the termination rate coefficient. Eq. 5.17 is used to extrapolate C_T^{obs} to ambient pressure at 80°C. The value of 733 obtained is in very good agreement with the literature data¹², ranging from 478 to 718.

5.2.4 Copolymerization of styrene and MMA

Copolymerizations of styrene and MMA were investigated at 80°C and at pressures between 300 and 1000 bar.

The MWDs obtained for copolymers ($f_S = 0.2$) in bulk and in scCO₂ at 80°C and 300 bar are pictured in Fig. 5.20. The MWDs in bulk and in scCO₂ are shifted to lower values with increasing CPhBF concentration. In addition, the MWDs in scCO₂ are shifted to lower values compared to bulk MWDs. For example, the copolymerization performed with 8·10⁻⁵ wt % of CPhBF (lowest CTA concentration in Fig. 5.20) generates M_w of 1.85·10⁵ g·mol⁻¹ and 5.7·10⁴ g·mol⁻¹ in bulk and in scCO₂, respectively. This indicates that the transfer activity of CPhBF is strongly increased due to the presence of scCO₂.

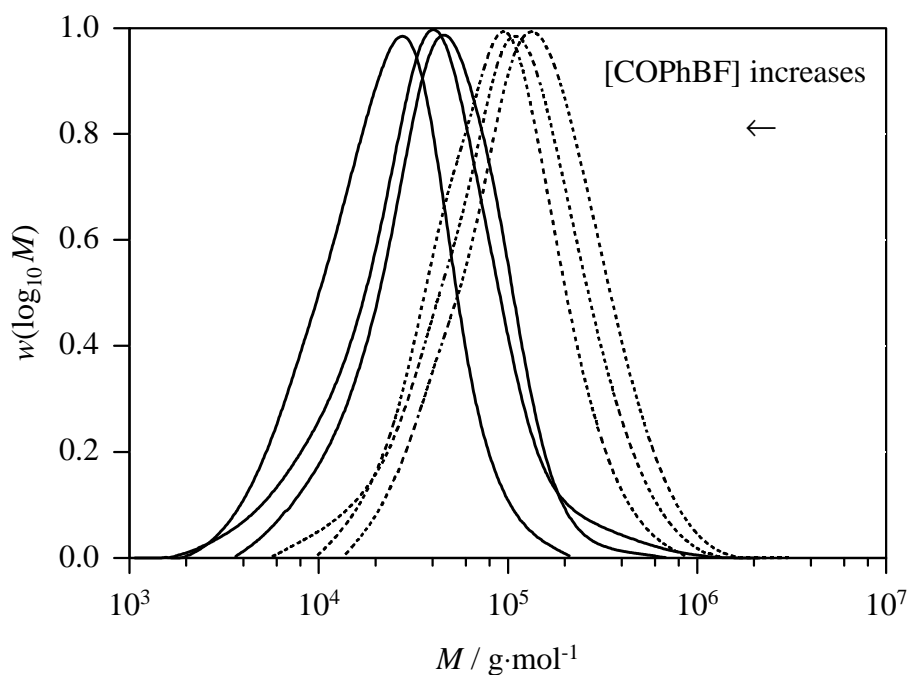


Figure 5.20: Molecular weight distributions of styrene-MMA copolymers ($f_S = 0.2$) obtained in 40 wt % $scCO_2$ (full line) and in bulk (dotted line) at $80^\circ C$ and 300 bar varying the amount of COPhBF. $[COPhBF]/[M]$ range is from 1.5×10^{-7} to 4.6×10^{-7} and from 1.5×10^{-7} to 5.8×10^{-7} in bulk and in $scCO_2$, respectively.

Fig. 5.21 summarizes the CLD plots obtained in styrene and MMA copolymerization with $f_S = 0.2, 0.5,$ and 0.8 , at $80^\circ C$, 300 bar, in bulk and in $scCO_2$. For copolymerization with f_S of 0.2 and 0.5, the C_T^{obs} values are approximately by a factor of 3 higher in $scCO_2$ than in bulk, which indicates a strong effect on C_T^{obs} of $scCO_2$ as a solvent. In polymerizations with $f_S = 0.8$, the bulk data are very scattered and the C_T^{obs} values are equivalent in both media, which indicates that $scCO_2$ has no significant influence in C_T^{obs} .

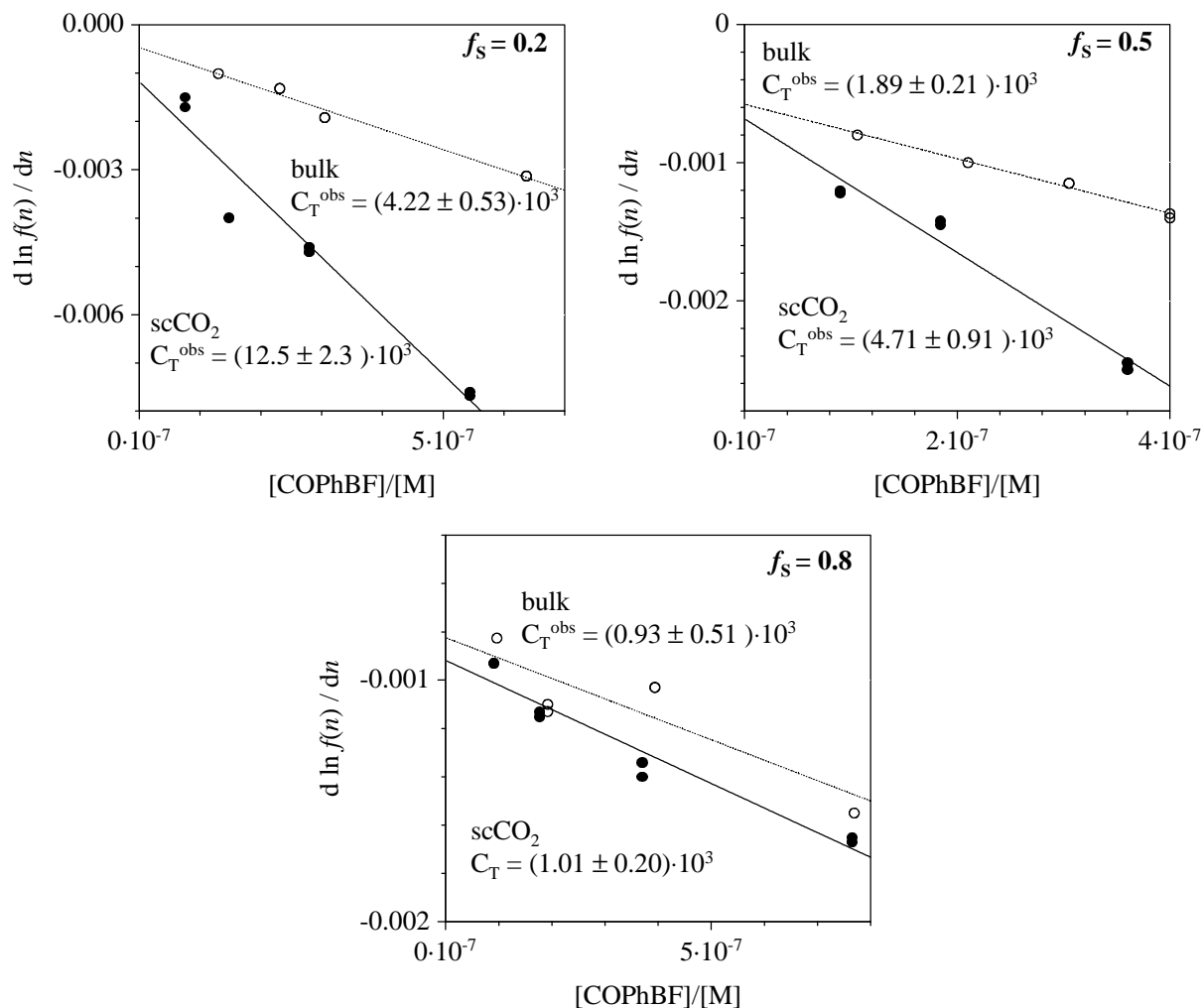


Figure 5.21: CLD plots for copolymerizations of styrene and MMA at f_s of 0.2, 0.5, and 0.8, 80°C, 300 bar, in 40 wt % $scCO_2$ (full circles) and in bulk (open circles).

The variation of C_T^{obs} with f_s for copolymerizations at 80°C, 300 bar in bulk and in $scCO_2$ is shown in Fig. 5.22. C_T^{obs} decreases with increasing f_s in both media, which indicates that C_T^{obs} in styrene polymerizations is lower than C_T^{obs} in MMA polymerizations. Indeed, at 300 bar in both media $C_{T,MMA}^{obs}$ is more than one order of magnitude higher than $C_{T,styrene}^{obs}$. The variation of C_T^{obs} with f_s is different in bulk and in $scCO_2$: C_T^{obs} in bulk shows a stronger decrease compared to C_T^{obs} in $scCO_2$, when a little amount of styrene is added in the copolymerization. C_T^{obs} in $scCO_2$ are $2.11 \cdot 10^4$ and $1.25 \cdot 10^4$ at $f_s = 0$ and 0.2, respectively, whereas C_T^{obs} in bulk are $1.41 \cdot 10^4$ and $4.22 \cdot 10^3$ at $f_s = 0$ and 0.2, respectively. At $f_s = 0.8$, C_T^{obs} are equivalent in bulk and in $scCO_2$. These findings and the preceding observations in the homopolymerizations suggest that at high f_s , C_T^{obs} are equivalent in bulk and in $scCO_2$.

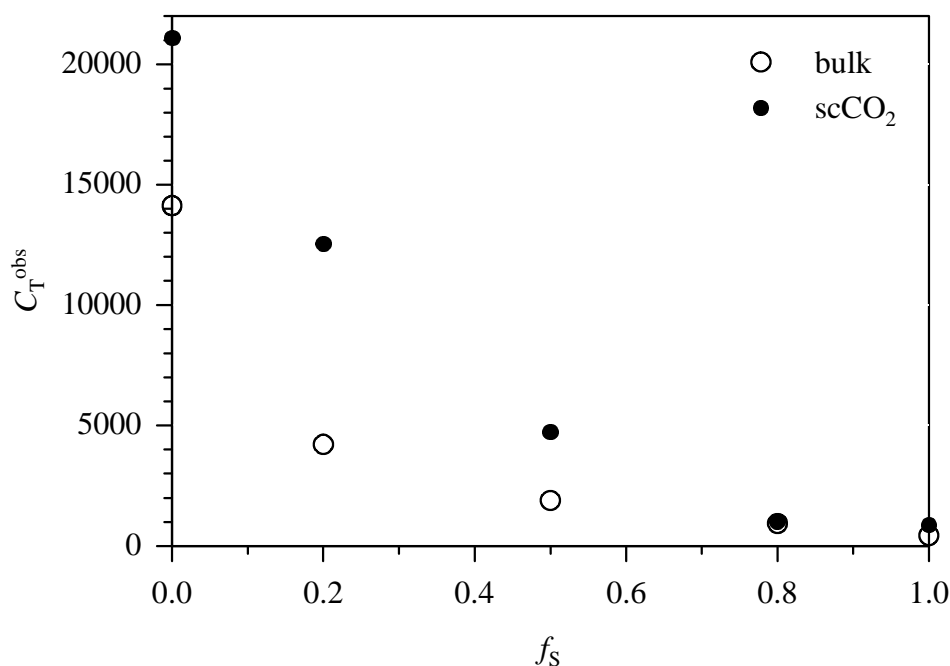


Figure 5.22: Variation of the chain-transfer constant with the mole fraction of styrene in the monomer feed for polymerization of styrene and MMA in bulk (open circles) and in scCO₂ (full circles) at 80°C and 300 bar. The experimental data are listed in Appendix 3.

The next plot shows the comparison of the variation of C_T^{obs} with f_S in bulk obtained in this work (80°C and 300 bar) and reported in literature⁹ (1 bar and 40°C).

The variation of C_T^{obs} with f_S is the same here and in the literature: C_T^{obs} decreases with increasing f_S . As already mentioned, literature reported that C_T^{obs} is independent on the temperature in MMA homopolymerization^{14,15,16}, whereas a decrease in C_T^{obs} is observed when the temperature increases in styrene homopolymerization¹⁴. C_T^{obs} reported at 40°C and 1 bar are slightly higher than C_T^{obs} determined in this work at 80°C and 300 bar. It is obvious that C_T^{obs} decreases with increasing pressure independently of the temperature.

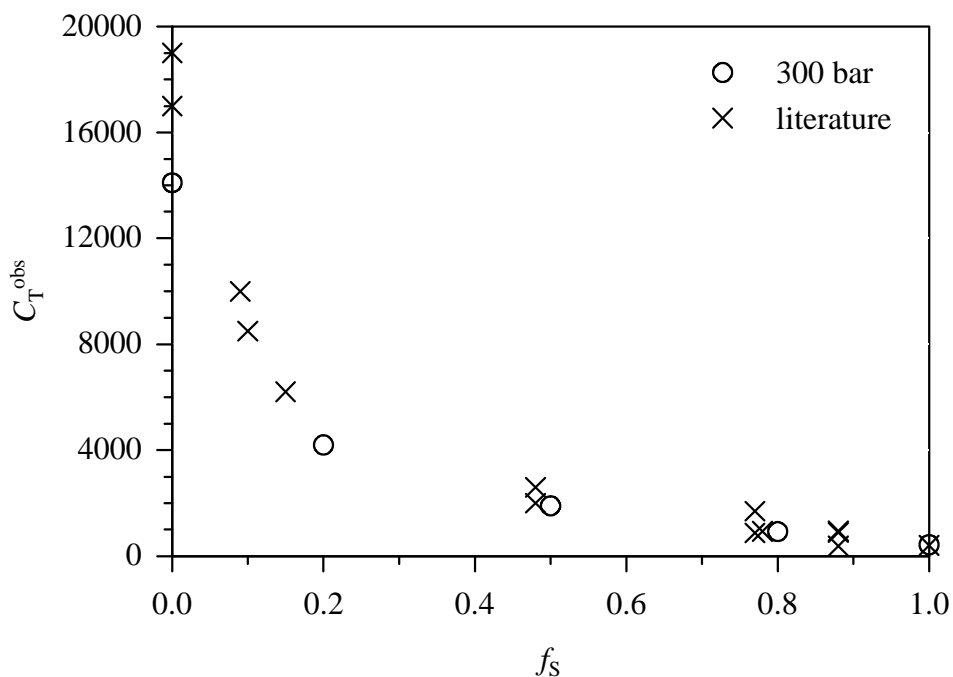


Figure 5.23: Dependence of the chain-transfer constant on the mole fraction of styrene in the monomer feed for copolymerizations in bulk at 80°C and 300 bar. The literature data measured in bulk at 40°C and 1 bar (×) are taken from ref. 9. Experimental data are listed in Appendix 3.

The corresponding k_{tr}^{obs} values were obtained from C_T^{obs} measured and the copolymerizations k_p data, listed in Appendix 1, which were obtained as explained in section 6. The variation of $\ln k_{tr}^{obs}$ with f_S is shown in Fig. 5.24: The left hand side (a) shows the variation of k_{tr}^{obs} in bulk and in scCO₂ and on the right hand side (b) k_{tr}^{obs} obtained in bulk are compared with the literature data.

Fig. 5.24a clearly shows that $\ln k_{tr}^{obs}$ decreases linearly with increasing f_S in bulk and in scCO₂. The lines fitted to the k_{tr}^{obs} data obtained in both media are parallel, which is also seen in Fig 5.24b. The variation of $\ln k_{tr}^{obs}$ with f_S is the same for the different systems, which indicates that the variation of $\ln k_{tr}^{obs}$ with f_S is independent of the reaction conditions (pressure, temperature, and reaction medium).

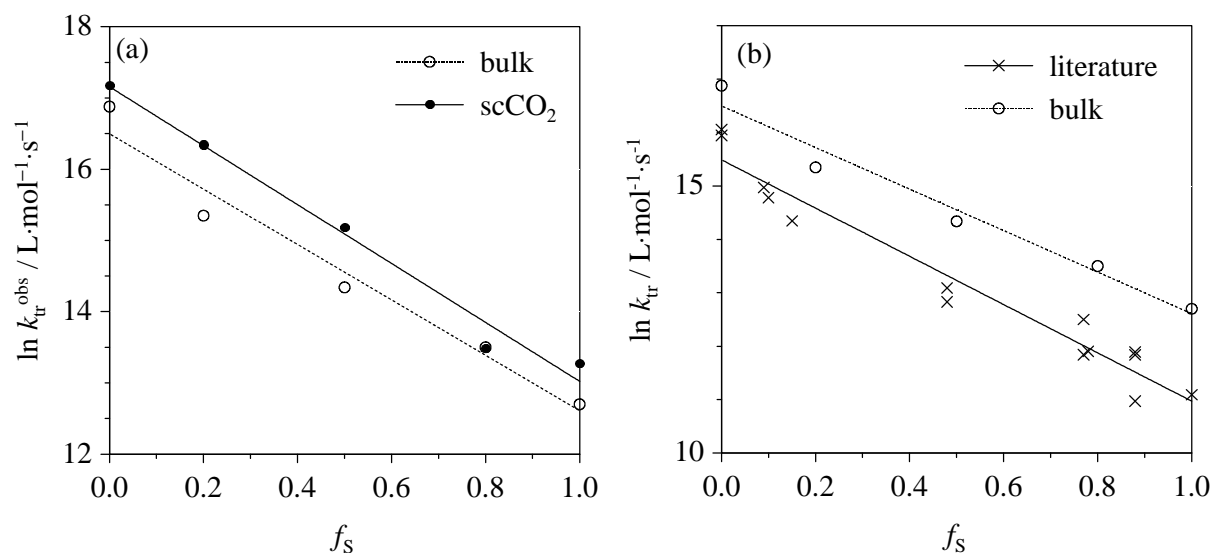


Figure 5.24: Variation of the chain-transfer rate coefficient with the mole fraction of styrene in the monomer feed for copolymerization of styrene and MMA in bulk (open circles) and in 40 wt % scCO₂ (full circles) at 80°C and 300 bar. The literature data (x) were calculated using the parameters (C_T^{obs} and k_p) determined in bulk at 40°C and 1 bar, which are listed in ref. 9. Experimental data are listed in Appendix 3.

As seen for MMA homopolymerizations, the k_{tr} values determined at $f_s = 0.2$ in scCO₂ are very high in the range of $10^7 \text{ L}\cdot\text{mol}^{-1}\cdot\text{s}^{-1}$ and are similar in size to the rate coefficients obtained for bimolecular termination reactions in free-radical polymerizations, which are known to be diffusion-controlled¹⁷.

Pressure dependence of k_{tr} and C_T

Fig. 5.25 shows the pressure dependence of C_T^{obs} and k_{tr}^{obs} for copolymerizations of styrene and MMA ($f_s = 0.5$) in bulk and in scCO₂ at 80°C and 300 bar.

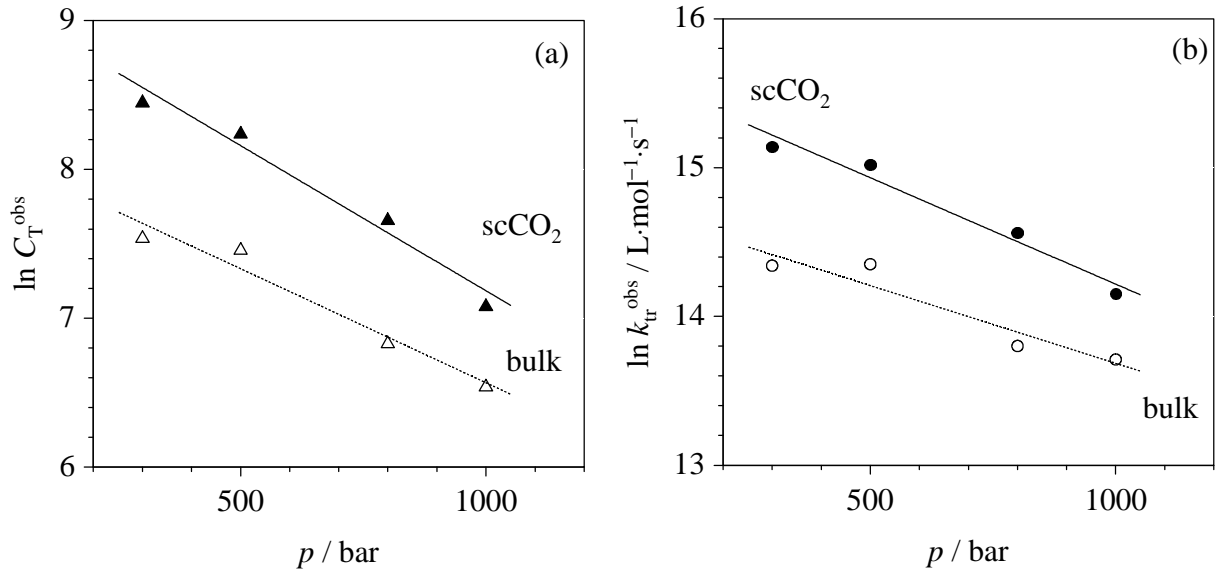


Figure 5.25: Pressure dependence of the chain-transfer rate constant (a) and of the chain-transfer rate coefficient (b) for copolymerizations of styrene and MMA ($f_S = 0.5$) at 80°C . Experimental data are listed in Appendix 3.

C_T^{obs} and $k_{\text{tr}}^{\text{obs}}$ decrease with increasing pressure in both media, which is slightly more pronounced in scCO_2 than in bulk.

The pressure dependence of C_T and k_{tr} may be expressed by Eqs 5.21-5.24.

$$\ln C_T^{\text{obs}} = (8.10 \pm 0.15) - (1.53 \pm 0.44) \cdot 10^{-3} (p / \text{bar}) \quad (5.21)$$

$$\ln [k_{\text{tr}}^{\text{obs}} / (\text{L}\cdot\text{mol}^{-1}\cdot\text{s}^{-1})] = (14.7 \pm 0.2) - (1.02 \pm 0.23) \cdot 10^{-3} (p / \text{bar}) \quad (5.22)$$

(bulk, $f_S = 0.5$, 80°C , $300 \leq p \leq 1000$ bar)

$$\ln C_T^{\text{obs}} = (9.14 \pm 0.17) - (1.95 \pm 0.48) \cdot 10^{-3} (p / \text{bar}) \quad (5.23)$$

$$\ln [k_{\text{tr}}^{\text{obs}} / (\text{L}\cdot\text{mol}^{-1}\cdot\text{s}^{-1})] = (15.6 \pm 0.1) - (1.43 \pm 0.19) \cdot 10^{-3} (p / \text{bar}) \quad (5.24)$$

(40 wt % scCO_2 , $f_S = 0.5$, 80°C , $300 \leq p \leq 1000$ bar)

The corresponding activation volumes in scCO_2 and in bulk are as follows:

$$\text{bulk: } \Delta V^\#(C_T^{\text{obs}}) = + (44.9 \pm 12.9) \text{ cm}^3\cdot\text{mol}^{-1} \quad \Delta V^\#(k_{\text{tr}}^{\text{obs}}) = + (29.9 \pm 6.8) \text{ cm}^3\cdot\text{mol}^{-1}$$

$$\text{scCO}_2: \Delta V^\#(C_T^{\text{obs}}) = + (57.2 \pm 14.1) \text{ cm}^3\cdot\text{mol}^{-1} \quad \Delta V^\#(k_{\text{tr}}^{\text{obs}}) = + (42.0 \pm 6.7) \text{ cm}^3\cdot\text{mol}^{-1}$$

The activation volumes for C_T^{obs} and $k_{\text{tr}}^{\text{obs}}$ indicate a strong pressure dependence in bulk and in scCO₂ as seen for the homopolymerization systems. Within experimental uncertainty, $\Delta V^\ddagger(k_{\text{tr}}^{\text{obs}})$ and $\Delta V^\ddagger(C_T^{\text{obs}})$ are similar in both media: In the range of +50 and +35 cm³·mol⁻¹ for C_T^{obs} and $k_{\text{tr}}^{\text{obs}}$, respectively. C_T^{obs} is extrapolated to ambient pressure via Eq. 5.21 resulting in $C_T^{\text{obs}} = 3.3 \cdot 10^3$, which is in very good agreement with the literature data of $3.3 \cdot 10^3$ reported at 40°C and $f_S = 0.48$.

5.2.5 Closing remarks

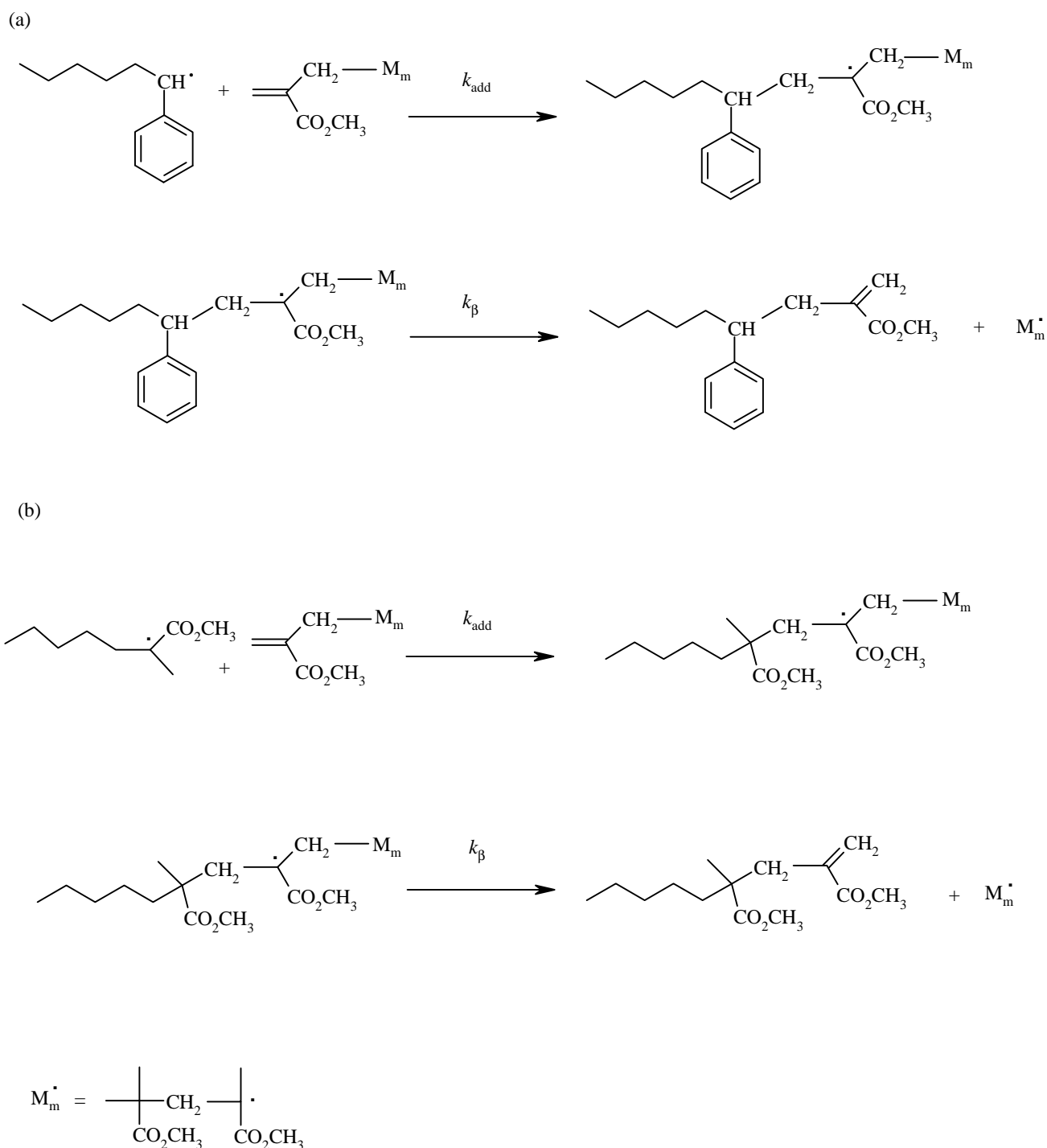
As mentioned before, the C_T^{obs} data calculated are based on the reaction scheme 5.2, such as all the C_T^{obs} values reported in the literature. However, recently a carbon-cobalt bond formation was directly measured in methyl acrylate polymerization¹⁸. The authors reported that this effect may be also seen in styrene homopolymerization. Thus, the $k_{\text{tr}}^{\text{obs}}$ values determined in this work in styrene and MMA copolymerizations and in styrene homopolymerization may be not accurate. $k_{\text{tr}}^{\text{obs}}$ determined in these conditions may be underestimated as explained in more details in section 5.4.

The Table below summarizes the results obtained for homo- and copolymerization of MMA and styrene in bulk and in scCO₂ at 80°C and 800 bar with CPhBF as catalytic chain-transfer agent.

MMA		
	C_T^{obs}	$k_{\text{tr}}^{\text{obs}}$
scCO₂	$(10.0 \pm 1.5) \cdot 10^3$	$(18.6 \pm 4.5) \cdot 10^6 \text{ L} \cdot \text{mol}^{-1} \cdot \text{s}^{-1}$
bulk	$(5.01 \pm 8.30) \cdot 10^3$	$(9.82 \pm 2.62) \cdot 10^6 \text{ L} \cdot \text{mol}^{-1} \cdot \text{s}^{-1}$
scCO₂ influence	influence in the entire pressure range	influence in the entire pressure range
DV[#] / cm³·mol⁻¹	<i>bulk</i> : + (68.7 ± 23.5) <i>scCO₂</i> : + (44.3 ± 12.1)	<i>bulk</i> : + (47.5 ± 15.8) <i>scCO₂</i> : + (31.5 ± 7.3)
styrene		
	C_T^{obs}	$k_{\text{tr}}^{\text{obs}}$
scCO₂	376 ± 45	$(3.12 \pm 0.72) \cdot 10^5 \text{ L} \cdot \text{mol}^{-1} \cdot \text{s}^{-1}$
bulk	237 ± 15	$(2.19 \pm 0.36) \cdot 10^5 \text{ L} \cdot \text{mol}^{-1} \cdot \text{s}^{-1}$
scCO₂ influence	no influence in the entire pressure range	no influence in the entire pressure range
DV[#] / cm³·mol⁻¹	<i>bulk</i> : + (45.6 ± 15.3) <i>scCO₂</i> : + (70.2 ± 20.3)	<i>bulk</i> : + (38.5 ± 9.6) <i>scCO₂</i> : + (54.6 ± 18.4)
styrene / MMA ($f_s = 0.5$)		
	C_T^{obs}	$k_{\text{tr}}^{\text{obs}}$
scCO₂	$(2.15 \pm 0.38) \cdot 10^3$	$(21.1 \pm 6.3) \cdot 10^5 \text{ L} \cdot \text{mol}^{-1} \cdot \text{s}^{-1}$
bulk	$(0.93 \pm 0.08) \cdot 10^3$	$(10.1 \pm 2.1) \cdot 10^5 \text{ L} \cdot \text{mol}^{-1} \cdot \text{s}^{-1}$
scCO₂ influence	influence in the entire pressure range	influence in the entire pressure range
DV[#] / cm³·mol⁻¹	<i>bulk</i> : + (44.9 ± 12.9) <i>scCO₂</i> : + (57.3 ± 14.1)	<i>bulk</i> : + (29.9 ± 6.8) <i>scCO₂</i> : + (42.0 ± 6.7)

5.3 MMA trimer as chain-transfer agent

Methyl methacrylate macromonomers have recently become of importance as precursors to block^{19,20}, graft copolymers²¹, and as chain-transfer agents^{22,23}. Currently there are data available on the chain-transfer constants of macromonomers only for few systems^{20,23,24,25}. In addition, these investigations were only made at ambient pressure for bulk polymerizations. MMA macromonomers are usually prepared via catalytic chain-transfer polymerization, which is able to produce low molecular weight. The most favoured reaction of a macromonomer in a polymerization is the radical addition-fragmentation or β -scission reaction. Scheme 5.3 illustrates the transfer reaction of MMA trimer as chain-transfer agent in styrene (a) and MMA (b) polymerization. The first step is the addition of the radical chain to the macromonomer, which creates a macroradical. The second step of the chain-transfer reaction is a β -scission reaction of the macroradical, releasing a dead polymer and a new radical species derived from the macromonomer, which in turn can initiate residual monomer. Moad et al.²³ performed a study with several MMA macromonomers of different chain length in MMA polymerization. The chain-transfer constant for MMA dimer has been reported to be one order of magnitude lower than MMA trimer (MMA₃), whereas a little increase in C_T is seen as chain length increases to tetramer, pentamer, etc. In addition, the transfer constants showed only a small temperature dependence and no variation with conversion. In this work MMA trimer was chosen as CTA in MMA and styrene polymerizations performed at 80°C. The fraction of MMA trimer, which was contained in the macromonomer mixture (dimer, trimer, tetramer, and pentamer) provided by DuPont Performance Coatings, was isolated by fractionated distillation under reduced pressure, as described in section 3.4.4. It has been seen that the distilled MMA trimer polymerizes after few days. Thus, all experiments with one monomer were carried out with the same MMA trimer fraction. After the homopolymerization studies, several distillations of the macromonomer mixture were performed. It was observed that MMA trimer polymerized immediately after the distillation. For this reason, the copolymerizations of styrene and MMA with MMA trimer as CTA are not investigated in this work.



Scheme 5.3: Reaction scheme for the chain transfer of MMA trimer in homopolymerization of styrene (a) and MMA (b).

As mentioned before, the determination of C_T reported in the literature for macromonomers as CTAs were only investigated at ambient pressure in bulk polymerizations. Thus, in this work chain-transfer constants and chain-transfer rate coefficients of MMA trimer as CTA are

determined in bulk and in 40 wt % solution of scCO_2 in styrene and MMA homopolymerizations. The pressure dependencies of C_T and k_{tr} are also investigated in both media since the pressure dependence has never been studied so far. The PLP technique is applied using a laser pulse repetition rate of 1 Hz and $[\text{DMPA}]$ of $0.2 \text{ mmol}\cdot\text{L}^{-1}$ (see section 4 for more details). The same range of MMA trimer concentration is used for both homopolymerizations.

The detailed discussion about MMA trimer as CTA in homopolymerizations of styrene and MMA is given in section 5.4.

5.3.1 Homopolymerization of styrene

Styrene homopolymerizations were carried out with MMA trimer as chain-transfer agent at 80°C in 40 wt % scCO_2 and in bulk, varying the pressure between 300 and 1500 bar.

The MWDs of PS obtained for polymerizations in scCO_2 at 80°C , 300 bar, and various amounts of MMA trimer are shown in Fig. 5.26.

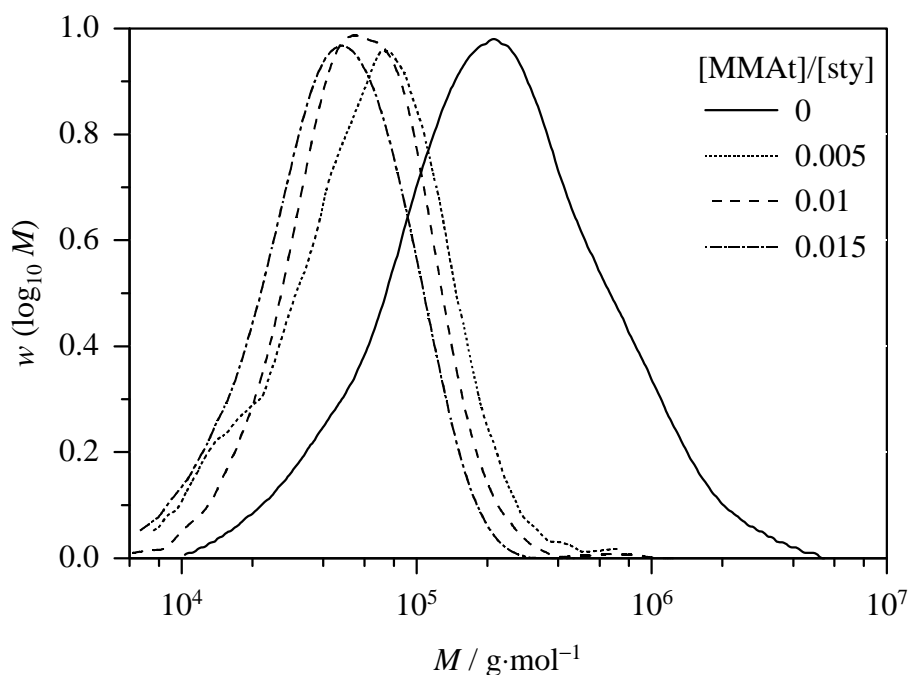


Figure 5.26: Molecular weight distributions of PS from polymerizations in 40 wt % scCO_2 at 80°C , 300 bar, and MMA trimer concentration as indicated.

The MWDs are shifted to lower molecular weights when the concentration of MMA trimer increases. In the absence of MMA trimer, the reaction yields polymer with a weight average

molecular weight of $3.77 \cdot 10^5 \text{ g} \cdot \text{mol}^{-1}$, and upon the addition of 1.5 wt % of MMA trimer ($[\text{MMA}t]/[\text{sty}] = 0.005$) M_w decreases to a value of $9.77 \cdot 10^4 \text{ g} \cdot \text{mol}^{-1}$. Therefore, the addition of only a small amount of CTA leads to a shift of the MWD to lower values.

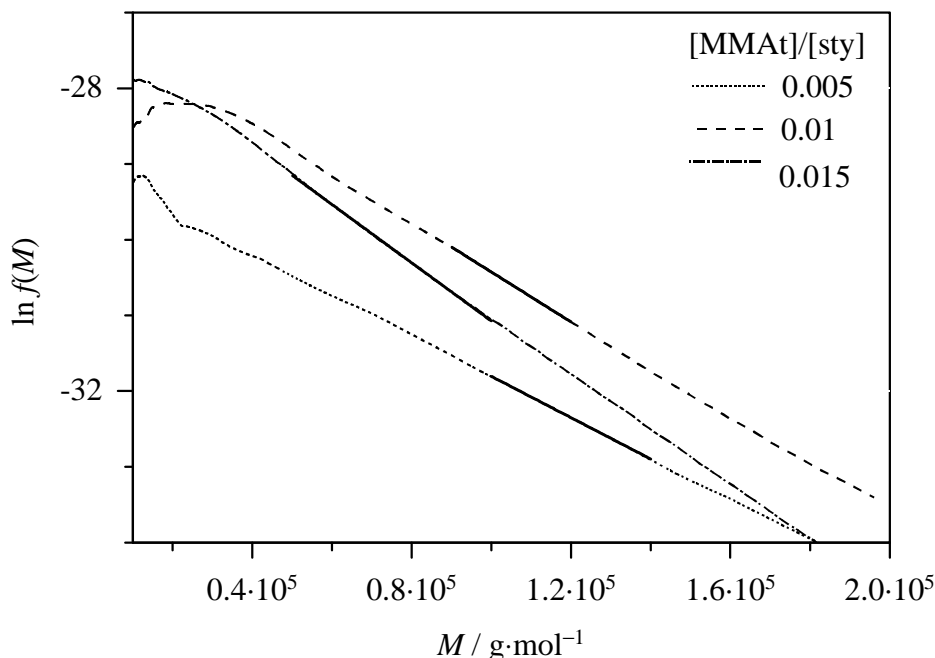


Figure 5.27: $\ln f(M)$ vs. M plots of PS from polymerizations in 40 wt % scCO_2 at 80°C and 300 bar with MMA trimer concentration as indicated. For more details see the text below.

The corresponding $\ln f(M)$ vs. M plots are pictured in Fig. 5.27. The bold line indicates the MW range for which the slope has been determined. The slope increases with increasing MMA trimer concentration as expected. Fig. 5.28 shows the so called CLD plots for styrene homopolymerizations at 80°C and 300 bar in scCO_2 and in bulk. The slopes, which give $-C_T$, are slightly different and the values of C_T determined are 0.173 ± 0.010 and 0.208 ± 0.024 in bulk and in 40 wt % scCO_2 , respectively. Within experimental uncertainty the chain-transfer constant obtained in scCO_2 is close to the bulk value, which indicates no significant influence of scCO_2 on the transfer activity of MMA trimer in styrene homopolymerization.

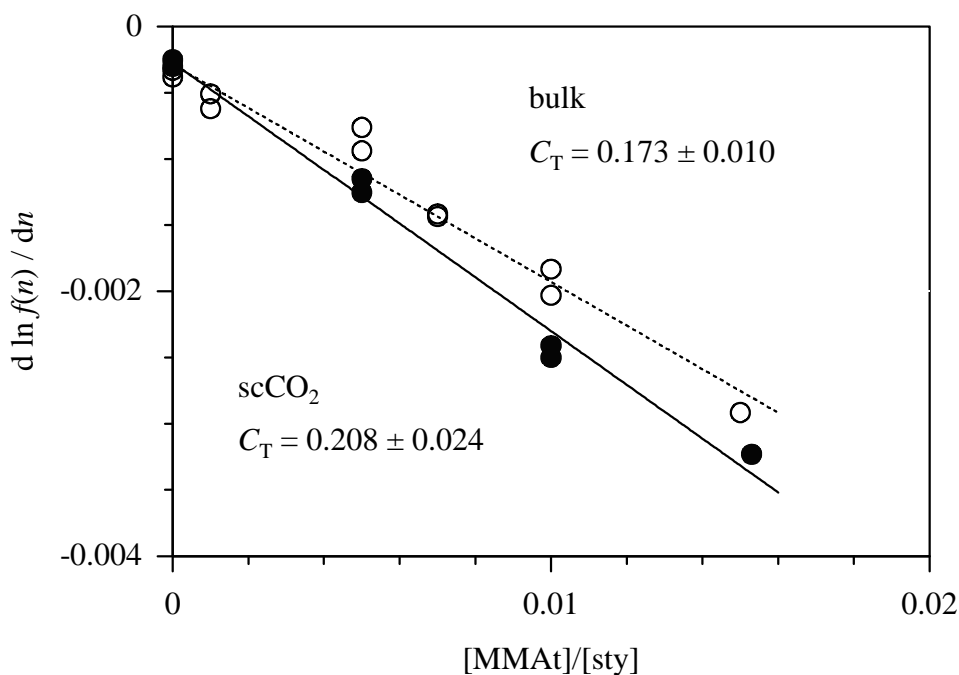


Figure 5.28: Determination of the chain-transfer constant from a plot of $d \ln f(n)/dn$ vs. $[MMA_t]/[sty]$ for styrene homopolymerizations at 80°C, 300 bar, in 40 wt % $scCO_2$ (solid line) and in bulk (dotted line).

Pressure dependence of C_T and k_{tr}

The pressure dependence of C_T and k_{tr} for the homopolymerization of styrene was studied at 80°C and pressures varying between 300 and 1500 bar*. The corresponding chain-transfer rate coefficients were determined from the C_T values obtained in this study and the propagation rate coefficients reported in the literature^{5,6} under the same conditions of pressure and temperature. The k_p values used are listed in Appendix 1.

Fig. 5.29 shows the pressure dependencies of C_T (a) and k_{tr} (b) for polymerizations at 80°C in $scCO_2$ and in bulk. C_T and k_{tr} decrease with increasing pressure in both media. It is shown that there is no significant difference in C_T and in k_{tr} in bulk and in $scCO_2$ over the entire pressure range: The $C_{T,bulk} / C_{T,scCO_2}$ values at 300 and 1500 bar are 0.83 and 0.93, respectively.

* As already explained, MMA trimer polymerizes after few days and styrene polymerization could only be studied at three pressures with the same batch of MMA trimer.

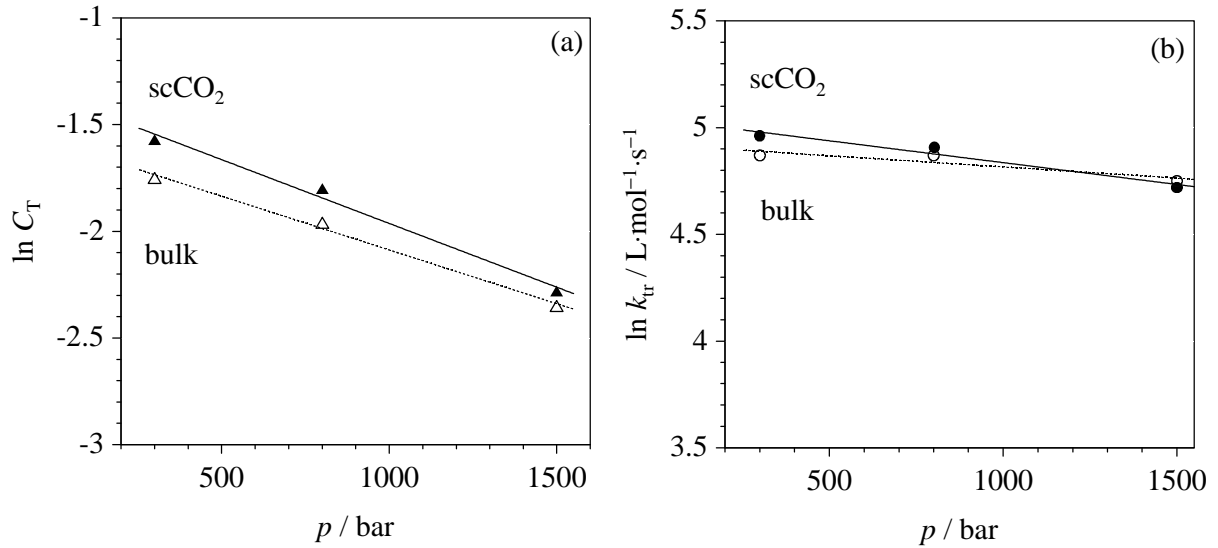


Figure 5.29: Pressure dependence of the chain-transfer constant (a) and of the chain-transfer rate coefficient (b) for styrene homopolymerizations at 80°C in 40 wt % scCO₂ and in bulk. Experimental data are reported in Appendix 4.

Eqs. 5.25 to 5.28 correspond to the linear fits of the experimental data for C_T and k_{tr} given in Fig. 5.29:

$$\ln C_T = - (1.58 \pm 0.47) - (5.05 \pm 1.64) \cdot 10^{-4} (p / \text{bar}) \quad (5.25)$$

$$\ln [k_{tr} / (\text{L} \cdot \text{mol}^{-1} \cdot \text{s}^{-1})] = (4.92 \pm 1.30) - (1.13 \pm 1.04) \cdot 10^{-4} (p / \text{bar}) \quad (5.26)$$

(bulk, 80°C, 300 ≤ p ≤ 1500 bar)

$$\ln C_T = - (1.31 \pm 0.37) - (6.37 \pm 1.40) \cdot 10^{-4} (p / \text{bar}) \quad (5.27)$$

$$\ln [k_{tr} / (\text{L} \cdot \text{mol}^{-1} \cdot \text{s}^{-1})] = (5.03 \pm 1.62) - (1.97 \pm 1.6) \cdot 10^{-4} (p / \text{bar}) \quad (5.28)$$

(40 wt % scCO₂, 80°C, 300 ≤ p ≤ 1500 bar)

According to $\delta (\ln k_{tr}) / \delta p = - \Delta V^\ddagger / (\text{R} \cdot T)$ and $\delta (\ln C_T) / \delta p = - \Delta V^\ddagger / (\text{R} \cdot T)$, the activation volumes for C_T and k_{tr} are calculated as:

$$\text{bulk: } \Delta V^\ddagger(C_T) = + (14.8 \pm 4.7) \text{ cm}^3 \cdot \text{mol}^{-1} \quad \Delta V^\ddagger(k_{tr}) = + (3.3 \pm 3.1) \text{ cm}^3 \cdot \text{mol}^{-1}$$

$$\text{scCO}_2: \Delta V^\ddagger(C_T) = + (18.7 \pm 4.1) \text{ cm}^3 \cdot \text{mol}^{-1} \quad \Delta V^\ddagger(k_{tr}) = + (5.8 \pm 4.7) \text{ cm}^3 \cdot \text{mol}^{-1}$$

The values of ΔV^\ddagger for C_T determined in $scCO_2$ and in bulk indicate a significant pressure dependence, whereas no pressure dependence is seen for k_{tr} . Considering the significant uncertainty determined in ΔV^\ddagger , ΔV^\ddagger for C_T and k_{tr} in bulk are close to the corresponding values in $scCO_2$. As these are the first data reported for styrene polymerization with MMA trimer as CTA, comparison with literature data is not possible.

5.3.2 Homopolymerization of MMA

MMA homopolymerizations were carried out at $80^\circ C$ in 40 wt % $scCO_2$, in bulk and pressures varying between 300 and 1500 bar.

Fig. 5.30 shows typical molecular weight distribution of PMMA from polymerizations in $scCO_2$ at $80^\circ C$ and 300 bar with the indicated amount of MMA trimer. The MWDs are shifted to lower molecular weights with increasing CTA concentration. In the absence of MMA trimer, the reaction yields polymer with M_w of $5 \cdot 10^5 \text{ g} \cdot \text{mol}^{-1}$, and upon addition of 3 wt % MMA trimer ($[MMA_t]/[MMA] = 0.01$) M_w decreases to a value of $2.4 \cdot 10^5 \text{ g} \cdot \text{mol}^{-1}$.

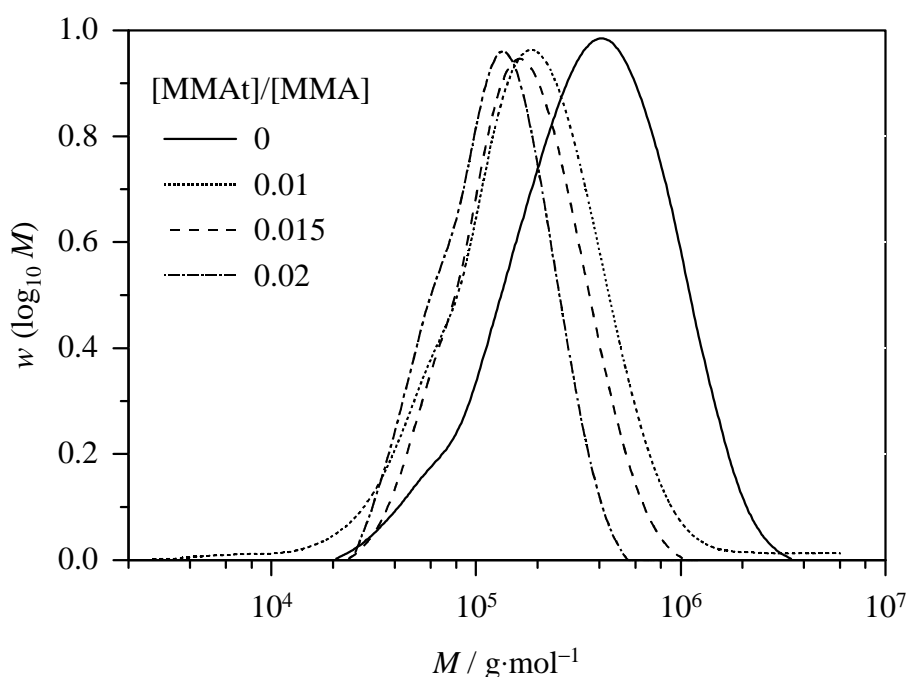


Figure 5.30: Molecular weight distributions of PMMA from polymerizations in 40 wt % $scCO_2$ at $80^\circ C$, 300 bar, and MMAAt concentration as indicated.

The corresponding $\ln f(M)$ vs. M plots are pictured in Fig. 5.31. The part of the distribution used to calculate C_T is indicated by the bold lines. The slope of this MW region is enhanced with increasing [MMA_t].

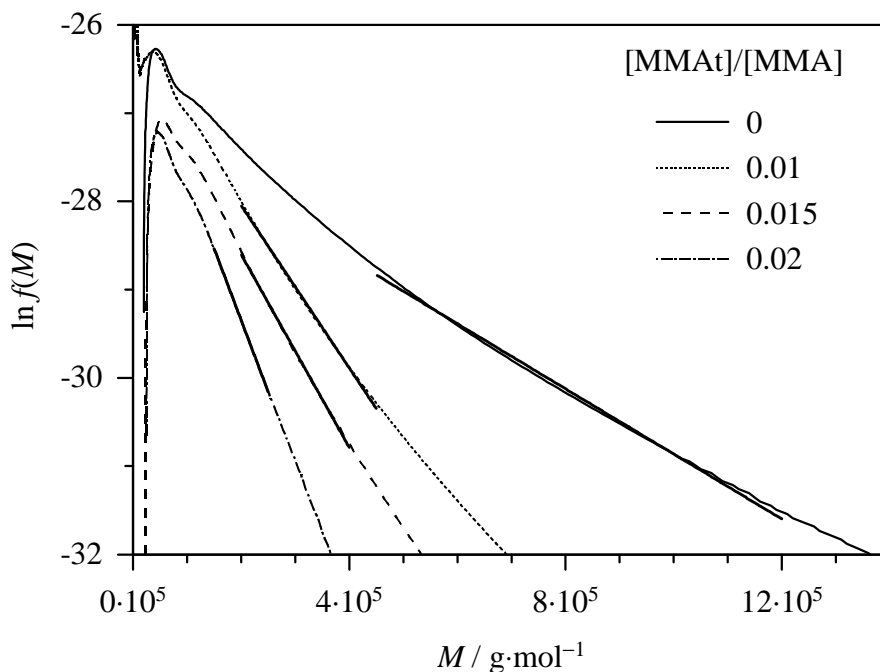


Figure 5.31: $\ln f(M)$ vs. M plots for MMA homopolymerizations in 40 wt % $scCO_2$ at $80^\circ C$ and 300 bar with MMA_t concentration as indicated.

Fig. 5.32 exhibits the CLD plots of MMA homopolymerizations at $80^\circ C$ and 300 bar in bulk and in $scCO_2$.

The C_T values obtained in $scCO_2$ and in bulk are 0.063 and 0.066, respectively. It is obvious that both C_T are identical, which indicates that $scCO_2$ as a solvent has no effect on the transfer activity of MMA trimer in MMA polymerization.

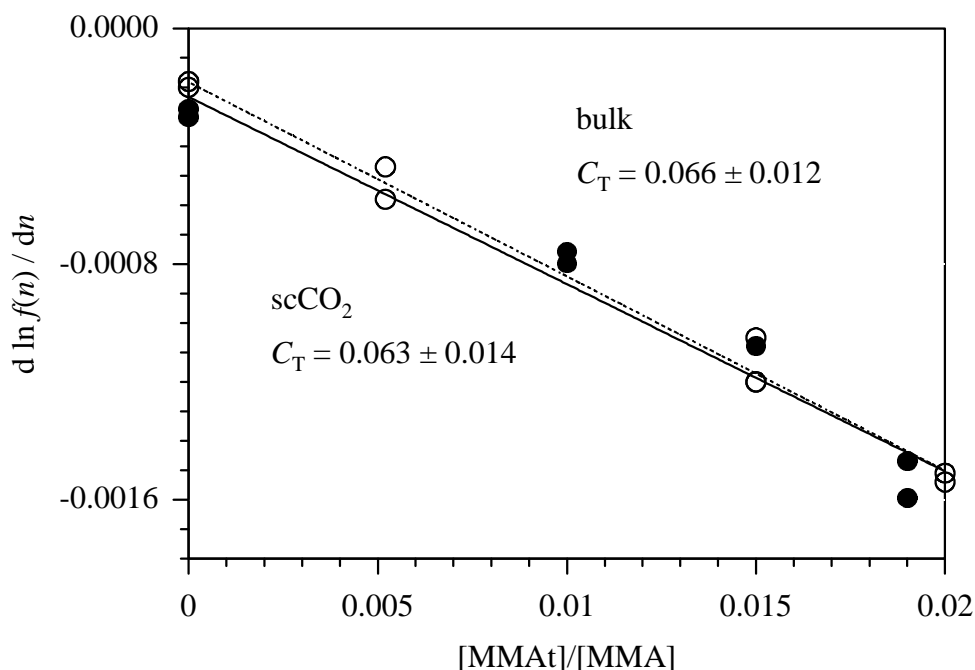


Figure 5.32: Determination of the chain-transfer constant from a plot of $d \ln f(n)/dn$ vs. $[MMA_t]/[MMA]$ for MMA homopolymerizations at 80°C, 300 bar, in 40 wt % $scCO_2$ (solid line) and in bulk (dotted line).

Pressure dependence of C_T and k_{tr}

The pressure dependence of C_T and k_{tr} for MMA homopolymerization was studied in a pressure range from 300 to 1500 bar. The values of k_{tr} were calculated with C_T values and k_p data given in Appendix 1 (for comparison see section 5.1.2).

Fig. 5.33 shows the pressure dependence of C_T and k_{tr} for polymerizations in $scCO_2$ and in bulk. In both media, C_T decreases with increasing pressure. It is obvious that C_T in $scCO_2$ and in bulk are very close, which confirms that $scCO_2$ has no influence on C_T in the entire pressure range. In contrast to C_T , k_{tr} is enhanced with pressure as seen in Fig. 5.33b. k_{tr} values determined in $scCO_2$ are slightly lower than in bulk. Nevertheless, within experimental uncertainty, k_{tr} is close in both media. In addition, the k_{tr} values determined in $scCO_2$ are 87.3 and 113 $L \cdot mol^{-1} \cdot s^{-1}$ at 300 and 1500 bar, respectively, which indicates a minor pressure dependence. The lines fitted to the k_{tr} data in both reaction media are parallel.

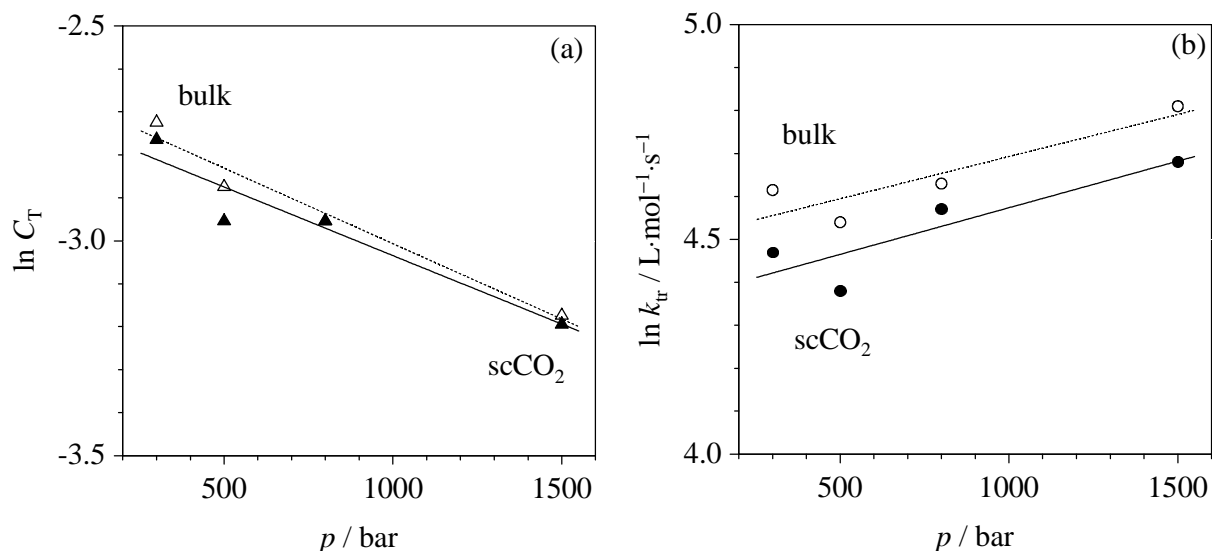


Figure 5.33: Pressure dependence of the chain-transfer constant (a) and of the chain-transfer rate coefficient (b) for MMA homopolymerizations in 40 wt % scCO₂ and in bulk at 80°C. Experimental data are reported in Appendix 4.

The expressions for the pressure dependence of C_T and k_{tr} are given by Eqs. 5.29-5.32.

$$\ln C_T = -(2.66 \pm 0.04) - (3.51 \pm 0.92) \cdot 10^{-4} (p / \text{bar}) \quad (5.29)$$

$$\ln [k_{tr} / (\text{L} \cdot \text{mol}^{-1} \cdot \text{s}^{-1})] = (4.5 \pm 0.06) + (1.96 \pm 0.97) \cdot 10^{-4} (p / \text{bar}) \quad (5.30)$$

(bulk, 80°C, 300 ≤ p ≤ 1500 bar)

$$\ln C_T = -(2.72 \pm 0.06) - (3.19 \pm 1.43) \cdot 10^{-4} (p / \text{bar}) \quad (5.31)$$

$$\ln [k_{tr} / (\text{L} \cdot \text{mol}^{-1} \cdot \text{s}^{-1})] = (4.36 \pm 0.07) + (2.17 \pm 1.53) \cdot 10^{-4} (p / \text{bar}) \quad (5.32)$$

(40 wt % scCO₂, 80°C, 300 ≤ p ≤ 1500 bar).

The corresponding activation volumes are as follows:

$$\text{bulk: } \Delta V^\ddagger(C_T) = + (10.3 \pm 2.7) \text{ cm}^3 \cdot \text{mol}^{-1}$$

$$\Delta V^\ddagger(k_{tr}) = - (5.8 \pm 2.8) \text{ cm}^3 \cdot \text{mol}^{-1}$$

$$\text{scCO}_2: \Delta V^\ddagger(C_T) = + (9.4 \pm 4.2) \text{ cm}^3 \cdot \text{mol}^{-1}$$

$$\Delta V^\ddagger(k_{tr}) = - (6.4 \pm 4.3) \text{ cm}^3 \cdot \text{mol}^{-1}$$

The values of ΔV^\ddagger for C_T and k_{tr} show different trends, which were already observed in Fig. 5.33. The activation volumes for C_T in bulk and in scCO₂ are approximately + 10 cm³·mol⁻¹,

which shows a significant decrease in C_T with pressure. In contrast, the ΔV^\ddagger values for k_{tr} in both media, which are around $-6 \text{ cm}^3 \cdot \text{mol}^{-1}$, indicate a slight increase in k_{tr} with pressure. The extrapolation of C_T in bulk to 1 bar via Eq. 5.29 gives a value of 0.07. Moad et al.²⁰ reported a value of 0.188 in bulk at 80°C and 1 bar, which is higher than the C_T of this work. The SEC analysis of the isolated fraction used in this work showed traces of MMA dimer, which may influence the C_T values. As previously mentioned, the transfer activity of MMA dimer is lower than for MMA trimer. Therefore, the presence of MMA dimer in the CTA contributes to a lower value of C_T as expected for pure MMA trimer. In the literature a C_T value²⁰ of 0.015 is reported for MMA dimer as CTA. Thus C_T of 0.07 extrapolated from Eq. 5.29 is in between the C_T values for MMA dimer and MMA trimer.

5.3.3 Summary

The Table below summarizes the results obtained for MMA and styrene homopolymerizations in bulk and in scCO₂ at 80°C with MMA trimer as chain-transfer agent. C_T and k_{tr} are given for polymerizations at 80°C and 800 bar.

MMA		
	C_T	k_{tr}
scCO₂	0.052 ± 0.002	$97.1 \pm 8.5 \text{ L}\cdot\text{mol}^{-1}\cdot\text{s}^{-1}$
bulk	0.053 ± 0.002	$103 \pm 8 \text{ L}\cdot\text{mol}^{-1}\cdot\text{s}^{-1}$
scCO₂ influence	no influence in the entire pressure range	no influence in the entire pressure range
DV[#] / cm³·mol⁻¹	<i>bulk</i> : $+(10.3 \pm 2.7)$	<i>bulk</i> : $-(5.8 \pm 2.8)$
	<i>scCO₂</i> : $+(9.4 \pm 4.2)$	<i>scCO₂</i> : $-(6.4 \pm 4.3)$
styrene		
	C_T	k_{tr}
scCO₂	0.165 ± 0.011	$136 \pm 18 \text{ L}\cdot\text{mol}^{-1}\cdot\text{s}^{-1}$
bulk	0.141 ± 0.009	$131 \pm 14 \text{ L}\cdot\text{mol}^{-1}\cdot\text{s}^{-1}$
scCO₂ influence	no influence in the entire pressure range	no influence in the entire pressure range
DV[#] / cm³·mol⁻¹	<i>bulk</i> : $+(14.8 \pm 4.7)$	<i>bulk</i> : $+(3.3 \pm 3.1)$
	<i>scCO₂</i> : $+(18.7 \pm 4.1)$	<i>scCO₂</i> : $+(5.8 \pm 4.7)$

5.4 Discussions

The experimental results presented in the preceding sections showed very different trends for k_{tr} . k_{tr} values obtained for polymerizations of MMA at 80°C and pressures varying between 300 and 1000 bar differ by orders of magnitude: Close to 10^2 , 10^3 and $10^7 \text{L}\cdot\text{mol}^{-1}\cdot\text{s}^{-1}$ for the MMA trimer, for DDM and for COPhBF, respectively. The scCO_2 influence on k_{tr} in MMA and styrene homo- and copolymerizations is dependent on the monomer-CTA system under consideration. As shown in the schemes 5.1, 5.2, and 5.3, the mechanisms of the transfer reaction are very different for the CTAs.

As mentioned in section 5.2, C_T^{obs} and k_{tr}^{obs} values determined in the presence of COPhBF in styrene-MMA homo- and copolymerizations are based on a direct abstraction of the hydrogen atom from the polymer radical by COPhBF, as illustrated in scheme 5.2. Recently it has been suggested that this scheme may be not adequate for the transfer reaction with COPhBF in styrene polymerization¹⁰. The different reaction schemes proposed for the transfer process in styrene polymerization are presented in the following part. Implications on C_T and k_{tr} values are discussed in section 5.4.1.3.

The first part of the discussion deals with the mechanism of the chain-transfer reaction for the different CTAs, in order to explain the difference on k_{tr} in styrene and MMA polymerizations. The second part deals with the k_{tr} values obtained for the different systems, which are discussed in terms of pressure dependence and scCO_2 influence.

5.4.1 Mechanism of the chain-transfer reaction

The table below summarizes the k_{tr} values ($\text{L}\cdot\text{mol}^{-1}\cdot\text{s}^{-1}$) obtained in styrene and MMA homo- and copolymerization in scCO_2 at 80°C and 300 bar.

f_S	$10^{-3}\cdot k_{tr,DDM}$	$10^{-5}\cdot k_{tr,COPhBF}^{\text{obs}}$	k_{tr,MMA_t}
0	1.14 ± 0.25	292 ± 100	87.3 ± 14.1
0.5	3.03 ± 0.62	37.6 ± 12.1	–
1	11.2 ± 2.1	5.79 ± 1.18	142 ± 23

5.4.1.1 DDM

The k_{tr} values, in the range from 10^3 to 10^4 L·mol⁻¹·s⁻¹, obtained in MMA and styrene polymerizations with DDM indicate a good transfer activity. The C_T values of 0.771 and 15.5 extrapolated or obtained at 80°C and ambient pressure in MMA and styrene bulk homopolymerizations, respectively, are in very good agreement with the literature data: Hutchinson et al.¹ reported C_T values of 0.711 and 15.6 in MMA and styrene homopolymerizations, respectively, under the same experimental conditions.

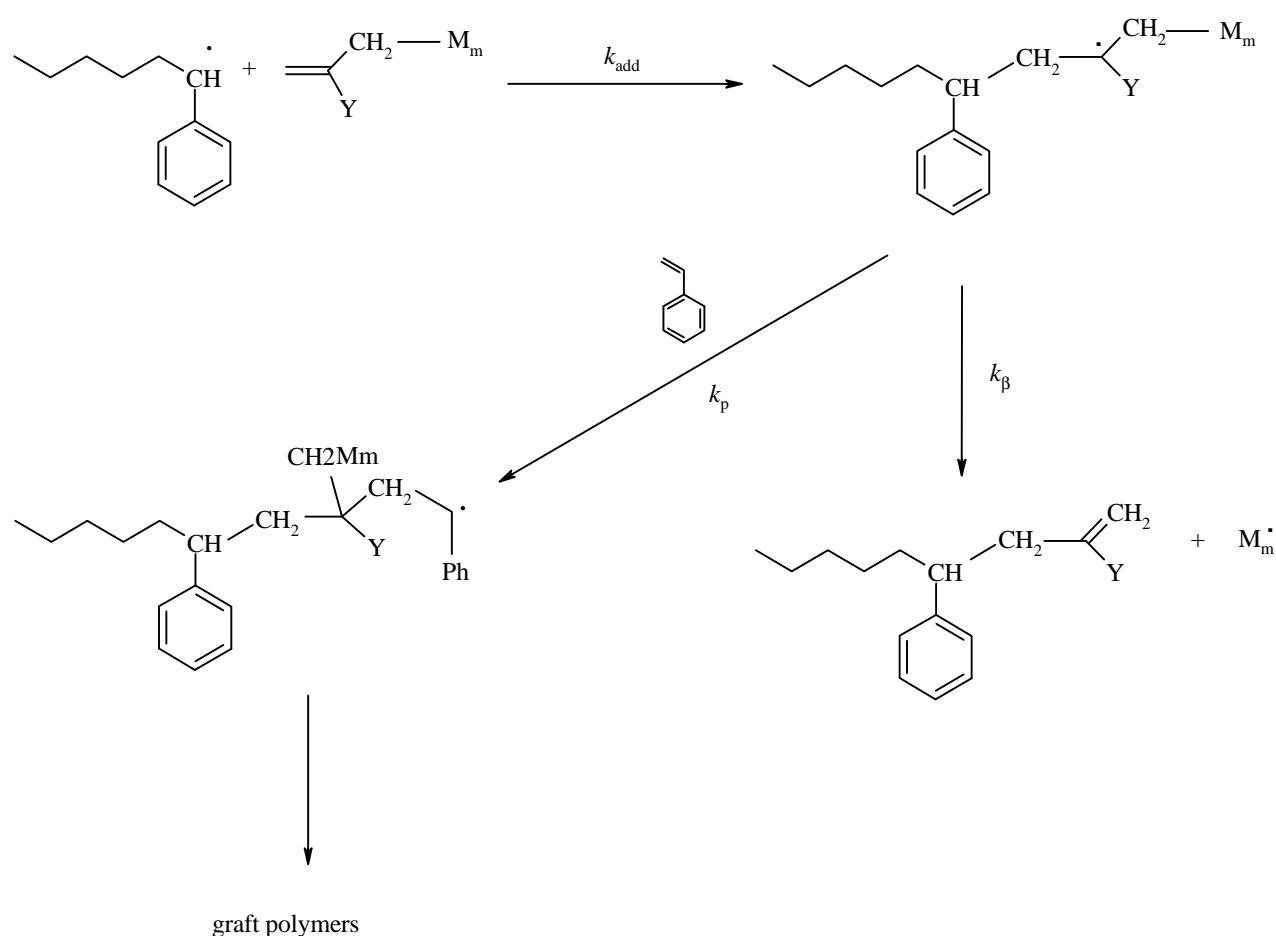
As described in scheme 5.1, the transfer reaction of DDM with a growing radical is composed of two steps: the abstraction of a hydrogen atom of DDM by the polymer radical and the addition of the thiyl radical formed with a monomer molecule. The hydrogen abstraction is the rate-determining step in the transfer process with DDM since it creates the polymer.

Styryl radicals are known to be very stable²⁶, which induces a very low propagation rate coefficient compared to methacrylates and acrylates monomers, e.g. at 300 bar and 80°C in bulk k_p for styrene is 763 L·mol⁻¹·s⁻¹ and for MMA is 1540 L·mol⁻¹·s⁻¹. If the reactivity of the styryl or methacrylic radical is the determining factor for the transfer rate, it is expected that the transfer reaction of DDM with styryl radicals should be slower than the transfer reaction with methacrylic radicals. However, the experimental results have shown that the hydrogen abstraction is clearly more difficult with methacrylic radicals, which are hindered due to the α -methyl group. Thus, it seems that not only the polymer radical reactivity determines the rate of the hydrogen abstraction. Interactions between DDM and polymer radicals may influence the rate of the transfer reaction. In addition, as styryl radicals propagate more slowly than methacrylic radicals, those are more prone to possible side reactions.

Tronche et al.²⁷ have shown that the rate of a hydrogen abstraction of octadecanethiol by a radical decreases by one order of magnitude when the radical contains polar substituents. An extreme example²⁸ for this polar effect is the reaction of a perfluoroalkyl radical with phenylthiol which is a factor of 500 less rapid than reaction of an alkyl radical. A styryl radical, which is obviously less polar than a methacrylic radical, is thus supposed to abstract more rapidly the hydrogen atom of DDM than a methacrylic radical. This observation is consistent with the results of this work, thus the polarity of the monomer seems to be an important factor in the transfer process of DDM.

5.4.1.2 MMA trimer

The mechanism of the transfer reaction of a macromonomer with a vinyl monomer is illustrated in scheme 5.3. Since chain transfer occurs via an addition-fragmentation mechanism, k_{tr} is composed of k_{add} and k_{β} , which are the addition and the β -scission rate coefficients, respectively. For efficient chain-transfer to occur it is important that the lifetime of the intermediate macroradical is short with respect to the lifetime of a propagating species. Moad et al.²³ found that there is no retardation in MMA polymerization carried out in the presence of macromonomers CTAs compared to experiments without CTA. They concluded that fragmentation is fast relative to addition. k_{tr} is thus determined by the reactivity of the MMA trimer double bond towards the addition of a propagating radical in MMA homopolymerization. In styrene homopolymerization it has been shown that a competition between fragmentation and copolymerization of the macroradical formed after addition of the styrene radical may occur in some cases²⁹, as illustrated in scheme 5.4 below.



Scheme 5.4: Competition between fragmentation and copolymerization in the chain-transfer process with macromonomer.

The competition between fragmentation and copolymerization has also been shown for acrylate polymerizations, which are non-sterically hindered monomers such as styrene. In contrast, the incorporation of macromonomers into polymethacrylates via copolymerization was seen to be close to zero³⁰.

In case of copolymerizations as side reaction, the molecular weight distribution of the polymer obtained should be broader, due to the presence of graft polymers, as compared to MMA homopolymerization where the copolymerization reaction does not take place. Such an observation was not made for the MWD of the polystyrene obtained here. MWDs obtained for styrene and MMA homopolymerizations have approximately the same polydispersity index ($PDI = M_w/M_n$), which characterizes the broadness of a molecular weight distribution.

The copolymerization of a styrene monomer and the macroradical may be compared to a styrene-MMA propagation reaction. Thus, it can be anticipated that the copolymerization rate will increase with pressure, as seen for k_p in MMA-styrene copolymerization³¹. The formation of graft polymers resulting from this copolymerization will be increased, and the yield of polymers issued from the transfer process will be reduced. A change in the MWD of the polymer obtained, thus an enhanced PDI, is expected when increasing pressure. This was not observed here, where PDI is almost constant with pressure. In summary, these observations confirm the absence of the copolymerization as side reaction in styrene homopolymerization under the experimental reaction conditions applied in this work, and thus the applicability of the calculated chain-transfer rate coefficients.

k_{tr} values obtained for MMA trimer as CTA in styrene and MMA homopolymerizations are very low, in the range of $10^2 \text{ L}\cdot\text{mol}^{-1}\cdot\text{s}^{-1}$, indicating a very slow chain-transfer process. In styrene homopolymerization k_{tr} is higher than in MMA homopolymerization. It should be kept in mind that the batches of MMA trimer used are different for styrene and MMA polymerization (see section 5.3). Although SEC analysis showed that both batches of macromonomer contain approximately the same amount of MMA dimer and MMA trimer, it can not be excluded that small differences in k_{tr} as seen in this work may be due to the use of different batches of CTA. It has been shown that C_T of MMA dimer is lower than C_T of MMA trimer in MMA homopolymerization²³.

In a recent study, Bon et al.³² performed polymerizations of styrene and MMA with an allyl bromide as CTA. The structure of an allyl bromide is comparable to the one of a MMA macromonomer since only M_m (see scheme 5.4) is different: $M_m = \text{Br}$ in case of the allyl bromide and $M_m = 2 \text{ MMA units}$ in case of the MMA trimer. In addition, the transfer reaction scheme proposed with an allyl bromide is an addition-fragmentation, such as here. The results

have shown that k_{tr} obtained in styrene polymerization is higher than in MMA polymerization, as seen in this work. Thus, the literature data support the experimental results of this work.

The rate-determining step of the transfer process in MMA and styrene homopolymerization with MMA trimer, which is the addition reaction, may be compared to the MMA and styrene-MMA propagation reactions, respectively. The propagation kinetics of the copolymerization of styrene and MMA is described satisfactorily by the implicit penultimate model^{31,33,34}. This implies that the cross-propagation coefficient, $k_{psty/MMA}$, of $1004 \text{ L}\cdot\text{mol}^{-1}\cdot\text{s}^{-1}$ is evaluated from the reactivity ratio³¹ $r_{styrene}$ (0.76) and from $k_{p,styrene}$ ($763 \text{ L}\cdot\text{mol}^{-1}\cdot\text{s}^{-1}$) determined at 300 bar and 80°C in bulk polymerization. $k_{p,MMA}$ is $1540 \text{ L}\cdot\text{mol}^{-1}\cdot\text{s}^{-1}$ under the same experimental conditions. The chain-transfer rate coefficients of styrene and MMA homopolymerization with MMA trimer, determined here at 300 bar and 80°C in bulk, are 131 and $101 \text{ L}\cdot\text{mol}^{-1}\cdot\text{s}^{-1}$, respectively. This indicates that MMA radicals are more reactive than styryl radicals with MMA as "comonomer", whereas styryl radicals are more reactive than MMA radicals with MMA trimer as "comonomer". Thus, MMA trimer is not comparable with MMA in terms of reactivity. In addition, MMA trimer is 7 times less reactive than MMA towards a styryl radical and 15 times less reactive than MMA towards a methyl methacrylic radical. It is obvious that the reactivity of MMA trimer with a growing radical is very low compared to the homopropagation reaction of the monomer. This finding may be explained by the bulkiness of the MMA trimer. The addition reaction of the MMA trimer with sterically hindered radicals such as methacrylic radical is clearly more difficult than with styryl radicals. Thus, as seen here k_{tr} in styrene homopolymerization is higher than in MMA homopolymerization with MMA trimer as CTA.

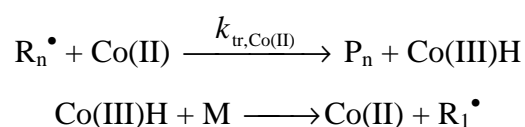
5.4.1.3 CPhBF

k_{tr} values determined for CPhBF as catalytic chain-transfer agent (CCTA) are approximately two orders of magnitude lower in styrene polymerization ($10^5 \text{ L}\cdot\text{mol}^{-1}\cdot\text{s}^{-1}$) than in MMA polymerization ($10^7 \text{ L}\cdot\text{mol}^{-1}\cdot\text{s}^{-1}$). The values of C_T obtained in Section 5.2 are in accordance with the literature data, which are reported to be for 60°C and ambient pressure in the range of 10^2 and 10^4 in styrene and MMA homopolymerizations³⁵, respectively. The k_{tr} values are in accordance with a diffusion-controlled transfer process in MMA polymerization (more details are given in the next part) and with a chemically-controlled process in styrene homopolymerization.

Catalytic chain transfer is most effective for tertiary propagating radicals such as in methacrylates, from which a hydrogen atom is abstracted from the α -carbon atom in the substituent^{36,37,38}, as seen in scheme 5.2. In contrast, for secondary radicals such as styryl, the chain-transfer reaction is less effective. Styrene lacks an α -methyl group, and hydrogen abstraction is proposed to occur from an internal β -H atom on the backbone^{47,39}. Abstraction of a hydrogen atom from the backbone is likely to be more difficult than from an α -methyl group due to steric hindrance and should yield lower k_{tr} values, which supports the results obtained in this work. This steric effect may be not sufficient to explain the strong difference in k_{tr} for styrene and MMA homopolymerizations. It may also be explained by the chain-transfer mechanism. No conclusive evidence exists regarding the actual chain-transfer mechanism other than presented in scheme 5.2, i.e., a hydrogen is abstracted from the growing radical, which is the rate-determining step and the hydrogen is transferred to the monomer. This mechanism seems to be the most conceivable and generally accepted mechanism to date. However, it is known from organometallic chemistry^{40,41,42} that many Co(II) complexes have the ability to form reversible Co–C bonds with organic radicals. Electron spin resonance (ESR) studies showed a decrease of Co(II) concentration in the catalytic chain-transfer polymerization of styrene, but not for MMA and this was attributed to a reversible Co–C bond formation³⁵. Recently, Roberts et al.¹⁸ directly observed the formation of cobalt-carbon bonds in CCT polymerization with methyl acrylate, with C_T being by orders of magnitude lower than for methacrylate polymerization. Therefore, it is obvious that the Co–C bond formation depends on the type of radical present in the system, and that the Co–radical complex is more stable when secondary (styrenic, acrylic) rather than tertiary (methacrylic) radicals are present. In some cases, such as acrylates, free-radical polymerization in the presence of Co-complexes leads to living polymerization characteristics^{43,44,45}.

Three different mechanisms are suggested for styrene polymerizations with COPhBF as CCTA, for more details see ref. 10.

Firstly, the well-known two-step mechanism involving Co–H intermediates as shown in scheme 5.2.



Scheme 5.2

The reaction scheme 5.2 is the most widely accepted version of the catalytic chain-transfer process and it is this mechanism on which all the C_T values published have been based upon. A clear and thorough discussion of this mechanism is given in ref. 46.

The second mechanism, given in scheme 5.5, is related to the reaction of a monomer molecule and a radical coordinately bound to the cobalt center.



Scheme 5.5

The third mechanism is similar to the second one but with the exception that the monomer (M) acts as a ligand of the cobalt center, see scheme 5.6. This mechanism was previously suggested by Haddleton and co-workers⁴⁷ to explain the decrease in C_T of a cobalt-complex for MMA polymerizations in solution of toluene as compared to bulk reactions. Solvent effects may be explained by the formation of a strong solvent-catalyst complex, leading to a decrease in active catalyst concentration. However, Davis et al.¹⁰ have not observed significant solvent effects of this nature except when using pyridine, which is known to be a very strong ligand.



Scheme 5.6

Considering that the reversible cobalt-carbon bond occurs in catalytic chain transfer of styrene polymerization, as illustrated in scheme 5.5 and 5.6, the effective concentration of CTA is probably lower than what one expects. Thus, the true $[\text{COPhBF}]/[\text{M}]$ ratios are lower than the $[\text{COPhBF}]_0/[\text{M}]$, which are used to determine C_T (see Eq. 4.17). This implies that C_T^{obs} is lower than the true C_T , C_T^{true} . This means that the true ratio will be obtained by a horizontal shift of the points to lower values on the CLD plot ($\Lambda \cdot M_0$ vs $[\text{COPhBF}]/[\text{M}]$), yielding a steeper slope and hence a higher C_T .

Since Λ in Eq. 4.7 is directly governed by the product of C_T and $[\text{CTA}]$, the relationship between the observed C_T and the true C_T is given by:

$$C_T^{\text{true}} \cdot [\text{COPhBF}]_{\text{true}} = C_T^{\text{obs}} \cdot [\text{COPhBF}]_{\text{initial}} \quad (5.1)$$

Thus, considering a transfer process with a reversible cobalt-carbon bond, the C_T^{true} might be easily accessible knowing the $[\text{COPhBF}]_{\text{true}}$ and using C_T^{obs} determined in this work assuming scheme 5.2 to occur.

In other words, $k_{\text{tr}}^{\text{obs}}$ may be underestimated and this may explain that catalytic chain-transfer polymerization of MMA is diffusion controlled and apparently chemically controlled in styrene. Considering the above finding, this difference may be actually smaller and its conceivable that catalytic chain-transfer in styrene is also diffusion controlled. Thus, it may be anticipated that k_{tr} values of styrene and MMA are in the same range, as seen for k_{tr} determined in the presence of DDM and MMA trimer. In addition, styrene and MMA have shown to have k_p and k_t values in the same range³¹.

5.4.2 Activation volume $DV^\#$ and scCO_2 influence on k_{tr}

The table below summarizes the activation volumes of k_{tr} , $\Delta V^\#(k_{\text{tr}}) / \text{cm}^3 \cdot \text{mol}^{-1}$, obtained in styrene and MMA homo- and copolymerization with the different CTAs at 80°C.

f_S		0	0.5	1
$\Delta V^\#(k_{\text{tr,DDM}})$	bulk	$-(5.3 \pm 3.7)$	$-(2.6 \pm 2.8)$	$-(4.5 \pm 1)$
	scCO_2	$-(4.4 \pm 2.9)$	$-(2.8 \pm 1.9)$	$-(1.8 \pm 3.5)$
$\Delta V^\#(k_{\text{tr,COPhBF}}^{\text{obs}})$	bulk	$+(47.5 \pm 15.8)$	–	–
	scCO_2	$+(31.5 \pm 7.3)$	–	–
$\Delta V^\#(k_{\text{tr,MMA trimer}})$	bulk	$-(5.8 \pm 2.8)$	–	$+(3.3 \pm 3.1)$
	scCO_2	$-(6.4 \pm 4.3)$	–	$+(5.8 \pm 4.7)$

Assuming the uncertainty on the $k_{\text{tr}}^{\text{obs}}$ values relative to the system styrene-COPhBF reported above, activation volumes are not discussed for styrene polymerizations with COPhBF as catalytic CTA.

5.4.2.1 DDM

In Section 5.1 it was shown that $\ln k_{\text{tr,copo}}$ in styrene-MMA polymerization varies linearly with the styrene content in the monomer feed, which holds for reactions in bulk and in scCO_2 and

for pressure ranging from 300 to 1000 bar. In addition, k_{tr} determined in scCO₂ is close to the bulk value in the entire pressure range independently of f_S . Thus, the activation volumes of k_{tr} measured in both reaction media are similar, as reported in the table above. This aspect is also seen for k_p obtained in styrene and MMA homo- and copolymerizations in the same conditions of experiment. Beuermann et al.⁵ showed that the propagation rate coefficients and consequently the pressure dependence of k_p for styrene in scCO₂ at 80°C are very close to the bulk data. In addition, k_p determined for MMA polymerizations at 80°C performed in this work, which are listed in Appendix 1, also show no influence of scCO₂. In addition, k_{tr} values indicate that the transfer reaction is chemically controlled, as already seen for the propagation reaction⁵.

The independence of k_{tr} on scCO₂ as a solvent suggests that the viscosity of the system is not a determining factor. This observation is in agreement with the results reported by Foster et al.⁴⁸. Investigations in bulk polymerizations of methacrylates with ester groups largely different in size (MMA and 2-phenoxyethyl methacrylate (POEMA)) showed for both monomers the same k_{tr} , despite a significant difference in the viscosity of the system: The viscosities of POEMA and MMA are 2.51 and 0.37 cP, respectively, at reaction conditions. It provides strong evidence that viscosity effects are negligible in a conventional chain-transfer reaction of these monomers. The insensitivity of ΔV^\ddagger on the reaction medium supports the view that the dynamics of the transfer reaction is essentially the same in both media. Madruga et al.³ report a similar effect: k_{tr} values for styrene and MMA homo- and copolymerizations in solution of benzene are similar to the corresponding bulk values. As seen in this work for scCO₂, the solvent effect is negligible in conventional transfer polymerizations in solvents of poor polarity. However, Gnanou et al.⁴⁹ investigated the polymerization of styrene in various solvents with different thiols containing an ester group. An increase of the polarity of the reaction medium results in an enhancement of k_{tr} . They explained that this is most likely due to the transferring functionality that is made more accessible to the growing radical in such media. It is in accordance with a study of Tronche et al.²⁷, which indicates an increase of the transfer rate of a radical with 1-butane thiol increasing the polarity of the solvent. Summary of the literature studies shows that solvents with high polarity increase the rate of the transfer process, whereas solvent with weak polar nature have no influence on k_{tr} . scCO₂ is a poor polar solvent, thus it is expected that there is no influence on k_{tr} using scCO₂ as a solvent. The results reported in this work are consistent with this observation.

Within experimental uncertainty, the pressure dependence of the transfer rate coefficient is not significant for styrene and MMA homo- and copolymerizations in both media. However a significant pressure dependence is observed in the propagation reaction^{5,50}: $\Delta V^\ddagger(k_p)$ for MMA and for styrene are around $-16 \text{ cm}^3 \cdot \text{mol}^{-1}$ and $-11 \text{ cm}^3 \cdot \text{mol}^{-1}$, respectively. k_p and k_{tr} are in the same range, thus a comparison of both processes is adequate. A difference between $\Delta V^\ddagger(k_p)$ and $\Delta V^\ddagger(k_{tr})$ is expected because the radical-monomer addition, in the propagation reaction, should be accompanied by a greater volume contraction than the transfer reaction, in which a thiyl-hydrogen bond must be broken. Tooney et al.⁵¹ reported that $\Delta V^\ddagger(k_{tr})$ for triethylamine in styrene homopolymerization at 60°C up to 4400 bar is in the range from -2 to $-3 \text{ cm}^3 \cdot \text{mol}^{-1}$, as seen for the values reported in this work. In both cases, transfer with DDM and triethylamine, the rate-determining step of the transfer process is a hydrogen abstraction of the CTA by the polystyryl radical. Walling and Pellon⁵² have indicated that $\Delta V^\ddagger(k_{tr})$ for carbon tetrachloride in styrene homopolymerization at 60°C up to 4000 bar is close to the $\Delta V^\ddagger(k_p)$ in the same conditions. In this last case, the rate determining step is a chlorine abstraction of the CTA by the polystyryl radical. This may indicate that ΔV^\ddagger for the transfer reaction is strongly dependent on the radius of the atom abstracted, thus on the CTA. In contrast, the nature of the polymer radical does influence the pressure dependence of the transfer reaction significantly.

In summary in MMA and styrene homo- and copolymerization, it has been shown here that scCO_2 , which is a solvent with a weak polar nature, has no influence on k_{tr} . The variation of k_{tr} with pressure is not significant as the abstracted atom, a hydrogen atom, is small. Thus, in styrene and MMA polymerization with DDM as CTA, k_{tr} is not influenced by the viscosity of the system.

5.4.2.2 MMA trimer

The k_{tr} values, and thus the activation volumes of k_{tr} , determined in styrene and MMA homopolymerizations are similar in bulk and in solution of scCO_2 , as reported in section 5.3. The k_{tr} values indicate a chemically-controlled transfer process. In an addition-fragmentation transfer process it has been shown that the rate-determining step is the addition reaction of the polymer radical and the MMA trimer²³. This step is comparable to a propagation reaction since in both cases the addition of a polymer radical with a vinyl oligomer (or monomer) occurs. Thus, k_{tr} determined in styrene and MMA homopolymerization are compared to k_p

styrene-MMA and MMA polymerization, respectively. Previous studies have shown that the values of $k_{p,MMA}$ and $k_{psty/MMA}$ determined in $scCO_2$ are very close to the bulk values under the same conditions of experiments of this work³¹. These observations are in accordance with the results obtained here, where no $scCO_2$ effect is seen for k_{tr} in the presence of MMA trimer (see Table above).

Within experimental uncertainty the enhancement of k_{tr} in MMA homopolymerization is not significant with increasing pressure and the pressure dependence of k_{tr} is close to the one observed with DDM as CTA ($\Delta V^\ddagger (k_{tr,DDM}) = - (5.3 \pm 3.7) \text{ cm}^3 \cdot \text{mol}^{-1}$ and $\Delta V^\ddagger (k_{tr,MMA}) = - (5.8 \pm 2.8) \text{ cm}^3 \cdot \text{mol}^{-1}$ in bulk polymerization). $\Delta V^\ddagger (k_{tr})$ obtained in styrene homopolymerization is close to zero. The positive activation volume for k_{tr} in styrene homopolymerization is probably due to the very low values determined for C_T , thus for k_{tr} , which increases the uncertainty of the data. In a chemically-controlled process, an addition reaction becomes faster with pressure, whereas a fragmentation is slowed down with pressure. Considering the results obtained, the addition to the double bond is the rate-determining step in the transfer process for MMA homopolymerization, as previously suggested by Moad et al.²³. In addition, since the fragmentation reaction is supposed to be faster, the macroradical formed is immediately transformed to a dead polymer and a new radical. As a consequence the volume variation of the system does not significantly change, which induces a low pressure dependence as seen in this work.

In summary, the activation volumes of k_{tr} determined in styrene and MMA homopolymerizations in the presence of MMA trimer are not significant and are not influenced by the presence of $scCO_2$ as a solvent. In addition, the values of $\Delta V^\ddagger (k_{tr})$ are close to the ones determined with DDM as CTA, which transfer process is chemically controlled.

5.4.2.3 CPhBF

The results obtained in MMA homopolymerization with CPhBF as CCTA suggest a significant $scCO_2$ influence on k_{tr} (k_{tr} at 80°C and 1000 bar are $14.5 \cdot 10^6$ and $5.5 \cdot 10^6 \text{ L} \cdot \text{mol}^{-1} \cdot \text{s}^{-1}$ in $scCO_2$ and in bulk, respectively) and high positive activation volumes are determined ($\Delta V^\ddagger (k_{tr})$ is around $+35 \text{ cm}^3 \cdot \text{mol}^{-1}$ in both media). These findings are in accordance with a diffusion-controlled transfer process.

In the literature⁵³ the kinetic results from catalytic chain-transfer reactions with methacrylates indicate also a diffusion-controlled transfer reaction. For methacrylates with ester groups of

different size, Arrhenius parameters for the transfer reaction are reported: Activation energies around $E_A(k_{tr}) = +23 \text{ kJ}\cdot\text{mol}^{-1}$, which induces $E_A(C_T) = 0 \text{ kJ}\cdot\text{mol}^{-1}$, and frequency factors around $A = 10^{10} \text{ L}\cdot\text{mol}^{-1}\cdot\text{s}^{-1}$. The significant $E_A(k_{tr})$ indicates the presence of a reaction barrier and the high A is atypical for a chemically-controlled bimolecular reaction between a polymeric radical and a small molecule^{54,55}, which is generally lower than $10^5 \text{ L}\cdot\text{mol}^{-1}\cdot\text{s}^{-1}$. It was also shown that k_{tr} decreases with increasing ester chain in a homologous series of methacrylates^{48,56}. This phenomenon was assigned to a diffusion-controlled transfer reaction and the individual k_{tr} value was directly proportional to the inverse viscosity of the monomer: e.g., the higher the viscosity, the lower k_{tr} . The results obtained in MMA homopolymerization in this work are in accordance with this observation: k_{tr} is enhanced in scCO₂ and decreases with increasing pressure. The presence of scCO₂ decreases the viscosity of the system, whereas high pressure increases the viscosity of the system. Davis et al.¹³ performed MMA polymerization in approximately 80 wt % scCO₂ at 50°C and 150 bar with CPhBF as CCTA. The reported k_{tr} in the range of $10^8 \text{ L}\cdot\text{mol}^{-1}\cdot\text{s}^{-1}$ is also consistent with a diffusion-controlled transfer reaction: k_{tr} increases strongly in the presence of scCO₂ and k_{tr} is very high, comparable to termination rate coefficients which are known to be diffusion controlled.

The following part will focus on the influence of the viscosity on the k_{tr} values because literature data and the results of this work clearly indicate a dependence of k_{tr} on the viscosity of the system. In addition, one of the special features of using scCO₂ as an alternate solvent is the very low viscosity of CO₂ compared to the monomer viscosity. The above mentioned k_{tr} value around 10^8 in the catalytic chain-transfer polymerization of MMA at 50°C and 150 bar in 80 wt % scCO₂ is one order of magnitude higher than the k_{tr} value around 10^7 extrapolated at 80°C and 150 bar in 40 wt % scCO₂ in Section 5.2.2. $E_A(k_{tr})$ was reported to be around + 23 kJ·mol⁻¹ so that k_{tr} increases with temperature. Therefore, if a temperature dependence is anticipated in scCO₂, k_{tr} at 50°C should be slightly lower than k_{tr} at 80°C. The reported above values are not in accordance with this finding. Thus, the difference in k_{tr} between literature data and this work is due to the different scCO₂ contents. This indicates that viscosity is an important parameter in MMA polymerization with CPhBF since the viscosity of the mixture with 80 wt % scCO₂ is lower than the one with 40 wt % scCO₂.

It may be considered that the presence of CPhBF does not influence the viscosity since only a small amount of CPhBF is used to prepare the solutions. At 80°C and 300 bar, the CO₂ viscosity of 658 μP is by about one order of magnitude lower than the MMA viscosity, estimated to be approximately 3000 μP. The CO₂ viscosity is taken from ref. 57, whereas the

MMA viscosity is estimated from the 30°C data given by Ogo et al.⁵⁸ and the 60°C data given by Foster et al.⁴⁸. The viscosity for MMA-CO₂ mixtures is not available in the literature. Therefore the viscosity of the mixture⁵ is estimated from the data of the pure components according to: $\ln h_{\text{mix}} = x(\text{CO}_2) \cdot \ln h(\text{CO}_2) + x(\text{MMA}) \cdot \ln h(\text{MMA})$, with the molar fractions $x(\text{CO}_2)$ and $x(\text{MMA})$ of CO₂ and MMA in the mixture. As in the work of Fischer et al.⁵⁹ polymer contributions are not taken into account, as the monomer conversion was below 4 % in all experiments of this work. A value of 1200 μP is estimated, which shows that the viscosity of the monomer-CO₂ mixture is significantly reduced compared to pure MMA. Thus the reduced viscosity may be the cause for the observed enhancement of k_{tr} in the presence of CO₂. This phenomenon was previously seen⁵ for the termination rate coefficient in styrene homopolymerization in scCO₂, which is also diffusion controlled.

The significant solvent effect observed in MMA homopolymerization may also be exerted via a ligation mechanism and partitioning of the catalyst. These two possibilities are discussed in the following part. In a recent work, it was shown that the solvent effects on catalytic chain-transfer (methacrylate polymerizations) are not significant for solvents that are weak ligands, such as toluene and butyl acetate⁵³. Solvent effect only becomes important for strong ligand such as pyridine. Neither toluene nor CO₂ are strong ligands and therefore it seems unlikely that the strong effects observed in polymerization in scCO₂ can be attributed to direct chemically interactions. An enhanced chain-transfer process may be possible if the local cobalt-complex concentration around the radical is increased. Klingler and Rathke⁶⁰ studied the hydrogenation of dicobalt octacarbonyl in scCO₂ and found no significant solvent effects in comparison to nonpolar organic solvents. Therefore it seems unlikely that the increase of k_{tr} in scCO₂ may be attributed to partitioning.

The activation volumes obtained for k_{tr} in MMA homopolymerization are surprisingly high ($\sim +35 \text{ cm}^3 \cdot \text{mol}^{-1}$) compared to other systems and kinetic parameters studied so far. For example, the activation volume of the termination reaction⁵⁰ in MMA homopolymerization $\Delta V^\ddagger(k_t)$ around $+16 \text{ cm}^3 \cdot \text{mol}^{-1}$ is lower than the value of $\Delta V^\ddagger(k_{\text{tr}})$ observed for the transfer reaction determined here. Both reactions, transfer and termination, are assumed to be diffusion controlled. The difference on ΔV^\ddagger of k_{tr} and k_t indicates the presence of a stronger reaction barrier in the transfer than in the termination process, thus a consequent pressure dependence. As discussed before, the viscosity of the system, which increases with increasing pressure, may also explain this phenomenon. However the pressure dependence of the viscosity, $\Delta V^\ddagger(\mu)$, is lower than the reported $\Delta V^\ddagger(k_{\text{tr}})$: $\Delta V^\ddagger(\mu) = +14 \text{ cm}^3 \cdot \text{mol}^{-1}$ for MMA⁵⁸.

Therefore, the strong pressure dependence observed for k_{tr} may not only be explained by a diffusion-controlled reaction. Other phenomenons may have additive effects, which induces such unusual activation volume.

Considering the mechanism proposed for MMA homopolymerization (Scheme 5.2) it may be supposed that the structure of the cobalt-complex changes during the abstraction of the hydrogen atom, which undergoes a significant variation of the volume of the system. This hypothesis could be verified by knowing the structure of the complex. A crystal analysis gives informations on the structure, which was not successful for this complex (see Section 3).

Another cobalt-complex was also used as a CTA in the literature⁶¹: the bis(difluoroboryl) dimethylglyoximato cobalt (II) (COBF). The structure of COBF is very close to the one of CPhBF: substituting phenyl groups by methyl groups. COBF was reported to have a transfer constant, thus k_{tr} , one order of magnitude higher than the one of CPhBF, which was explained by the restricted mobility of CPhBF due to the presence of phenyl groups. Thus, the abstraction of a hydrogen atom is made more difficult with CPhBF. It may be anticipated that the mobility of the CPhBF molecules is much more restricted with increasing pressure due to the enhancement of the viscosity. Thus, k_{tr} will strongly decrease with increasing pressure, which is consistent with the results of this work.

In summary, the viscosity of the system is a significant rate-determining factor in the MMA homopolymerization with CPhBF as CTA, thus k_{tr} is higher in the presence of $scCO_2$ as a solvent. In addition, the bulky CPhBF molecule contributes to a strong and positive activation volume of k_{tr} .

5.5 References

1. Hutchinson, R. A.; Paquet, D. A.; Mc Minn, J. H. *Macromolecules* **1995**, 28, 5655.
2. De la Fuente, J. L.; Madruga, E. L. *J. Polym. Sc., Polym. Chem. Ed.* **1998**, 36, 2913.
3. De la Fuente, J. L.; Madruga, E. L. *J. Polym. Sc., Polym. Chem. Ed.* **2000**, 38, 170.
4. Isemer, C.; Wahl, A. private communication.
5. Beuermann, S.; Buback, M.; Isemer, C.; Lacik, I.; Wahl, A. *Macromolecules*, in preparation for publications.
6. Buback, M.; Kuchta, F.-D. *Macromol. Chem. Phys.* **1995**, 196, 1887.
7. Beuermann, S.; Buback, M.; Russell, G. T. *Macromol. Rapid. Commun.* **1994**, 15, 351.

8. Gridnev, A.; *J. Polym. Sci., Polym. Chem. Ed.* **2000**, 38, 1753.
9. Heuts, J. P. A.; Kukulj, D.; Foster, D. J.; Davis, T. P. *Macromolecules* **1998**, 31, 2894.
10. Heuts, J. P. A.; Foster, D. J.; Davis, T. P. *ACS symposium series 768, Transition Metal Catalysis in Macromolecular Design* **2000**, p 254.
11. Kowollik, C.; Davis, T. P. *J. Polym. Sci., Polym. Chem.* **2000**, 38, 3303.
12. Heuts, J. P. A.; Foster, D. J.; Davis, T. P.; Yamada, B.; Yamazoe, H.; Azukizawa, M. *Macromolecules* **1999**, 32, 2511.
13. Foster, D. J.; Heuts, P. A.; Lucien, F. P.; Davis, T. P. *Macromolecules* **1999**, 32, 5514.
14. Kukulj, D.; Davis, T. P. *Macromol. Chem. Phys.* **1998**, 199, 1697.
15. Heuts, J. P. A.; Foster, D. J.; Davis, T. P. *Macromolecules* **1998**, 31, 6034.
16. Haddleton, D. M.; Maloney, D. R.; Suddaby, K. G.; Muir, A. V. G.; Richards, S. N. *Macromol. Symp.* **1996**, 111, 37.
17. Russell, G. T. *Macromol. Theory. Simul.* **1995**, 4, 497.
18. Roberts, G. E.; Heuts, J. P. A.; Davis, T. P. *Macromolecules* **2000**, 33, 7765.
19. Krstina, J.; Moad, G.; Rizzardo, E.; Winsor, C. L.; Berge, C. T.; Fryd, M. *Macromolecules* **1995**, 28, 5381.
20. Moad, G.; Moad, C. L.; Krstina, J.; Rizzardo, E.; Berge, C. T.; Darling, T. R. PCT Int. Appl. WO 9615157, *Chem. Abstr.* **1996**, 125, 299554.
21. Rizzardo, E.; Meijs, G. F.; Thang, S. H.; *Macromol. Symp.* **1995**, 98, 101.
22. Darmon, M. J.; Berge, C. T.; Antonelli, J. A.; US 5362826, *Chem. Abstr.* **1993**, 120, 299554.
23. Moad, L. C.; Moad, G.; Rizzardo, E.; Thang, S. H. *Macromolecules* **1996**, 29, 7717.
24. Harrison, D. M. *Appl. Sc., The Chemistry of ω -unsaturated Oligomers and Polymers.* Swinburne Institute of Technology, **1988**.
25. Tanaka, H.; Kawa, H.; Sato, T. *J. Polym. Sci., Part A: Polym. Chem.* **1989**, 27, 1741.
26. Lechner, M. D.; Gehrke, K.; Nordmeier, E. H. *Makromolekulare Chemie*, Birkhäuser Verlag, Basel **1993**.
27. Tronche, C.; Martinez, F.; Horner, J. H.; Newcomb, M.; Senn, M.; Giese, B. *Tetrahedron. Lett.* **1996**, 37, 5845
28. Rong, X. X.; Pan, H. Q.; Dolbier, W. R.; Smart, B. E. *J. Am. Chem. Soc.* **1994**, 116, 521.
29. Colombani, D.; Chaumont, P. *Prog. Polym. Sci.* **1996**, 21, 439.
30. Berge, C. T.; Darmon, M. J.; Antonelli, J. A. *US Patent US 5*, **1994**, 362, 826.
31. Isemer, C. *Ph.-D Thesis* **2000**, Göttingen.

32. Bon, S. E.; Morsley, S. R.; Waterson, C.; Haddleton, D. M. *Macromolecules* **2000**, 33, 5818.
33. Coote, M. L.; Zammit, M. D.; Davis, T. P. Willett, G. D. *Macromolecules* **1997**, 30, 8182.
34. Coote, M. L.; Johnston, L. P.; Davis, T. P. *Macromolecules* **1997**, 30, 8191.
35. Heuts, J. P. A.; Foster, D. J.; Davis, T. P. *Macromolecules* **1999**, 32, 2511.
36. Sanayei, R. A.; O'Driscoll, K. F. *J. Macromol.Sci.* **1989**, A26, 1137.
37. Enikolopyan, N. S.; Smirnov, B. R.; Ponomarev, G. V.; Belgovskii, I. M.; *J Polym. Sci. Polym. Chem. Ed.* **1981**, 19, 879
38. Smirnov, B. R.; Morozaza, I. S.; Marchenko, A. P.; Markevic, M. A.; Pushchaeva, I. M.; Enikolopyan, N. S. *Dokl. Akad. Nauk. SSSR (Engl. Transl.)* **1980**, 253, 891.
39. Smirnov, B. R.; Plotnikov, V. D.; Ozerkovskii, B. V.; Roschupkin, V. P.; Enikolopyan, N. S. *Polym. Sci. USSR (Engl. Transl.)* **1981**, 23, 2894.
40. Brookhart, M.; Green, M. L. H.; Wong, L. L. *Prop. Inorg. Chem.* **1988**, 36,1.
41. Halpern, J.; Rempel, G. L.; Ng, F. T. *J. Am. Chem. Soc.* **1979**, 101, 7124.
42. Gridnev, A. A.; Belgovskii, I. M.; Enikolopyan, N. S. *Dokl. Akad. Nauk USSR (Engl. Trans.)* **1986**, 289, 1408.
43. Wayland, B. B., Posznik, G.; Mukerjee, S. L.; Fryd, M. *J. Am. Chem. Soc.* **1994**, 116, 7643.
44. Wayland, B. B.; Basicckes, L.; Mukerjee, S. L.; Wie, M.; Fryd, M. *Macromolecules* **1997**, 30, 8109.
45. Wayland, B. B.; Mukerjee, S.; Posznik, G.; Woska, D. C.; Basicches, L.; Gridnev, A. A.; Fryd, M.; Ittel, S. D. *In Controlled Radical Polymerization*; Matyjaszewski, K.; Ed.; ACS Symposium Series, 685; American Chemical Society: Washington, DC, **1998**, 305.
46. Gridnev, A. A.; Wayland, B. B.; Fryd, M. *Organometallics* **1996**, 15, 5116.
47. Haddleton, D. M.; Maloney, D. R.; Suddaby, K. G.; Muir, A. V. G.; Richards, S. N. *Macromol. Symp.* **1996**, 111, 37.
48. Foster, D. J.; Heuts, J. P. A.; Davis, T. P. *Polymer* **2000**, 41, 1385.
49. Businelli, L.; Gnanou, Y.; Maillard, B. *Macromol. Chem. Phys.* **2000**, 201, 2805.
50. Beuermann, S.; Buback, M.; Russell, G. T. *Macromol. Rapid. Commun.* **1994**, 15, 351.
51. Tooney, C. A.; Weale, K. E. *Transactions of the Faraday Society* **1962**, 58, 2446.

52. Walling, C.; Pellon, J. *J. Am. Chem. Soc.* **1957**, 79, 4776.
53. Heuts, J. P. A.; Foster, D. J.; Davis, T. P. *Macromolecules* **1999**, 32, 3907.
54. Beuermann, S.; Buback, M.; Davis, T. P.; Gilbert, R. G.; Hutchinson, R. A.; Olaj, O. F.; Russell, G. T.; Schweer, J.; van Herk, A. M. *Macromol. Chem. Phys.* **1997**, 198, 1545.
55. Heuts, J. P. A.; Gilbert, R. G.; Radom, L. *Macromolecules* **1995**, 28, 8771.
56. Mironychev, V. Y.; Mogilevich, M. M.; Smirnov, B. R.; Shapiro, Y. Y.; Golikov, J. V. *Polym. Sci. USSR* **1986**, 28, 2103.
57. Stephan, K.; Lucas, K. *Viscosity of Dense Fluids*, Plenum, New York **1979**.
58. Ogo, Y.; Kyonati, T. *Makromol. Chem.* **1978**, 179, 2407.
59. Fischer, J. P.; Mücke, G.; Schulz, G. V. *Ber. Bunsenges. Physik. Chem.* **1970**, 73, 1077.
60. Klingler, R. J.; Rathke, J. W. *J. Am. Chem. Soc.* **1994**, 116, 4772.
61. Sanayei, S. A.; O'Driscoll, K. F. *J. Macromol. Sci.* **1989**, A26(8), 1137.

6. Kinetic modeling

In order to understand the results obtained for chain-transfer rate coefficients, $k_{tr,copo}$, in styrene-MMA copolymerizations with DDM and CPhBF as CTAs, $k_{tr,copo}$ are modeled applying the terminal and the penultimate unit effect models. As explained in section 5.2, k_{tr}^{obs} obtained in styrene-MMA homo- and copolymerization with CPhBF are based on the transfer process described in scheme 5.2, which assumes a direct hydrogen abstraction by the Co(II) species. Recently¹ it has been suggested that other transfer reactions may occur in the catalytic chain-transfer reaction of CPhBF in the presence of styrene as comonomer. However, no conclusive evidence exists regarding the actual chain-transfer mechanism other than presented in scheme 5.2. Thus, in the following part k_{tr}^{obs} in styrene and MMA copolymerizations are also modeled.

The fractions of endgroups, Φ_A , formed are estimated for styrene-MMA copolymers.

The program package PREDICI[®] is used to simulate the molecular weight distribution of polymers obtained in the presence of DDM for styrene and MMA copolymerization. The results are compared to the corresponding experimental MWDs in order to confirm or disprove the predictions made in section 6.2, whether a terminal or a penultimate unit model describes the transfer process. In case of CPhBF, MWDs are modeled via PREDICI[®] in MMA homopolymerization.

6.1 Theoretical background

6.1.1 Simulations of k_{tr} applying terminal and PUE models

Free-radical copolymerization

In a copolymer system, the number of reactions occurring is higher than in free-radical homopolymerization, due to the presence of different types of radicals and monomers.

Chain growth proceeds via four distinct propagation steps², i.e., the addition of monomers A and B to propagating chains terminating in A or B, as shown in the following reaction scheme:



k_{pAA} and k_{pBB} refer to the homopropagation, and k_{pAB} and k_{pBA} to cross-propagation.

This model is called the terminal or Lewis-Mayo model, which considers only the influence of the terminal unit of a macroradical on the propagation rate coefficient and copolymer composition.

Within the terminal model, the mole fraction of monomer A in the instantaneously formed copolymer, F_A , can be expressed as a function of the mole fraction of the monomer A in the monomer feed, f_A :

$$F_A = \frac{r_A f_A^2 + f_A f_B}{r_A f_A^2 + 2 f_A f_B + r_B f_B^2} \quad (6.2)$$

where, r_A is the monomer reactivity ratio given by

$$r_A = \frac{k_{\text{pAA}}}{k_{\text{pAB}}} \quad (6.3)$$

The propagation rate coefficient, $k_{\text{p,copo}}$, is given by the expression:

$$k_{\text{p,copo}} = \frac{r_A f_A^2 + 2 f_A f_B + r_B f_B^2}{(r_A f_A / k_{\text{pAA}}) + (r_B f_B / k_{\text{pBB}})} \quad (6.4)$$

In general, the terminal model is found to adequately describe the copolymer composition (Eq. 6.2), but it fails to describe the average propagation rate coefficient, simultaneously^{2,3}.

Several models have been proposed to account for the discrepancy between the terminal model predictions and the experimentally found average propagation rate coefficients^{2,3}. The most frequently used model is the so-called "Penultimate Unit Effect" (PUE) model, which assumes that the radical reactivity is affected by the preceding unit on the chain as well. PUE model was first formulated by Merz et al.⁴. This model has attracted a lot of attention due to the work of Fukuda et al.⁵. In the penultimate model the radical reactivities s (e.g., $s_A = k_{pBAA} / k_{pAAA}$) are defined in addition to the reactivity ratios r (e.g., $r_{AA} = k_{pAAA} / k_{pAAB}$). These radical reactivities describe the effect of the penultimate unit on the homopropagation rate. A complete description of the development of the penultimate model can be found at ref. 6.

The following scheme summarizes all equations describing the kinetic coefficients in the implicit PUE (IPUE) model. More details about IPUE model are found at refs. 7 and 6.

$$\bar{k}_{pAA} = \frac{k_{pAAA}(r_A f_A + f_B)}{r_A f_A + \frac{f_B}{s_A}} \quad (6.5) \quad \bar{k}_{pBB} = \frac{k_{pBBB}(r_B f_B + f_A)}{r_B f_B + \frac{f_A}{s_B}} \quad (6.6)$$

$$r_A = \frac{\bar{k}_{pAA}}{k_{pAB}} \quad (6.7) \quad r_B = \frac{\bar{k}_{pBB}}{k_{pBA}} \quad (6.8)$$

$$s_A = \frac{k_{pBAA}}{k_{pAAA}} \quad (6.9) \quad s_B = \frac{k_{pABB}}{k_{pBBB}} \quad (6.10)$$

The mean homopropagation rate coefficients, \bar{k}_{pii} , are calculated using the mean reactivity ratio, r , the radical reactivities, s , homopropagation rate coefficients, k_{piii} , and the monomer mole fractions using Eqs. 6.5 and 6.6.

Both the instantaneous copolymer composition and the propagation rate coefficient implicitly contain the ratio of the two propagating radical concentrations, A_{AB} , of which an expression (Eq. 6.11) can be derived from the steady state assumption in all propagating radical concentrations. This ratio is important as it is basically a weighting factor for the contributions of the reactions of either radical to the overall observed kinetics and copolymer composition.

From this ratio the fraction of the different propagating terminal radicals, ϕ_A , is easily derived and given by Eq. 6.12⁸.

$$A_{AB} = \frac{[RA \cdot]}{[RB \cdot]} = \frac{\bar{k}_{pBB} r_A f_A}{\bar{k}_{pAA} r_B f_B} \quad (6.11)$$

$$\phi_A = \frac{A_{AB}}{1 + A_{AB}} \quad (6.12)$$

Considering the PUE model the fraction of propagating penultimate radicals, ϕ_{AA} , may be expressed as:

$$\phi_{AA} = \phi_A - \phi_{BA} = \frac{r_A \cdot f_A \cdot \phi_A}{r_A \cdot f_A + \frac{f_B}{s_A}} \quad (6.13)$$

The population ϕ_{BB} is calculated analog to ϕ_{AA} .

ϕ_{AA} , ϕ_{AB} , ϕ_{BB} and ϕ_{BA} are the fractions of the propagating terminal radicals AA, AB, BB, and BA, respectively.

Copolymerizations in the presence of a chain-transfer agent

In the literature it is shown that different propagating radicals have an impact on the propagation kinetics, by evidence of their propagation rate coefficients values⁹. Modeling of the termination rate coefficient, $k_{t,copo}$, as a function of the initial monomer feed in the reaction mixture has been thoroughly addressed by Fukuda et al.¹⁰. These models such as for the propagation rate coefficients apply the terminal and penultimate unit effect models. In case of transfer reaction in a copolymerization, the polymer radicals which react with the chain-transfer agent should also be differentiated. Thus, it is expected that a similar effect as seen for the propagation and termination reactions might exist for the chain-transfer reaction.

The present work extends to chain-transfer reaction the models based on the terminal and penultimate unit effect, which were proposed for propagation and termination reactions.

The reactions shown in Eqs. 6.14a and 6.14b are those for a general chain-transfer process in a chain-transfer copolymerization considering only the terminal unit of a macroradical. Both reactions have an associated chain-transfer rate coefficient, $k_{tr,A}$ and $k_{tr,B}$.



These two chain-transfer reactions will contribute to an observed chain-transfer rate coefficient, $k_{tr,copo}$, which can be expressed as an average of the two individual rate coefficients, weighted by the radical fractions.

$$\text{Model A:} \quad k_{tr,copo} = \phi_A \cdot k_{tr,A} + (1 - \phi_A) \cdot k_{tr,B} \quad (6.15)$$

Model A, which is described by Eq. 6.15, assumes that penultimate unit effects are negligible in the chain-transfer reaction. This assumption is not readily tested, and it is difficult to make an a priori estimate of the magnitude of potential penultimate unit effects.

In case of a penultimate unit effect in the transfer reaction, four (penultimate) transfer coefficients are taken into account, which are associated with the equations below.



The corresponding chain-transfer rate coefficient for the copolymerization is simply given by the following Eq. 6.17.

$$\text{Model B:} \quad k_{tr,copo} = k_{tr,AA} \cdot \phi_{AA} + k_{tr,BB} \cdot \phi_{BB} + k_{tr,AB} \cdot \phi_{AB} + k_{tr,BA} \cdot \phi_{BA} \quad (6.17)$$

Bamford et al.¹¹ proposed Model B for the estimation of C_T .

Model B is also used to predict the termination rate coefficient in copolymerization assuming an arithmetic mean approximation¹⁰ for the determination of k_t for reactions between two different "penultimate" free radicals. In this case, the model assumes that the polymer radical with endgroup AB terminates with the same radical (endgroup AB). Thus, the number of penultimate termination rate coefficients is reduced from ten to four. More details about this model are given in ref. 10. A second model, here Model C, differs from the last one in that a geometric mean approximation is applied. Model C is converted to k_{tr} simulation since the transfer reaction scheme considers also four reactions (Eqs. 6.16a-6.16d) when a PUE is taken into account.

Model C is described by the following Eq. 6.18.

$$\text{Model C: } k_{tr,copo}^{0.5} = k_{tr,AA}^{0.5} \cdot \phi_{AA} + k_{tr,BB}^{0.5} \cdot \phi_{BB} + k_{tr,AB}^{0.5} \cdot \phi_{AB} + k_{tr,BA}^{0.5} \cdot \phi_{BA} \quad (6.18)$$

Once $k_{tr,copo}$ is known as a function of the initial monomer feed for the two systems of this work, styrene-MMA copolymerizations in the presence of DDM and CPhBF as CTAs, a thorough analysis of the experimental data by model A is carried out in the next section. For models B and C, the experimental data (k_{tr}) is fitted to derive the variables $k_{tr,AB}$ ($C_{T,AB}$) and $k_{tr,BA}$ ($C_{T,BA}$). An error function for the calculation of residuals is defined and the individual residuals are weighted such that both contributions are of similar size. The error function usually is:

$$\text{error} = \sum \sqrt{(\text{data}_{\text{exp}} - \text{data}_{\text{model}})^2} \quad (6.19)$$

The least squares fitting procedure according to Levenberg-Marquardt^{12,13} is started and the program provides a set of optimum parameters.

6.1.2 Endgroups estimate

The most important aspects of free-radical polymerization with and without chain-transfer agent were outlined (k_p and k_{tr}) in the preceding part. These concepts are now combined for the prediction of the fraction of a particular endgroup in chain-transfer copolymerization. It is clear that for a particular endgroup to be formed, the radicals of desired nature and a large reactivity of these radicals towards the chain-transfer agent are required. Thus, the probability of the formation of an endgroup of type A is defined as the product of the probability of finding a radical type A and the probability of RA^\bullet reacting with CTA. The former probability is given by the fraction of RA^\bullet radicals, ϕ_A , as given by Eq. 6.12. The probability of radicals reacting with the chain-transfer agent, $P(A/CTA)$, is given by the ratio of the rate of reaction with CTA and all possible reaction rates involving RA^\bullet radicals (Eqs 20-21)^{14,15,16,17}. The transfers to monomer are assumed to be negligible in case of a styrene-MMA copolymerization in the reaction conditions¹⁸. In a transfer dominated system, transfer events largely dominate termination events (see Chap. 4). Thus, terminations by combination and disproportionation may be negligible.

$$P(A/CTA) = \frac{\text{rate of } RA^\bullet \text{ reacting with CTA}}{\sum_{\text{all possible } x} \text{rate of } RA^\bullet \text{ reacting with } x} \quad (6.20)$$

$$P(A/CTA) = \frac{k_{tr,A} \cdot [RA^\bullet] \cdot [CTA]}{(k_{tr,A} \cdot [CTA] + k_{pAA} \cdot [A] + k_{pAB} \cdot [B]) \cdot [RA^\bullet]} \quad (6.21)$$

Using, $C_{T,A} = \frac{k_{tr,A}}{k_{pAA}}$ and Eq. 6.3 gives:

$$P(A/CTA) = \frac{C_{T,A} [CTA]}{C_{T,A} [CTA] + [A] + [B]r_A^{-1}} \quad (6.22)$$

where, $C_{T,A}$ and $[CTA]$ are the chain-transfer constant for homopolymerization of A and the concentration of chain-transfer agent, respectively. $[A]$ and $[B]$ are the concentrations of monomer A and B, respectively.

The calculation of $P(A/CTA)$ only involves the knowledge of kinetic parameters, which are already required for the modeling of the chain-transfer coefficient. To derive an expression for the fraction of A endgroups, Φ_A , the probability of forming an A endgroup, i.e., $\phi_A \cdot P(A/CTA)$, needs to be normalized by the overall probability of forming an endgroup. If this is taken into account, the fraction of A endgroups is given by Eq. 6.23^{14,15,16,17}.

$$\Phi_A = \frac{\phi_A \cdot P(A/CTA)}{\phi_A \cdot P(A/CTA) + (1 - \phi_A) \cdot P(B/CTA)} \quad (6.23)$$

6.1.3 Simulation tool PREDICI[®]

The kinetic model described in this work is implemented into the simulation program PREDICI[®] (Polyreaction distributions by Countable System Integration) developed by M. Wulkow^{19,20}. The program uses a highly efficient algorithm, called discrete hp-algorithm for solving complex sets of countable differential equations. An integrated function interpreter enables the coupling of rate coefficients of elementary reaction steps with individual species concentrations, conversion, copolymer composition, number and weight average of the formed polymer or chain lengths of individual species. As a special feature of PREDICI[®], the full molecular weight distribution can be derived without any assumption of closure conditions.

6.2 Simulation of k_{tr} applying terminal and PUE models

In this section, the copolymerization behavior of styrene and MMA in terms of the fraction of propagating styrene radicals, ϕ_s , is modeled. The applicability of models A through C (Eqs. 6.15, 6.17, 6.18) is tested for the description of a conventional (DDM) and a catalytic (COPhBF) chain transfer reaction in the copolymerization of styrene and MMA.

6.2.1 Free-radical copolymerization

Fig. 6.1 shows the variation of ϕ_s with the mole fraction of styrene in the monomer feed for copolymerizations of styrene and MMA in bulk and in $scCO_2$ at $80^\circ C$ and 300 bar applying the terminal and IPUE models in Eq. 6.11 (A and B correspond to styrene and MMA, respectively).

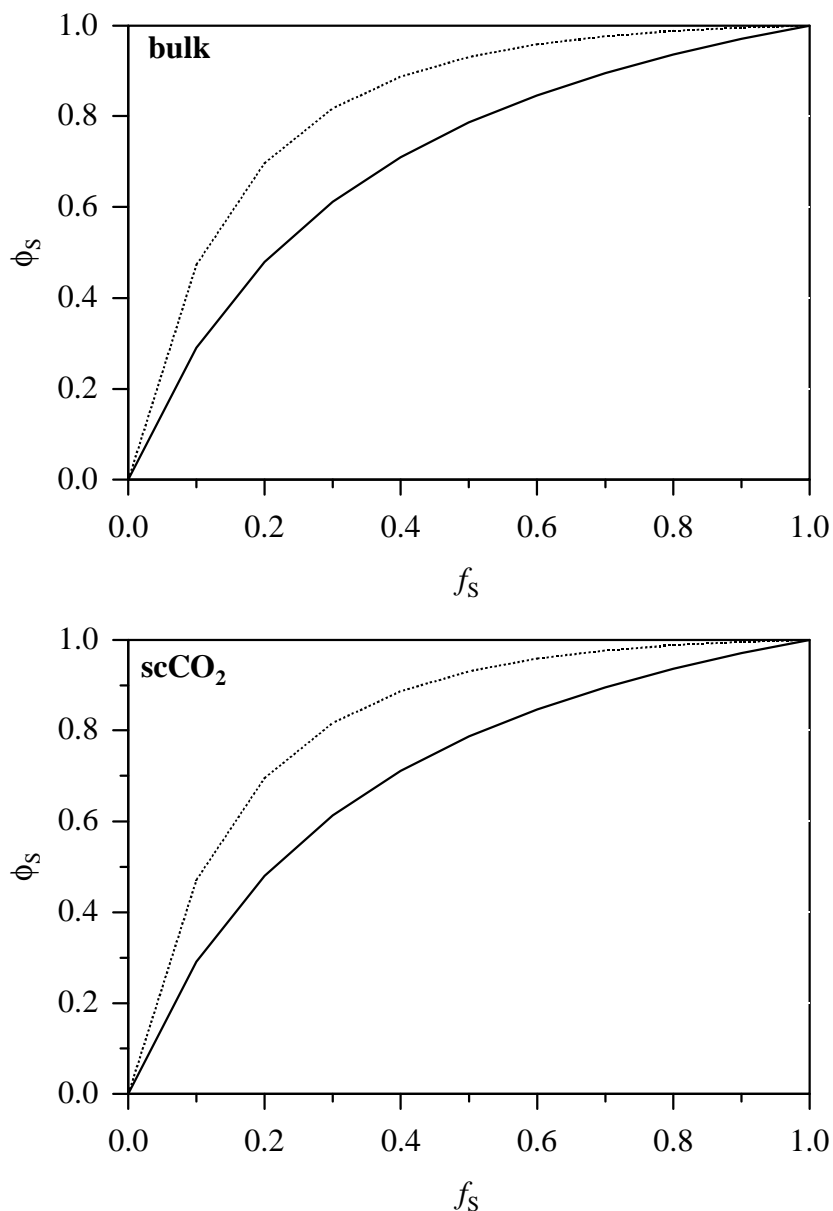


Figure 6.1: Fraction of propagating styrene radicals as a function of f_s in styrene-MMA copolymerization in bulk and in $scCO_2$ at $80^\circ C$ and 300 bar. Implicit penultimate predictions (dotted line) and terminal predictions (solid line).

The parameters used to calculate ϕ_S are collected in Table 6.1.

	MMA		styrene	
	bulk	scCO ₂	bulk	scCO ₂
$k_p / \text{L}\cdot\text{mol}^{-1}\cdot\text{s}^{-1}$	1540	1382	740	685
IPUE model	$r_B = 0.43$	$r_B = 0.50$	$r_A = 0.85$	$r_A = 0.87$
	$s_2 = 10$	$s_B = 10$	$s_A = 0.5$	$s_A = 0.5$
Terminal model	$r_B = 0.41$	$r_B = 0.47$	$r_A = 0.82$	$r_A = 0.86$

Table 6.1: Parameters used to determine f_S at 80°C and 300 bar in bulk and in scCO₂ via the IPUE and the terminal models. $k_{p,\text{styrene}}$, $k_{p,\text{MMA}}$, r , and s are taken from refs. 9, 21 and 22.

Fig. 6.1 shows that the fraction of propagating styrene radicals increases with increasing f_S . The simple terminal model and the more complex IPUE model give qualitatively the same trend for ϕ_S .

As indicated in the literature, k_p decreases with increasing the mole fraction of styrene in the monomer feed^{9,23,24}. Therefore, k_p styrene is lower than k_p MMA in the same conditions of experiment. It has already been reported that the k_p behavior in styrene and MMA copolymerization is well described by the IPUE model^{9,23,24}. Thus, in this work ϕ_S and $k_{p,\text{copo}}$ are determined applying the IPUE model.

In Fig. 6.1, the fraction of the radicals derived from the slower propagating monomer, styrene, is always larger than the corresponding fraction in the monomer feed. For example, at $f_S = 0.5$, the corresponding ϕ_S value is around 0.9. Thus, even at low f_S styryl radicals are the dominant radicals in the copolymerization system. Basically this means that the styrene radicals have a longer life time before they propagate and in the meantime are more prone to possible side reactions. It is indeed this behavior that is used in endgroup control. Therefore, in section 6.4, the study will be focused on styrene as endgroup.

6.2.2 Copolymerization in the presence of DDM

Fig. 6.2 shows the k_{tr} values for copolymerizations of styrene and MMA in $scCO_2$ with DDM as CTA at $80^\circ C$ and 300 bar obtained experimentally (circles) and via models A through C (lines). The experimental k_{tr} data, which were determined in section 5.1, are listed in Appendix 2. The reported values show that k_{tr} in bulk and in $scCO_2$ are similar. Thus, copolymerizations k_{tr} in bulk are not modeled since it is expected to have the same trend as k_{tr} copolymerization in $scCO_2$.

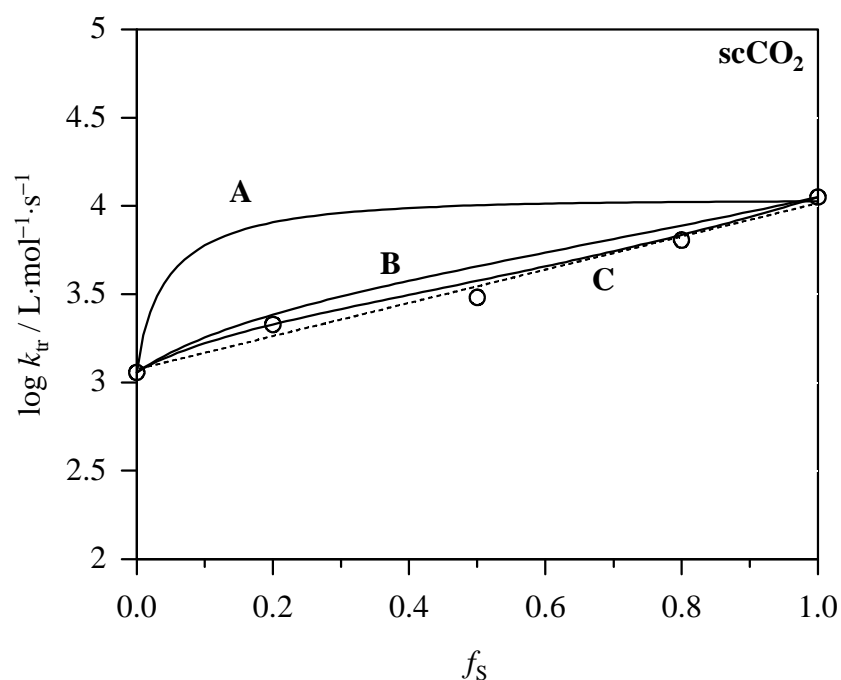


Figure 6.2: Chain-transfer rate coefficients of styrene-MMA copolymerizations in 40 wt % $scCO_2$ with DDM as chain-transfer agent at $80^\circ C$, 300 bar plotted against the mole fraction of styrene. The lines (A) through (C) correspond to the copolymerization k_{tr} models given in the text of Section 6.1.1. The dotted lines correspond to the linear fit of the experimental data listed in Appendix 2.

The copolymerization transfer rate coefficients for the penultimate radicals, $k_{tr,AB}$ and $k_{tr,BA}$, as obtained from fitting the $k_{tr,copo}$ data to model C are listed in Table 6.2. The rate coefficients $k_{tr,AB}$ and $k_{tr,BA}$ obtained are between the homotransfer rate coefficients and are very close to each other. This would allow to reduce the number of parameters for $k_{tr,copo}$ modeling.

$\log k_{tr,AB} / \text{L}\cdot\text{mol}^{-1}\cdot\text{s}^{-1}$	$\log k_{tr,BA} / \text{L}\cdot\text{mol}^{-1}\cdot\text{s}^{-1}$
3.17	3.47

Table 6.2: Transfer rate coefficients for penultimate radicals as deduced from models C for styrene (A) and MMA (B) copolymerizations at 80°C and 300 bar in scCO₂ using DDM as CTA.

In both cases, for the experimental data and the predictions, the addition of the slowly propagating monomer styrene to the copolymer system, leads to an increase of k_{tr} . As can be seen upon inspection of Fig. 6.2, the plot of $\log k_{tr}$ vs f_S is clearly linear for the values experimentally determined. It is obvious that models C and B, which assume four kinds of penultimate free radicals species, allow for a good representation of the experimental data. Model C provides a better representation of the experimental data. In other words, the simple terminal model, described by model A, does not allow for an accurate description of the chain-transfer rate coefficient for DDM as CTA and the more complex PUE model is required.

The fraction of propagating styryl radicals is the dominant radical endgroup even at low f_S as seen in Fig. 6.1. The results obtained in section 5.1 have shown that k_{tr} in styrene homopolymerization is higher than k_{tr} in MMA homopolymerization. Thus, it is expected that k_{tr} significantly increases even at low f_S , as depicted by the model A in Fig. 6.2. This effect is not seen for DDM, which confirms that the simple terminal model does not allow for an accurate description of k_{tr} for DDM as CTA.

Such PUE model considers steric factors, in particular a shielding of the free-radical chain end. Substituents on the terminal and on the penultimate unit should contribute to this effect. The values of $k_{tr,AB}$ and $k_{tr,BA}$ determined with model C are close to $k_{tr,AA}$ determined in MMA homopolymerization. This indicates that MMA, which is sterically hindered, strongly influences the transfer process as terminal and penultimate unit.

6.2.3 Copolymerization in the presence of CPhBF

k_{tr} values for copolymerizations of styrene and MMA in bulk and in scCO₂ with CPhBF as CTA at 80°C and 300 bar obtained experimentally (circles) and via models A through C (lines) are pictured in Fig. 6.3. The experimental k_{tr}^{obs} data, which were determined

considering scheme 5.2 to be valid, are listed in Appendix 3. Copolymerization k_{tr}^{obs} are modeled in both media since the reported values show an influence of $scCO_2$ as a solvent on k_{tr}^{obs} .

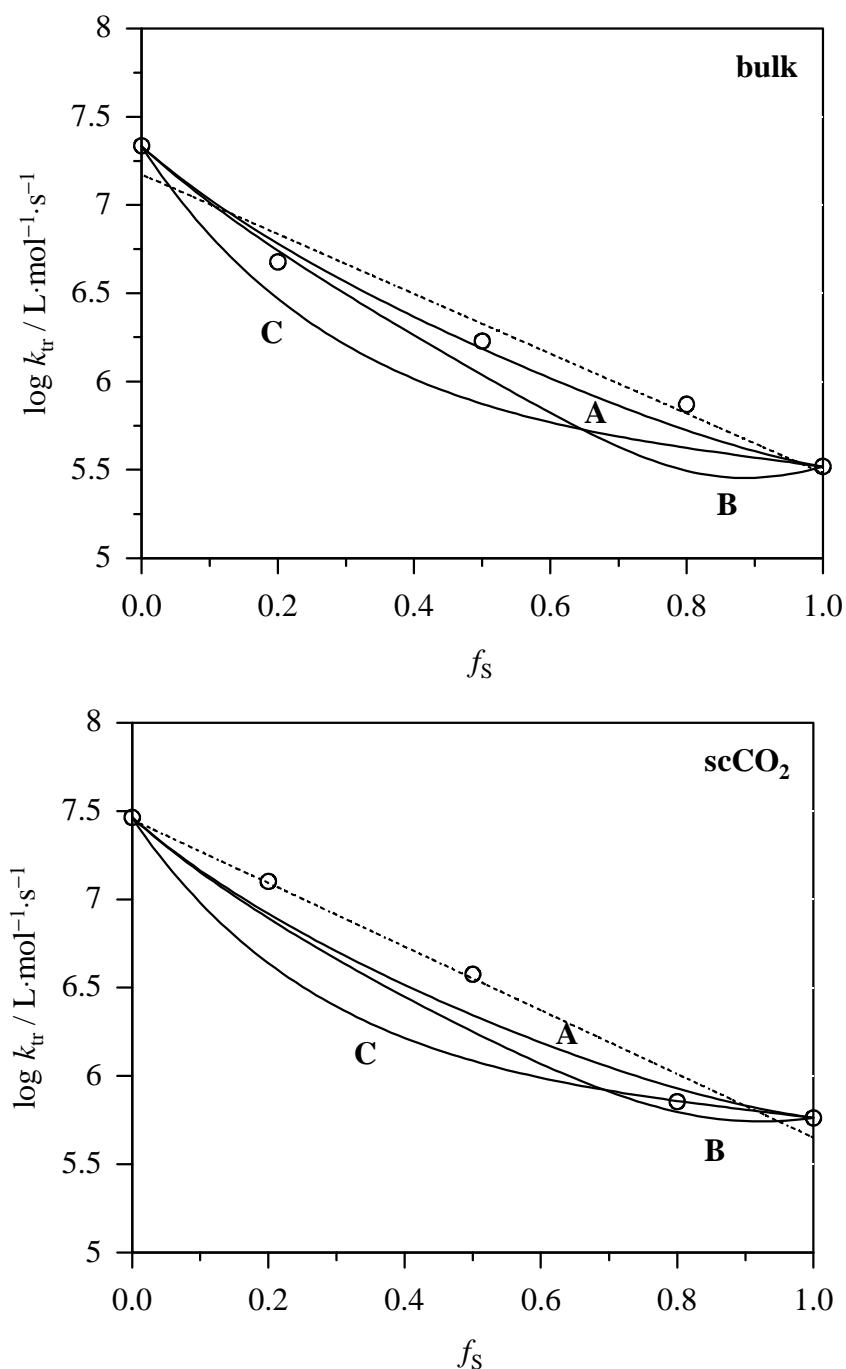


Figure 6.3: Chain-transfer rate coefficients of styrene-MMA copolymerizations in bulk and in 40 wt % $scCO_2$, at 80°C, 300 bar with $COPhBF$ as chain-transfer agent plotted against the mole fraction of styrene. The lines (A) through (C) correspond to the copolymerization k_{tr} models given in the text of Section 6.1.1. The dotted lines correspond to the linear fit of the experimental data which are listed in Appendix 3.

Fig. 6.3 shows that in both cases, models A through C and experimental data, k_{tr}^{obs} decreases with increasing f_S . As reported in Appendix 3, the uncertainties of the experimental data are relatively significant. Thus, it may be anticipated that within experimental uncertainty model A, which considers only two types of radicals, provides a better description of k_{tr}^{obs} for COPhBF as catalytic chain-transfer agent in bulk and in $scCO_2$. The terminal model is sufficient to describe the k_{tr}^{obs} in styrene and MMA copolymerization with COPhBF.

In case of COPhBF, k_{tr}^{obs} in styrene homopolymerization is lower than k_{tr}^{obs} in MMA homopolymerization (see Section 5.2). If the terminal model describes the transfer reaction well, k_{tr}^{obs} should significantly decrease for f_S from 0 to 2. The values of k_{tr}^{obs} reported in Appendix 2, clearly show this effect (k_{tr}^{obs} in bulk at 300 bar are $2.16 \cdot 10^7$ and $4.64 \cdot 10^6$ $L \cdot mol^{-1} \cdot s^{-1}$ for $f_S = 0$ and 0.2, respectively). Thus, a terminal model is expected for the description of the transfer process with COPhBF as catalytic CTA.

6.3 Modeling of full molecular weight distributions of styrene-MMA copolymers via PREDICI^â

6.3.1 Experimental considerations

In this section, the modeling of full molecular weight distributions, MWDs, of polymers is investigated. As described in the preceding section, IPUE has already been demonstrated to describe the propagation rate coefficients^{9,21,22} for copolymerization of styrene (S) and MMA (M). k_{pSSS} and k_{pMMM} are the propagation rate coefficients of styrene and MMA homopolymerization, respectively. The propagation rate coefficients, k_{pSM} , k_{pMS} , \bar{k}_{pSS} , \bar{k}_{pMM} are determined using Eqs. 6.5-6.8. k_{pSSS} , k_{pMMM} , r_S and r_M are listed in Table 6.1 for the conditions required.

The general reaction scheme used for the copolymerization of styrene and MMA with a transfer agent is as follows:

Initiation	$I^\bullet + S \rightarrow RS_1^\bullet$	k_{pSSS}
	$I^\bullet + M \rightarrow RM_1^\bullet$	k_{pMMM}
Propagation	$RS_n^\bullet + S \rightarrow RS_{n+1}^\bullet$	\bar{k}_{pSS}
	$RM_n^\bullet + M \rightarrow RM_{n+1}^\bullet$	\bar{k}_{pMM}
	$RS_n^\bullet + M \rightarrow RM_{n+1}^\bullet$	k_{pSM}
	$RM_n^\bullet + S \rightarrow RS_{n+1}^\bullet$	k_{pMS}
Termination (combination and disproportionation)	$RS_n^\bullet + RS_m^\bullet \rightarrow P_{n+m}, P_n + P_m$	$k_{tc,S}, k_{td,S}$
	$RM_n^\bullet + RM_m^\bullet \rightarrow P_{n+m}, P_n + P_m$	$k_{tc,M}, k_{td,M}$
	$RS_n^\bullet + RM_m^\bullet \rightarrow P_{n+m}, P_n + P_m$	$k_{tc,copo}, k_{td,copo}$
Transfer to monomer	$RS_n^\bullet + S \rightarrow P_n + S_1^\bullet$	$k_{trM,S}$
	$RM_n^\bullet + M \rightarrow P_n + M_1^\bullet$	$k_{trM,M}$
	$RS_n^\bullet + M \rightarrow P_n + M_1^\bullet$	$k_{trM,copo}$
	$RM_n^\bullet + S \rightarrow P_n + S_1^\bullet$	$k_{trM,copo}$

Scheme 6.1: Typical reaction scheme for copolymerizations of styrene (S) and MMA (M). $k_{t,c}$ and $k_{t,d}$ are the termination rate coefficients for combination and disproportionation, respectively. k_{trM} is the chain-transfer rate coefficients to monomer.

The modeling of MWDs via PREDICI[®] was carried out for polymerizations in bulk and in scCO₂ at 300 bar and 80°C. The termination rate coefficients, k_{tc} and k_{td} , are obtained considering that the ratio of combination and disproportionation is 7 as suggested in ref. 25. As already mentioned, in a transfer dominated system the termination events are negligible as compared to the transfer events. In addition, in styrene-MMA copolymerization the transfer rate coefficients to monomer are very low. Therefore, the following approximations are applied. $k_{tc,copo}$, $k_{td,copo}$ and $k_{trM,copo}$ are the arithmetic average values of the corresponding homo values. These coefficients are listed in Table 6.3.

	$k_{tc} / \text{L}\cdot\text{mol}^{-1}\cdot\text{s}^{-1}$		$k_{trM} / \text{L}\cdot\text{mol}^{-1}\cdot\text{s}^{-1}$
	bulk	scCO ₂	
MMA	$5\cdot 10^7$	10^8	0.06
	ref. 9*	ref. 9*	ref. 18
styrene	10^8	$8\cdot 10^8$	0.07
	ref. 21	ref. 21	ref. 18

Table 6.3: Kinetic coefficients used for modeling the molecular weight distribution of styrene and MMA polymerizations in bulk and in 40 wt % scCO₂ at 80°C and 300 bar. * The initiator used was AIBN.

In the PLP-SEC MWDs, the laser pulse rate is also a very important parameter, which determines the initial radical concentration, c_R^O . c_R^O is given by Eq. 6.24 as follows:

$$c_R^O = 2 \cdot \Phi \cdot \frac{n_{\text{abs}}}{V} \quad (6.24)$$

where Φ is the primary quantum yield, n_{abs} is the number of absorbed photons and V is the irradiated volume. The primary quantum yield is the product of the laser efficiency j and the initiator efficiency f and corresponds to a value of 0.24 for DMPA²⁶. According to the Beer-Lambert's law, the number of absorbed photons can be calculated by Eq. 6.25.

$$n_{\text{abs}} = \frac{E_p}{E_\lambda} \cdot (1 - 10^{-ecd}) \quad (6.25)$$

E_p , the energy of a single laser pulse, is measured using a laser power meter for known laser pulse repetition rate. E_λ is the energy of one mol of photons at the laser wavelength of 351 nm. e is the molar absorption coefficient of the initiator molecule at 351 nm, which is $200\cdot 10^3 \text{ cm}^2\cdot\text{mol}^{-1}$ for DMPA, c is the photoinitiator concentration and d is the optical path length.

The radical concentration used for the simulation via PREDICI[®] is estimated to be $1.5 \cdot 10^{-6}$ mol·L⁻¹.

Broadening of the MWD

Previously, it has been reported that a simulated MWD should be broadened in order to account for the broadening due to axial dispersion in experimental SEC analysis²⁷. The SEC set-up used for the determination of the polymer MWD shows only very little broadening, which may be characterized by a σ -value of 0.03-0.04 ref. 27. The procedure to determine this broadening value has been described by Buback and coworkers²⁸. Fig. 6.4 shows a comparison between MWDs as obtained via PREDICI[®] simulation (lines) and MWDs which were broadened applying a σ -value of 0.04 (x).

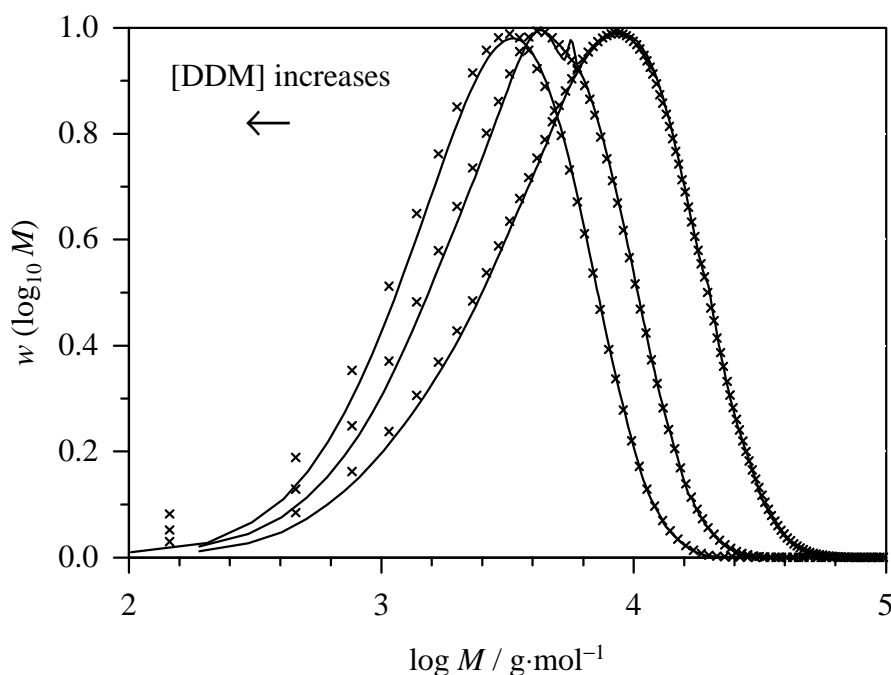


Figure 6.4: MWDs obtained from simulations without (lines) and after applying broadening (x) for copolymerizations of styrene and MMA ($f_S = 0.5$) at 80°C, 300 bar in scCO₂. $[DDM]/[M] = 0.005, 0.01, 0.015$.

It is obvious from Fig. 6.4 that the impact of broadening MWDs is not significant. Especially the high molecular weight region of the distribution used in the CLD method (see section 4) is

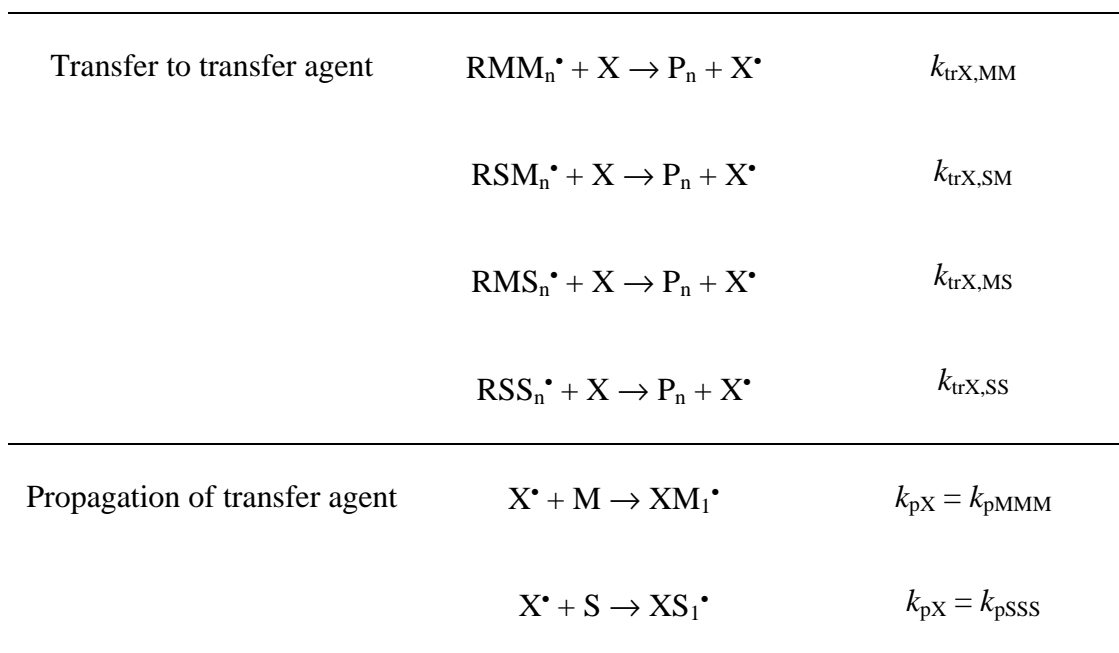
not affected by broadening. Thus, MWDs obtained from modeling presented in the following Sections are given without applying any broadening.

6.3.2 DDM as chain-transfer agent

The modeling of MWD for styrene-MMA polymer with DDM is investigated in order to confirm the prediction of the presence of penultimate effect in the transfer process. The validity of the transfer rate coefficients, $k_{tr,AB}$ and $k_{tr,BA}$, determined in section 6.2 is also tested.

Reaction scheme

In the following modeling of MWD, PUE model is applied as it has been suggested in section 6.2 to describe the transfer process well. The mechanism followed is shown in scheme 6.2.



Scheme 6.2: Chain-transfer reactions for copolymerizations with DDM.

$k_{trX,MM}$ and $k_{trX,SS}$ are the chain-transfer rate coefficients for MMA and styrene homopolymerizations, respectively. $k_{trX,SM}$ and $k_{trX,MS}$ correspond to the chain-transfer rate coefficients of the penultimate unit radicals SM and MS, respectively, which were estimated

using model C in section 6.2 ($k_{trX,SM}$ and $k_{trX,MS}$ are $k_{tr,AB}$ and $k_{tr,BA}$, respectively and are listed in Table 6.2).

The propagation rate coefficient of the transfer agent with a monomer A, k_{pX} , is assumed to be similar to the homopropagation rate coefficient of A, k_{pAAA} .

Modeling of MWDs and k_{tr}

PREDICI[®] simulations of MWD were investigated for styrene-MMA copolymerizations ($f_S = 0.1, 0.4$ and 0.6) at 80°C and 300 bar in bulk. Fig. 6.5 shows, as example, the modeled MWDs obtained for polymerizations in bulk with $f_S = 0.1$ in the presence of different amounts of DDM. As k_{tr} is not influenced by the presence of scCO_2 as compared to the bulk value, the same results are expected in both media.

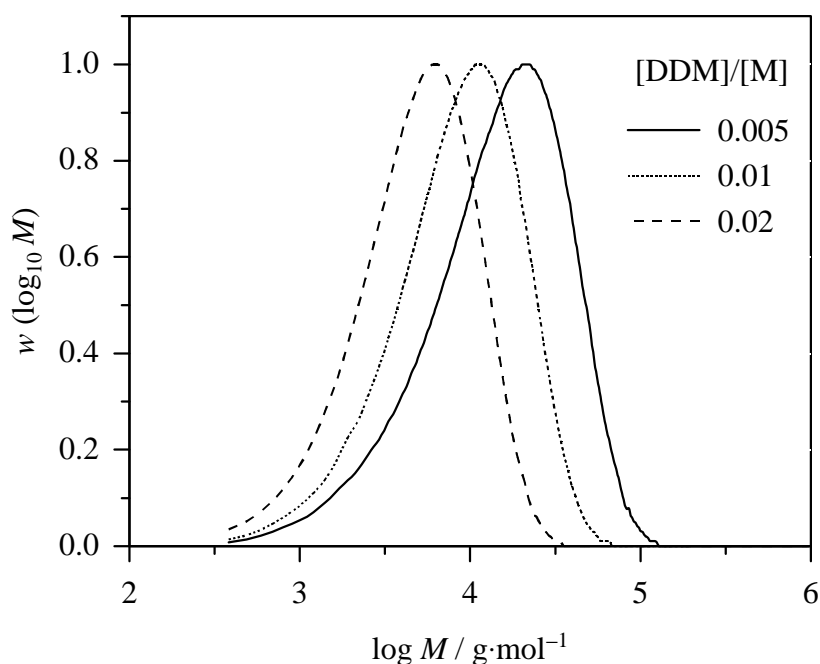


Figure 6.5: Simulated molecular weight distributions for copolymerizations of styrene and MMA ($f_S = 0.1$) at 80°C , 300 bar with different amounts of DDM.

As expected, Fig. 6.5 shows that MWD obtained via PREDICI[®] is shifted to lower MW values increasing the amount of DDM.

In order to compare k_{tr} values obtained experimentally in section 5.2 and k_{tr} values obtained by modeling the MWD via PREDICI[®], chain-transfer rate coefficients were determined using the

same method (CLD method as explained in section 4). Fig. 6.6 pictures $\log k_{tr}$, derived from modeling (full circle) and experimentally determined (open circle), as a function of f_S for copolymerizations of styrene and MMA in bulk at 80°C and 300 bar.

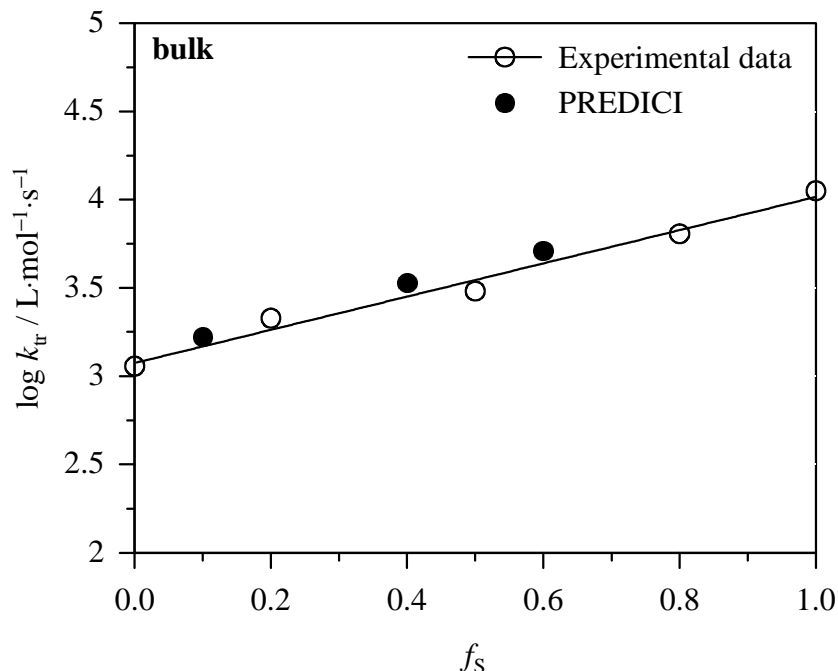


Figure 6.6: $\log k_{tr}$ obtained from MWDs modeled with PREDICI^â (full circle) and obtained experimentally (open circle) for bulk copolymerizations of styrene and MMA at 80°C and 300 bar as a function of the mole fraction of styrene in the monomer feed.

Fig. 6.6 shows a very good agreement between the k_{tr} values, determined via PREDICI[®] using $k_{tr,AB}$ and $k_{tr,BA}$ reported in table 6.2, and the k_{tr} values obtained experimentally. As mentioned before, the plot of $\log k_{tr}$ vs. f_S is linear, which induces that knowing homopolymerizations k_{tr} values, copolymerization k_{tr} may be estimated at each f_S .

It is clear that the kinetic model and the kinetic coefficients, $k_{tr,AB}$ and $k_{tr,BA}$, applied here are available to describe the copolymerization of styrene-MMA in bulk with DDM as CTA via PREDICI[®].

The present work indicates that styrene-MMA copolymerization with DDM as CTA is adequately represented by the PUE model in the transfer reaction.

In order to confirm that terminal model does not allow for an accurate description of the transfer process with DDM, few MWDs were modeled considering a terminal model for the

transfer reaction with DDM. In this case only two transfer reactions are taken into account associated to the MMA and styrene homopropagation transfer rate coefficients.

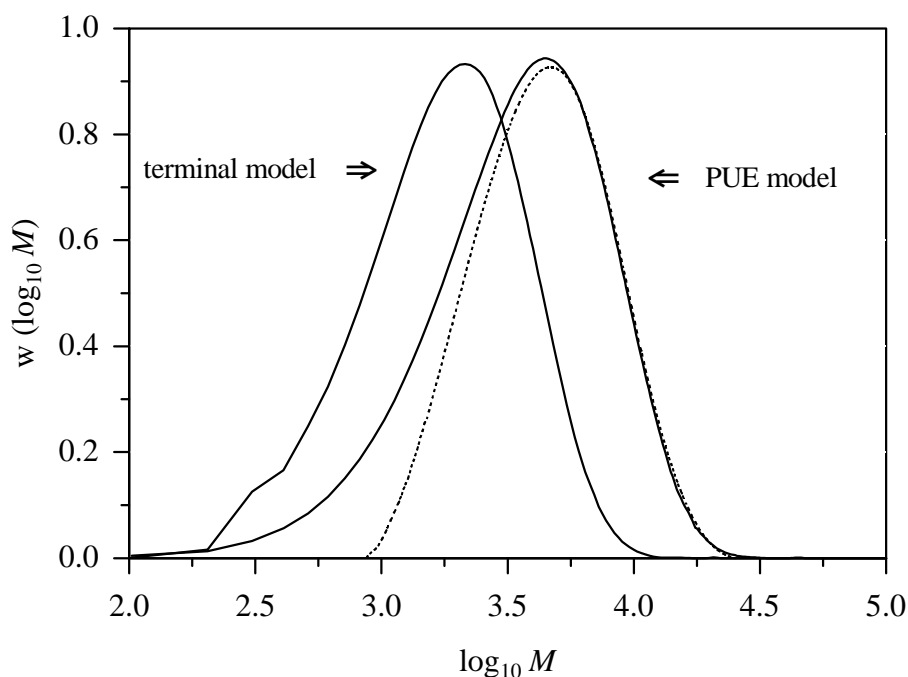


Figure 6.7: Simulated (solid line) and experimental (dotted line) molecular weight distributions for the copolymerization of styrene and MMA ($f_S = 0.5$) in bulk at 80°C and 300 bar with $[\text{DDM}]/[\text{sty}] = 0.01$.

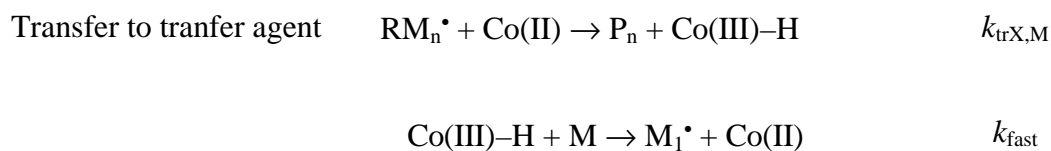
Fig. 6.7 shows, as example, the MWD obtained for bulk polymerizations at 80°C , 300 bar, and $f_S = 0.5$. As expected the MWD modeled using PUE model in the transfer reaction is in very good agreement with the experimental MWD. In contrast, the modeled MWD obtained considering a terminal model in the transfer reaction, is shifted to lower values of MW compared to the experimental MWD. This provides strong evidence that terminal model is not sufficient to allow a good representation of the transfer process with DDM.

6.3.3 CPhBF as catalytic chain-transfer agent

As mentioned in section 5.4, k_{tr}^{obs} determined in styrene and MMA homo- and copolymerization are based on scheme 5.2. The fraction of propagating styryl radicals is very large at low f_S as seen in Fig. 6.2. Thus, it is not adequate to perform the modeling of MWD for styrene-MMA copolymer even at low f_S since the transfer scheme for radical terminated styrene is unclear. In the next part investigations into MWDs for MMA homopolymerization are performed.

Reaction scheme

The mechanism of the catalytic chain-transfer reaction in MMA homopolymerization is illustrated in Scheme 6.3. The rate determining step within this reaction sequence is the hydrogen abstraction by the Co(II) complex, which is believed to proceed with a rate coefficient, $k_{trX,M}$, which is k_{tr} determined for MMA homopolymerization. The second step of the transfer reaction, which initiates a new radical, is considered to be fast.



Scheme 6.3: Catalytic chain-transfer reactions for MMA homopolymerization with CPhBF.

Modeling of MWDs

The MWDs obtained via PREDICI[®] for MMA homopolymerizations at 80°C, 300 bar, in bulk and in scCO₂ are pictured in Fig. 6.8. The k_{tr}^{obs} used are listed in Appendix 3.

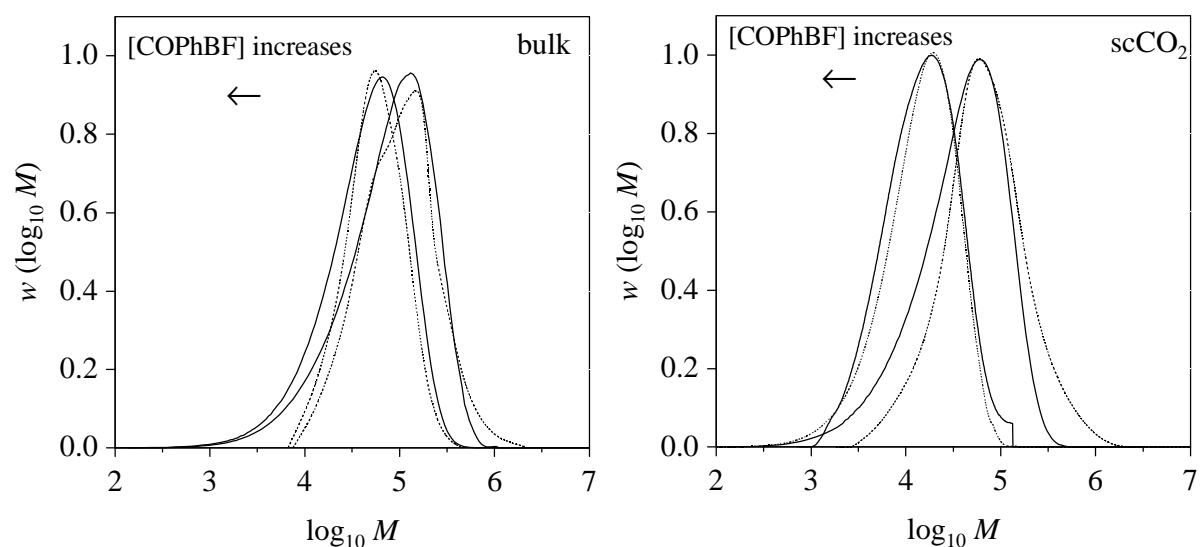


Figure 6.8: Simulated (solid line) and experimental (dotted line) molecular weight distributions for MMA homopolymerizations in bulk and in $scCO_2$ at $80^\circ C$ and 300 bar with $[COPhBF]/[MMA] = 5.4 \cdot 10^{-7}$, $1.5 \cdot 10^{-7}$ and $8.8 \cdot 10^{-8}$, $1.5 \cdot 10^{-7}$ in $scCO_2$ and in bulk, respectively.

The shape and peak position of the experimental and modeled MWDs are slightly different, which may be explained by uncertainties in the COPhBF concentration. As explained in Section 3, the amount of complex used is small and thus uncertainty in the concentration may significantly shift the MWD distribution. However the high molecular weight region, which is used for determining k_{tr} , is not affected. Thus, k_{tr}^{obs} values determined in MMA homopolymerization following scheme 5.2 are considered as accurate.

6.3.4 Closing remarks

In this work PREDICI[®] can not be considered as an effective method to verify the validity of k_{tr} experimentally obtained, assuming that the implemented transfer coefficients are directly derived from the experimental MWD. Nevertheless, transfer rate coefficients and transfer process have been precisely determined for the system styrene-MMA with DDM as CTA.

Hutchinson et al.²⁹ have reported that C_T of DDM is identical for methacrylates with different ester sizes. Thus, by way of k_{tr} reported in this work and other kinetics coefficients reported in the literature, PREDICI[®] appears to be a powerful tool for simulation of homo-, copo- or even terpolymerizations of styrene and methacrylates with DDM as CTA over a wide range of temperature and pressure.

6.4 Endgroups estimate

Fig. 6.2 has shown that the more slowly propagating radicals are the more reactive radical towards DDM, leading to an increase of k_{tr} with increasing f_S . This latter behavior is exactly what is required for an effective endgroup control. The addition of styrene leads to an increase in ϕ_S and an increase in the overall chain-transfer probability. The a priori prediction that at some monomer feed composition with $f_S \ll 1$, the nature of the dominant endgroups will be that of styrene, i.e., $\Phi_S = 1$.

The predictions made by Eq. 6.23 on the fraction of styrene endgroups, Φ_S , for styrene-MMA copolymers in $scCO_2$ with DDM as CTA, are shown in Fig. 6.9. The monomer concentrations are calculated from mole fraction, density and molecular weight of the monomers. The CTA concentration is obtained considering that $[CTA]/[sty]$ are 0.015, which were the conditions of the measurements (see section 5.1).

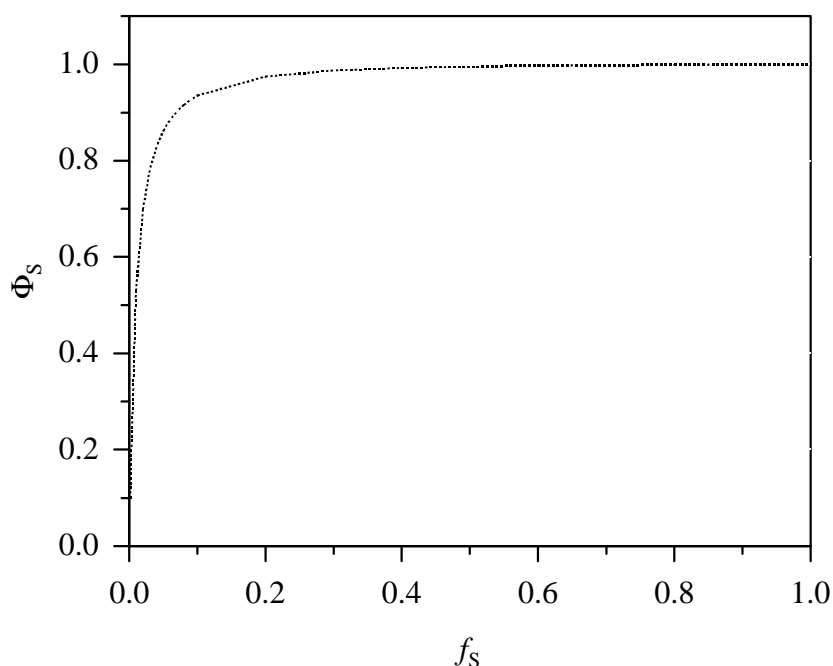


Figure 6.9: Fraction of styrene endgroups as a function of the mole fraction of styrene in the monomer feed for styrene-MMA copolymerizations in 40 wt % $scCO_2$ at 80°C and 300 bar with DDM as CTA.

Φ_S strongly increases for $f_S < 0.1$ and then stays almost constant by Φ_S close to 1. The fraction of styrene endgroups in the styrene-MMA copolymer depends on the affinity of styrene to

CTA. In Fig. 6.9, the qualitative expectations are clearly recognized. The synergistic effects in copolymerization with DDM lead to a situation in which nearly all chains have a styrene endgroup at $f_S = 0.1$. The amount of DDM was also varied and no significant effect is observed on Φ_S : Φ_S slightly increases by decreasing [DDM].

Davis et al.³⁰ found the same synergistic effect as for DDM here for the copolymerization of styrene and α -methyl styrene with CPhBF as CTA, where α -methyl styrene is the more slowly propagating monomer. It was shown that the addition of α -methyl styrene to the system leads to an increase in the fraction of propagating α -methyl styrene radicals and an increase in overall chain-transfer probability. The kinetic modeling was performed assuming scheme 5.2 available for the transfer process.

In case of CPhBF, the more slowly propagating radicals, styryl, are less reactive towards CPhBF and this induces a decrease of k_{tr} with increasing f_S . In this case, there are two opposing effects for the production of a certain endgroup; Addition of styrene leads to an increase in ϕ_S but the overall chain-transfer probability decreases. Overall, no prediction of the nature of the dominant endgroups in this system can be given.

In summary, the fraction of endgroup in a copolymer is controlled by the nature of monomer and chain-transfer agent. In a styrene-MMA comonomer mixture, the monomer required as the endgroup needs to display a very low reactivity towards addition to another monomer, but a high reactivity towards the CTA. The monomer making up the main chain of the polymer should be highly reactive towards addition to monomer and be relatively unreactive towards the CTA³⁰. These observations were also confirmed in the literature³⁰ for other systems.

6.5 References

1. Heuts, J. P. A.; Foster, D. J.; Davis, T. P. *ACS symposium series 768, Transition Metal Catalysis in Macromolecular Design* **2000**, p 254.
2. Fukuda, T.; Kubo, K.; Ma, Y. D. *Prog. Polym Sci* **1992**, 17, 87.
3. Maxwell, I. A.; Aerdt, A. M.; German, A. L. *Macromolecules* **1993**, 26, 1956.
4. Merz, E.; Alfrey, T.; Goldfinger, G. *J. Polym. Sci.* **1946**, 1, 75.
5. Fukuda, T.; Ma, Y.-D.; Inagaki, H. *Macromolecules* **1995**, 18, 1985.

6. Fukuda, T.; Ma, Y.-D.; Inagaki, H. *Makromol. Chem. Rapid Commun.* **1987**, 8, 495.
7. Fukuda, T.; Ma, Y.-D.; Inagaki, H.; Kubo, M. *Macromolecules* **1991**, 24, 370.
8. Odian, G. *Principles of Polymerization*, 2nd Ed., Wiley: New York, **1981**.
9. Isemer, C. *Ph.-D Thesis* **2000**, Göttingen.
10. Fukuda, T.; Die, N.; Ma, Y.-D. *Macromol. Symp.* **1996**, 111, 305.
11. Bamford, C. H. J. *Chem. Soc.* **1976**, 72, 2805.
12. *Data reduction and error analysis for the Physical Sciences*, Bevington, A.; McGraw-Hill: New York, **1969**.
13. *Numerical Recipes*, Press, Flannery, Teukolsky, Vetterling, Cambridge University Press: Cambridge **1989**.
14. Heuts, J. P. A.; Kukulj, D.; Foster, D. J.; Davis, T. P. *Macromolecules* **1998**, 2894, 31.
15. Kukulj, D.; Heuts, J. P. A.; Davis, T. P. *Macromolecules* **1998**, 31, 6034.
16. Galbraith, M. N.; Moad, G.; Solomon, D. H.; Spurling, T. H. *Macromolecules* **1987**, 20, 675.
17. Heuts, J. P. A.; Coote, M. L.; Davis, T. P.; Johnston, L. P. M. *Im Controlled Radical Polymerization*; Matyjaszewski, K.; Ed.; ACS Symposium Series, vol 685; American Chemical Society: Washington, DC, **1998**, p 120.
18. *Polymer Handbook*, 3rd ed.; Brandup, A.; Immergut, E. H. Eds.; Wiley-Interscience: New York, **1989**.
19. Wulkow, M. *Macromol. Theory Simul.* **1996**, 5, 393.
20. Wulkow, M., CiT GmbH, Oldenburger Str. 200, 26180 Rastede.
21. Beuermann, S.; Buback, M.; Isemer, C.; Lacik, I.; Wahl, A. *Macromolecules*, in preparation for publications.
22. Beuermann, S.; Buback, M.; Russell, G. T. *Macromol. Rapid. Commun.* **1994**, 15, 351.
23. Coote, M. L.; Zammit, M. D.; Davis, T. P. Willett, G. D. *Macromolecules* **1997**, 30, 8182.
24. Coote, M. L.; Johnston, L. P.; Davis, T. P. *Macromolecules* **1997**, 30, 8191.
25. Moad, G.; Salomon, D. H. *in Comprehensive Polymer Science*, G. Allen, J. C. Bevington, Eds., vol 3, Chap. 11, Pergamon Press, New York **1989**.
26. Fouassier, J. P.; Jacques, P.; Lougnot, D. J. *J. Rad. Cur.* **1983**, 4, 9.
27. van Boxtel, H. C. M. *Ph.- D. Thesis* **2000**, Göttingen.
28. Buback, M.; Busch, M.; Lämmel, R. A. *Macromol. Theory Simul.* **1996**, 5, 845.

29. Hutchinson, R. A.; Paquet, D. A.; Mc Minn, J. H. *Macromolecules* **1995**, 28, 5655.
30. Heuts, P. A.; Morrison, D. A.; Davis, T. P. *In Controlled/Living Radical Polymerization*; Matyjaszewski, K.; Ed.; ACS Symposium Series, vol 768; American Chemical Society: Washington, DC, **2000**, p 313.

7. Closing remarks

This work has shown that using various chain-transfer agents, different orders of magnitude of chain-transfer rate coefficients are accessible. In styrene and MMA homo- and copolymerizations in the presence of DDM and MMA trimer as chain-transfer agents, k_{tr} values are in the range of 10^3 and 10^2 L·mol⁻¹·s⁻¹, respectively. The transfer process is chemically controlled. In both cases, DDM and MMA trimer as CTAs, k_{tr} is not influenced by the presence of scCO₂ as a solvent and the pressure dependence of k_{tr} is not significant. For MMA homopolymerizations in the presence of CPhBF as catalytic CTA, k_{tr} obtained in scCO₂ is significantly higher than in bulk, e.g. at 1000 bar and 80°C k_{tr} values are $145 \cdot 10^5$ and $55.1 \cdot 10^5$ L·mol⁻¹·s⁻¹ in scCO₂ and in bulk, respectively. In addition, the activation volume for k_{tr} of + 35 cm³·mol⁻¹ is high. These observations are consistent with a diffusion-controlled transfer process.

The particular case of styrene polymerization with CPhBF indicates that the observed k_{tr} values may be underestimated, since it may not be ruled out that the concentration of active Co(II) species may be reduced due to the formation of a reversible cobalt-carbon bond (Co(III)). This transfer process is not clear so far and true rate coefficients related to actual concentration of Co(II) species in the system are not available. The data presented here and in the literature are not reliable to draw any mechanistic conclusions. However, it has been shown that this equilibrium between Co(II) and Co(III) species does not occur in MMA homopolymerization¹.

The decrease of Co(II) species concentration in styrene polymerizations¹ has been observed from indirect analytical method such as electron spin resonance (ESR). It may be interesting to analyze directly the polystyrene formed using matrix-assisted laser desorption ionization time of flight mass spectrometry (MALDI-TOF-MS), thereby permitting the direct observation of the cobalt-carbon bond in styrene polymerization. This technique was successfully used to analyze poly(methyl acrylate) chains formed by catalytic chain-transfer polymerization with a cobalt complex as chain-transfer agent².

In case of a direct observation of the cobalt-carbon bond, the active CPhBF concentration should be reduced, thus the true k_{tr} , k_{tr}^{true} , should be higher than k_{tr}^{obs} . Assuming the validity of scheme 5.2 and taking into consideration the equilibrium between the two species, Co(II) and Co(III), it should be possible to determine k_{tr}^{true} , knowing the concentration of active Co(II) molecules and k_{tr}^{obs} values determined in this work ($k_{tr}^{obs} \cdot [Co(II)]_{initial} = k_{tr}^{true} \cdot [Co(II)]_{active}$).

One approach to determine the active cobalt concentration may be to monitor the Co(II) species during the polymerization by ESR.

The big pressure dependence of k_{tr} obtained in MMA homopolymerization with CPhBF is also explained by the bulkiness of the CTA molecule. By increasing the pressure, the mobility of the CPhBF molecule is much more restricted, which induces a decrease in k_{tr} . This assumption may be tested by studying the pressure dependence of k_{tr} for a less sterically hindered catalytic chain-transfer agent. The bis(difluoroboryl) dimethylglyoximate cobalt (II), COBF, appears to be a good candidate as the structure of this complex is close to the one of CPhBF, substituting the phenyl groups by methyl groups. In addition, COBF is much less sterically hindered than CPhBF. COBF has already shown to have a higher transfer rate coefficient than CPhBF in MMA homopolymerization^{3,4}, because hydrogen abstraction is facilitated using COBF. Thus, if the high activation volume of k_{tr} for CPhBF is due to the bulkiness of the CTA molecule, it is expected that using COBF as catalytic CTA leads to a lower activation volume.

7.1 References

1. Heuts, J. P. A.; Foster, D. J.; Davis, T. P.; Yamada, B.; Yamazoe, H.; Azukizawa, M. *Macromolecules* **1999**, 32, 2511.
2. Roberts, G. E.; Heuts, J. P.A.; Davis, T. P. *Macromolecules* **2000**, 33, 7765.
3. Kukulj, D.; Davis, T. P., Suddaby, K. G.; Haddleton, D. M.; Gilbert, R. G. *J. Polym. Sci. Pol. Chem.* **1997**, 35, 859.
4. Kukulj, D.; Davis, T. P. *Macromol. Chem. Phys.* **1998**, 199, 1697.

8. Abbreviations

a	Mark-Houwink parameter
a_{copo}	Mark-Houwink parameter of a copolymer
A	absorbance
A_{AB}	instantaneous copolymer composition
AIBN	azobisisobutyronitril
c	initiator concentration
CCTA	catalytic chain-transfer agent
C_{I}	chain-transfer constant for transfer to initiator
CLD	chain-length distribution
C_{M}	chain-transfer constant for transfer to monomer
COBF	bis(difluoroboryl) dimethylglyoximato cobalt (II)
COPhBF	bis(difluoroboryl) diphenylglyoximato cobalt (II)
C_{p}	chain-transfer constant for transfer to polymer
C_{R}^0	effective initial radical concentration
C_{T}	chain-transfer constant for transfer to chain-transfer agent
CTA	chain-transfer agent
d	optical path length
DDM	<i>n</i> -dodecyl mercaptan
DMPA	2,2-Dimethoxy-2-phenylacetophenone
DP_{n}	number average degree of polymerization in the presence of CTA
DP_{no}	number average degree of polymerization in the absence of CTA
E_{A}	activation energy
E_{λ}	energy of one mole of photons at the wave length λ
E_{p}	energy of one laser pulse
ESR	electron spin resonance
ε	molar absorption coefficient
f_{i}	mole fraction of component <i>i</i> in the monomer mixture
F_{i}	mole fraction of component <i>i</i> in the polymer mixture
$f(M)$	number molecular weight distribution
ϕ_{A}	fraction of the propagating radical with a terminal unit A
ϕ_{AB}	fraction of the propagating radical with a penultimate unit A and a terminal unit B

Φ_A	fraction of A endgroups
Φ	primary quantum yield
Int_0	peak integral before pulsing
Int_p	peak integral after pulsing
IPUE	Implicit penultimate unit effect
K	Mark-Houwink parameter
K_{copo}	Mark-Houwink parameter of a copolymer
k_d	decomposition rate coefficient
k_p	propagation rate coefficient
k_{pAA}	propagation rate coefficient in a homopolymerization of monomer A
k_{pAB}	propagation rate coefficient for the reaction of a macroradical with terminal unit A and monomer B
\bar{k}_{pAB}	average k_{pAB}
k_{pABC}	propagation rate coefficient for the reaction of a macroradical with penultimate unit A and terminal unit B with a monomer C
$k_{p,copo}$	propagation rate coefficient in a copolymerization
k_t	termination rate coefficient in a homopolymerization
$k_{t,c}$	termination rate coefficient for termination by combination
$k_{t,copo}$	termination rate coefficient in a copolymerization
$k_{t,d}$	termination rate coefficient for termination by disproportionation
$k_{tr,A}$	chain-transfer rate coefficient in a homopolymerization of monomer A
$k_{tr,AB}$	chain-transfer rate coefficient of a radical with penultimate unit A and terminal unit B
$k_{tr,I}$	chain-transfer rate coefficient for transfer to initiator
$k_{tr,M}$	chain-transfer rate coefficient for transfer to monomer
$k_{tr,P}$	chain-transfer rate coefficient for transfer to polymer
$k_{tr,X}$	chain-transfer rate coefficient for transfer to chain-transfer agent
Λ	slope of the $\ln f(M)$ vs M plot
Λ_{high}	slope of the $\ln f(M)$ vs M plot in the high molecular weight region
Λ_{peak}	slope of the $\ln f(M)$ vs M plot in the peak molecular weight region
M	monomer
MMA	methyl methacrylate
MMA _t	methyl methacrylate trimer
M_n	number average molecular weight

M_0	monomer molecular weight
M_w	weight average molecular weight
MWD	molecular weight distribution
M_Z	Z average molecular weight
n_{abs}	number of absorbed photons
p	pressure
P(A/CTA)	probability of the formation of an endgroup of type A
PLP	pulsed-laser polymerization
PMMA	poly(methyl methacrylate)
PS	polystyrene
PUE	penultimate unit effect
r_i	reactivity ratio (homo propagation to cross propagation)
R_p	rate of propagation
R_t	rate of termination
R_{tr}	rate of transfer
S	styrene
S	probability of propagation
SEC	size-exclusion chromatography
s_i	radical reactivity ratio
t	time
T	absolute temperature
ΔV^\ddagger	activation volume
V	irradiated volume
X	monomer conversion
x	number of pulses

9. Appendix

Appendix 1

Propagation rate coefficients in styrene-MMA copolymerizations in bulk and in scCO₂ determined at 80°C applying the PLP-SEC method.

The data of the homopropagation k_p are taken from the literature and determined in this work (see section 5.1). The data of the copolymerization k_p are estimated applying the Implicit Penultimate Unit Effect model following Eqs. 6.4-6.10 in section 6. r and s values are listed in Table 6.1.

f_s	p / bar	$k_{p,bulk}$ $L \cdot mol^{-1} \cdot s^{-1}$	$k_{p,scCO_2}$ $L \cdot mol^{-1} \cdot s^{-1}$
0	300	1540 ^(a)	1382 ^(b)
0	500	1653 ^(a)	1597 ^(b)
0	800	1961 ^(a)	1860 ^(b)
0	1000	2197 ^(a)	1970 ^(c)
0	1500	2922 ^(a)	2776 ^(c)
0.2	300	1108 ^(d)	1014 ^(d)
0.2	500	1224 ^(d)	1120 ^(d)
0.2	800	1390 ^(d)	1267 ^(d)
0.2	1000	1516 ^(d)	1386 ^(d)
0.2	1500	1884 ^(d)	1730 ^(d)
0.5	300	894 ^(d)	804 ^(d)
0.5	500	977 ^(d)	875 ^(d)
0.5	800	1096 ^(d)	983 ^(d)
0.5	1000	1188 ^(d)	1167 ^(d)
0.5	1500	1449 ^(d)	1305 ^(d)

f_s	p / bar	$k_{p,\text{bulk}}$ $\text{L}\cdot\text{mol}^{-1}\cdot\text{s}^{-1}$	k_{p,scCO_2} $\text{L}\cdot\text{mol}^{-1}\cdot\text{s}^{-1}$
0.8	300	791 ^(d)	713 ^(d)
0.8	500	865 ^(d)	773 ^(d)
0.8	800	968 ^(d)	861 ^(d)
0.8	1000	1048 ^(d)	940 ^(d)
0.8	1500	1273 ^(d)	1143 ^(d)
1	300	763 ^(e)	685 ^(f)
1	500	828 ^(e)	742 ^(f)
1	800	929 ^(e)	830 ^(f)
1	1000	1004 ^(e)	901 ^(f)
1	1500	1216 ^(e)	1096 ^(f)

^(a) Beuermann, S.; Buback, M.; Russell, G. T. *Macromol. Rapid. Commun.* **1994**, 15, 351.

^(b) measured in this work.

^(c) extrapolated.

^(d) estimated applying the IPUE model.

^(e) Buback, M.; Kuchta, F.-D. *Macromol. Chem. Phys.* **1995**, 196, 1887.

^(f) Beuermann, S.; Buback, M.; Isemer, C.; Lacik, I.; Wahl, A. *Macromolecules*, in preparation for publications.

Appendix 2

Chain-transfer rate coefficients and chain-transfer constants of styrene-MMA homo- and copolymerizations in bulk and in 40 wt % scCO₂ at 80°C in the presence of DDM as chain-transfer agent.

<i>p</i> / bar	wt % CO ₂	<i>f_s</i>	<i>C_T</i>		$10^{-3}k_{tr}$
			Mayo	CLD	L·mol ⁻¹ ·s ⁻¹
300	40	0	0.790	0.811 ± 0.098	1.14 ± 0.25
300	0	0	0.663	0.702 ± 0.071	1.08 ± 0.21
500	40	0	0.751	0.771 ± 0.066	1.24 ± 0.22
500	0	0	0.531	0.599 ± 0.042	0.991 ± 0.165
800	40	0	0.585	0.669 ± 0.052	1.25 ± 0.22
800	0	0	0.609	0.604 ± 0.048	1.18 ± 0.20
1000	40	0	0.641	0.639 ± 0.052	1.28 ± 0.23
1000	0	0	0.552	0.514 ± 0.035	1.16 ± 0.18
300	40	0.2	1.90	2.10 ± 0.15	2.13 ± 0.36
300	0	0.2	2.10	2.03 ± 0.08	2.22 ± 0.35
1	0	0.5	3.85	3.83 ± 0.45	2.98 ± 0.73
300	40	0.5	3.65	3.77 ± 0.35	3.03 ± 0.62
300	0	0.5	3.26	3.34 ± 0.25	2.98 ± 0.55
500	40	0.5	3.54	3.66 ± 0.52	3.20 ± 0.84
500	0	0.5	3.42	3.25 ± 0.48	3.17 ± 0.89
800	40	0.5	3.16	3.24 ± 0.43	3.19 ± 0.87
800	0	0.5	3.05	2.88 ± 0.35	3.16 ± 0.89
1500	40	0.5	2.58	2.64 ± 0.39	3.44 ± 0.98
1000	0	0.5	2.45	2.73 ± 0.25	3.24 ± 1.25

p / bar	wt % CO ₂	f_s	C_T		$10^{-3}k_{tr}$
			Mayo	CLD	Lmol ⁻¹ s ⁻¹ CLD
300	40	0.8	7.82	8.98 ± 1.25	6.40 ± 1.62
300	0	0.8	7.75	8.14 ± 0.96	6.44 ± 1.47
1	0	1	–	15.5 ± 1.2	10.6 ± 1.9
300	40	1	–	16.3 ± 1.5	11.2 ± 2.1
300	0	1	–	14.6 ± 1.8	11.2 ± 1.4
500	40	1	–	15.5 ± 1.3	11.5 ± 2.1
800	40	1	–	14.8 ± 0.8	12.3 ± 1.9
1500	40	1	–	11.0 ± 0.8	12.1 ± 2.1
1500	0	1	–	11.2 ± 0.9	13.4 ± 2.7

Appendix 3

Chain-transfer rate coefficients and chain-transfer constants observed in styrene and MMA homo- and copolymerizations in bulk and in 40 wt % scCO₂ at 80°C in the presence of CPhBF as chain-transfer agent. The C_T determination is based on Eq. 4.17 (see section 4), which was derived assuming scheme 5.2 to be valid for catalytic chain-transfer polymerization.

p / bar	wt % CO ₂	f_s	$10^{-2} \times C_T^{\text{obs}}$		$10^{-5} k_{\text{tr}}^{\text{obs}}$
			Mayo	CLD	L mol ⁻¹ s ⁻¹
300	40	0	220	211 ± 51	292 ± 100
300	0	0	128	141 ± 22	216 ± 55
500	40	0	166	157 ± 17	252 ± 52
500	0	0	102	80.0 ± 5.3	131 ± 22
800	40	0	140	100 ± 15	186 ± 45
800	0	0	55.0	50.1 ± 8.3	98.2 ± 26.2
1000	40	0	74	73.6 ± 24.7	145 ± 62
1000	0	0	22.5	25.1 ± 6.2	55.1 ± 19.1
300	40	0.2	111	125 ± 23	126 ± 39
300	0	0.2	39.4	42.2 ± 5.3	46.4 ± 9.6
300	40	0.5	50.5	47.1 ± 9.1	37.6 ± 12.1
300	0	0.5	23.7	18.9 ± 2.1	16.9 ± 3.7
500	40	0.5	37.4	38.2 ± 2.5	33.4 ± 5.7
500	0	0.5	16.6	17.5 ± 1.1	17.1 ± 2.8
800	40	0.5	32.5	21.5 ± 3.8	21.1 ± 6.3
800	0	0.5	10.5	9.30 ± 0.85	10.1 ± 2.1
1000	40	0.5	10.4	12.0 ± 1.4	14.0 ± 3.2

p / bar	wt % CO ₂	f_s	$10^{-2} \times C_1^{\text{obs}}$		$10^{-5} k_{\text{tr}}^{\text{obs}}$
			Mayo	CLD	$\text{L} \times \text{mol}^{-1} \times \text{s}^{-1}$
1000	0	0.5	7.16	7.12 ± 2.5	8.47 ± 4.1
300	40	0.8	9.85	10.1 ± 2.0	7.15 ± 2.33
300	0	0.8	9.73	9.34 ± 5.11	7.38 ± 5.19
300	40	1	7.52	8.46 ± 0.80	5.79 ± 1.18
300	0	1	4.31	4.35 ± 2.34	3.29 ± 2.27
500	40	1	3.98	4.08 ± 0.35	3.02 ± 0.53
500	0	1	3.12	3.25 ± 0.26	2.69 ± 0.48
800	40	1	3.55	3.76 ± 0.45	3.12 ± 0.72
800	0	1	2.15	2.37 ± 0.15	2.19 ± 0.36
1000	40	1	1.05	1.20 ± 0.23	1.08 ± 0.31
1000	0	1	1.12	1.30 ± 0.12	1.31 ± 0.27

Appendix 4

Chain-transfer rate coefficients and chain-transfer constants in styrene and MMA homopolymerizations in bulk and in 40 wt % scCO₂ at 80°C in the presence of MMA trimer as chain-transfer agent.

Styrene homopolymerization

<i>p</i> / bar	wt % CO ₂	<i>C_T</i>		<i>k_{tr}</i> / L·mol ⁻¹ ·s ⁻¹
		Mayo	CLD	CLD
300	40	0.198	0.208 ± 0.024	142 ± 23
300	0	0.164	0.173 ± 0.010	131 ± 14
800	40	0.167	0.165 ± 0.011	136 ± 18
800	0	0.122	0.141 ± 0.009	131 ± 14
1500	40	0.089	0.102 ± 0.009	112 ± 21
1500	0	0.085	0.095 ± 0.003	115 ± 11

MMA homopolymerization

<i>p</i> / bar	wt % CO ₂	<i>C_T</i>		<i>k_{tr}</i> / L·mol ⁻¹ ·s ⁻¹
		Mayo	CLD	CLD
300	40	0.096	0.063 ± 0.014	87.3 ± 14.1
300	0	0.063	0.066 ± 0.012	101 ± 08
500	40	0.037	0.052 ± 0.011	83.2 ± 25.2
500	0	0.052	0.057 ± 0.003	94.1 ± 14.5
800	40	0.043	0.052 ± 0.002	97.1 ± 8.5
800	0	0.043	0.053 ± 0.002	103 ± 8
1500	40	0.041	0.041 ± 0.006	113 ± 27
1500	0	0.039	0.042 ± 0.005	123 ± 16

Acknowledgments

To my supervisor, Prof. Dr. M. Buback, I am indebted for the opportunity for this foray into scientific research which I have enjoyed, and learnt from.

Many thanks to Dr. S. Beuermann for encouragement, interest throughout and helpful discussions.

At the practical level, many thanks to Dr. Hans Peter Vögele for his ability to keep everything running and also for his friendship. Many thanks to Dorit Nelke, Eric Minaux and Mark Egorov for their vigilant proof reading and advice on the preparation of this thesis. Many thanks to the Buback Abteilung as a whole for the very pleasant and cooperative working environment.

Special thanks to Dorit Nelke, Matthias Müller, Achim Feldermann and Michael Jürgens for the advice, discussion, company and friendship. I would like to specially thank Heike Rohmann for friendship, for advice and everything else which is hard to put in a paper.

Many thanks to Dr. Igor Iacík for the measurement of numerous MWDs, for the advice, discussion and friendship.

It is a pleasure to acknowledge Prof. Dr. J. Magull who allows me to prepare the cobalt complex. Special thanks to Ruth Dinger and Ulrich Schaller for their help.

I am indebted to the Deutschen Forschungsgemeinschaft, to the European Graduate School and to the European Union for the financial supports.

Je tiens à remercier Eric pour son soutien pendant toute la durée de ma thèse, pour son amitié et ses conseils.

Enfin un remerciement tout particulier à ma mère qui m'a soutenue pendant toute la durée de mes études et pour son amitié.

Curriculum Vitae

Personal information

22.01.1974 Born in Beirut, Lebanon

Education & qualification

1979 - 1984 Elementary School in Villeneuve d'Acsg, France.

1984 - 1992 GCE A Levels in Maths, Physics/Chemistry Biology, History
Queneau High School, Villeneuve d'Acsg.

1992 - 1994 Technological University Institute of Chemistry, University of
Lille, France.

1994 - 1997 Graduation at the University of Lille, France.

Since April 1998 Research toward doctorate in the Institute for Physical Chemistry,
University of Göttingen, in the research group of Prof. Dr. M.
Buback, Germany.

Ap. 1998 - Ap. 1999 Member of the Graduiertenkolleg "Kinetic und Selectivität
chemischer Prozesse in verdichteter fluider Phase".

Ap. 1999 - Sept. 2000 Member of the european project "Superclean Chemistry 2".

Since Sept. 2000 Member of the European Graduate School "Microstructural
Control in Free-Radical Polymerization".

Experience

May - June 1994 Technical training at Norsohaas (water analysis laboratory).

July - Nov. 1995 Technical training at "Institut de Recherche dans l'Industrie
Sucrière" (sugar analysis laboratory).

Sept. 1996 - Sept. 1997 Scientific worker at the University of Lille.

Since April 1998 Scientific worker at the University of Göttingen.